AMIL2DA

Advanced MIPAS level 2 data analysis [amil'tu:da]

Contract No. EVG1-CT-1999-00015
An EC research project co-funded by the Energy, Environment and Sustainable Development Program within the topic 'Development of Generic Earth Observation Technologies'

Final Report

July 1, 2000 - June 30, 2003

co-ordinated by Thomas von Clarmann

http://www.fzk.de/imk/imk2/ame/amil2da

Study Team: T.von Clarmann (IMK)(coordinator)
M. Birk (DLR)
H. Bovensmann (UB)
A. Bracher (UB)
A. Burgess (OU)
S. Ceccherini (IFAC)
A. Doicu (OU)
A. Dudhia (OU)
H. Fischer (IMK)
J.-M. Flaud (LPM)
B. Funke (IAA)
M. García-Comas (IAA)
S. Gil-López (IAA)
N. Glatthor (IMK)
S. Hilgers (DLR)
M. Höpfner (IMK)
V. Jay (OU, now RAL)
S. Kellmann (IMK)
B.J. Kerridge (RAL)
E. Kyrölä (FMI)
A. Linden (IMK)
M. López-Puertas (IAA)
M. López-Valverde (IAA)
F.-J. Martín-Torres (IMK)
M. Milz (IMK)
V. Payne (OU)
J. Reburn (RAL)
M. Ridolfi (IFAC)
C.D. Rodgers (OU)
F. Schreier (DLR)
G. Schwarz (DLR)
R. Siddans (RAL)
T. Steck (IMK)
G.P. Stiller (IMK)
J. Tamminen (FMI)
G. Wagner (DLR)
D.Y. Wang (IMK)
R. Wells (OU)

Chapter 1

Management Report

Reporting period: 1.7.2002 – 30.6.2003

1.1 Objectives of the Reporting Period

The Michelson Interferometer for Passive Atmospheric Sounding (MIPAS) on the Envisat earth observation satellite developed by the European Space Agency (ESA) provides vertical profiles of atmospheric species relevant to several mostly inter-linked problems in ozone chemistry and global change. Routine data analysis under ESA responsibility covers only six species (H_2O, O_3, N_2O, CH_4, HNO_3, NO_2) as well as pressure and temperature. The MIPAS data, however, contains much more information of other atmospheric trace species of very high scientific value. Thus, the exploitation of MIPAS data with respect to the retrieval of many more scientifically interesting species such as the complete nitrogene family, chlorine source gases and reservoirs, greenhouse gases, ozone precursors, aerosols etc as well as the analysis of the six key species by means of data processors of higher sophistication than the operational ESA code are of high interest for better understanding of the ozone-chemistry and global change. The main goal of AMIL2DA project is to fill this gap and to ensure quality and intercomparability of these independently generated value-added data products, which are generated by innovative data analysis and retrieval approaches developed by participating groups.

A major objective of AMIL2DA was the development and adaption of the data analysis codes to the MIPAS requirements as well as validation of these processors. While cross-validation of radiative transfer models and a blind test retrieval study were to a major part finished in the first two years of the project, the main objectives in the reporting period were related to real MIPAS measurement data: intercomparison of real data retrievals carried out with these data processors; detection of deficiencies of processors; removal of these deficiencies and upgrading of processors. Further objectives of AMIL2DA included a characterization of the MIPAS instrument and the processing schemes by various means as well as validation of the data with other instruments.

1.2 Scientific/Technical Progress Made in Different Work Packages According to the Planned Timeschedule:

All workpackages could be successfully finished by end of the project period. Due to delayed Envisat launch all workpackages based on real MIPAS data had to be shifted towards the end of the project period. By rescheduling them in parallel rather than sequential, also these workpackages (WP 5000) could be completed in time. By these activities the functionality of the MIPAS instrument as well as the data processors was proven. Finally, recommendations for potential changes of the operational processor were given to ESA (WP 6000).

Final Gantt chart Update:

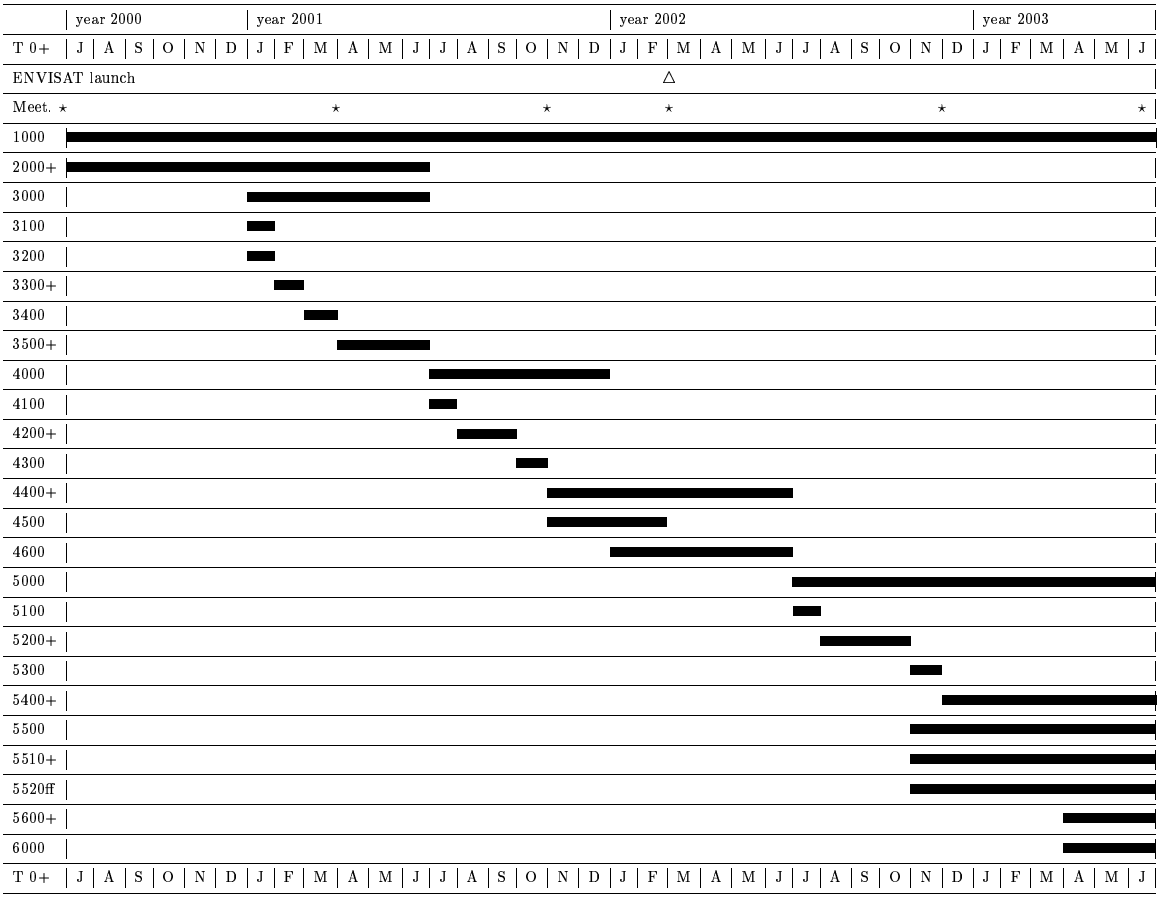

Table with comparison between planned and used manpower and financial resources by Work Packages and partners:

Manpower Matrix (for organisations working on AC basis, table entries are additional personnel only): This table includes only manpower charged to EC. Actually a lot more manpower went into each WP, which was funded by external sources.

Work-Package No	IMK	Oxford Univ.	DLR	IFAC	RAL	LPM	IAA	Univ. Bremen	FMI
1000 planned	3+6								
used	3+6								
5000 planned	27.25+18.5	7+3.5	19	11	14	4	12.5	0+3	3
used	27.25+18.5	7+3.5	19	11	16	4	12.5	5+0	3
6000 planned				7					
used				7					

Financial Resources Matrix

Work-Package No	IMK	Oxford Univ.	DLR	IFAC	RAL	LPM	IAA	Univ. Bremen	FMI
1000 planned	16886								
used	18652								
5000 planned	153384	56534	91424	61904	102926	31517	46680	2000	12542
used	169427	80171	71818	40357	127184	39516	33332	37033	10176
6000 planned				39392					
used				25682					

1.3 Milestones and Deliverables Obtained:

Milestones:

The following milestones have been achieved within the reporting period:

1. (M8) Explanation and removal of systematic residuals in best fit spectra (23 June 2003)

2. (M10) Fifth Project Meeting (25/26 November 2002)
3. (M11) Final product validation (23 June 2003)
4. (M12) Final Presentation (23/24 June 2003)

Deliverables:

The following deliverables have been provided:

Deliverables list

Deliverable No	Deliverable title	Delivery date	Nature	Dissem. level
D45 (5210)	Retrieved observational and atmospheric parameters along with error estimates; residual spectra of IMK	12/02	Da	RE
D46 (5220)	Retrieved observational and atmospheric parameters along with error estimates; residual spectra of Oxf. Univ.	12/02	Da	RE
D47 (5230)	Retrieved observational and atmospheric parameters along with error estimates; residual spectra of DLR	12/02	Da	RE
D48 (5240)	Retrieved observational and atmospheric parameters along with error estimates; residual spectra of IFAC	12/02	Da	RE
D49 (5250)	Retrieved observational and atmospheric parameters along with error estimates; residual spectra of RAL	12/02	Da	RE
D50 (1000)	Report on Progress observed from 4/02 to 7/02, with Mid-Term Assessment Report as an annex	7/02	Re	RE
Cost	Cost statement 1/07/01-30/06/02	31/08/02		
D51 (5300)	Diagnostics	7/02	Re	RE
D52 (1000)	Quarterly Report	10/02	Re	RE
D53 (5410)	Second upgrade of IMK retrieval strategy	6/03	Me	RE
D54 (5420)	Second upgrade of Oxf. Univ. retrieval strategy	6/03	Me	RE
D55 (5430)	Second upgrade of DLR retrieval strategy	6/03	Me	RE
D56 (5440)	Second upgrade of IFAC retrieval strategy	6/03	Me	RE
D57 (5450)	Second upgrade of RAL retrieval strategy	6/03	Me	RE
D58 (1000)	Quarterly Report	1/03	Re	RE

Deliverable No	Deliverable title	Delivery date	Nature	Dissem. level
D59 (5510)	Documentation on characterization of the best-fit residuals in terms of NLTE effects. Better understanding of the retrieval codes	6/03	Re	PU
D60 (5511)	Documentation on characterization of the best-fit residuals in terms of NLTE effects by using the MIPAS data. Better understanding of the retrieval codes	6/03	Re	PU
D61 (5512)	Documentation on characterization of the best-fit residuals in terms of NLTE effects by using the 'NLTE free' retrieved quantities from GOMOS and SCIAMACHY. Better understanding of the retrieval codes and possibly NLTE populations of some levels	6/03	Re	PU
D62 (5513)	Documentation on characterization of the best-fit residuals in terms of NLTE effects in terms of Day/Night MIPAS spectra. Better understanding of the retrieval codes	6/03	Re	PU
D63 (5520)	Auxiliary list of spectroscopic data	6/03	Da	PU
D64 (5530)	Assessment of microwindows	6/03	Re	PU
D65 (5540)	Characterization of the MIPAS instrument	6/03	Re	PU
D66 (5550)	Assessment of *a priori* data	6/03	Re	PU
D67 (5560)	Assessment of other reasons for systematic residuals	6/03	Re	PU
D68 (1000)	Quarterly Report	4/03	Re	RE
D69 (5600)	Comparison against external data	6/03	Re	PU
D70 (5610)	Comparison against GOMOS	6/03	Re	PU
D71 (5620)	Comparison against SCIAMACHY data	6/03	Re	PU
D72 (5630)	Comparison against external data	6/03	Re	PU
D73 (6000)	Processor IROE-R review	6/03	Re	PU
D74 (1000)	Glossy Brochure #2	7/03	Re	PU
D75 (1000)	Final Report Upgrade	7/03 10/03	Re Re	PU PU
Cost	Cost statement 1/07/02-30/06/03 09/03			

1.4 Deviations From the Work Plan or/and Time Schedule and Their Impact to the Project

The following deliverables were delayed:

Deliverable	scheduled date	actual date	impact on project
D45 (5210)	06/02	12/02	delay of subsequent WP
D46 (5220)	06/02	12/02	delay of subsequent WP
D47 (5230)	06/02	12/02	delay of subsequent WP
D48 (5240)	06/02	12/02	delay of subsequent WP
D49 (5250)	06/02	12/02	delay of subsequent WP
D53 (5410)	11/02	06/03	none
D54 (5420)	11/02	06/03	none
D55 (5430)	11/02	06/03	none
D56 (5440)	11/02	06/03	none
D57 (5450)	11/02	06/03	none
D59 (5510)	04/03	06/03	none
D60 (5511)	04/03	06/03	none
D61 (5512)	04/03	06/03	none
D62 (5513)	04/03	06/03	none
D63 (5520)	04/03	06/03	none
D64 (5530)	04/03	06/03	none
D65 (5540)	04/03	06/03	none
D66 (5550)	04/03	06/03	none
D67 (5560)	04/03	06/03	none

1.5 Co-ordination of the Information Between Partners and Communication Activities

1. **Organised meetings**
   - Co-ordination Meeting (Florence, 25-26 November 2002)
   - Final Meeting (Karlsruhe 23-24 June 2003)
2. **Conference attendance**
   - Fourth International Radiative Transfer Modelling Workshop, 8–11 July 2002, Bredbeck, Germany;
   - ASA 2002 - Atmospheric Spectroscopy Application, 25–28 August 2002, Moscow, Russia;
   - ENVISAT Calibration Review Workshop, 9–13 September 2002, Noordwijk, The Netherlands;

- 6th European Symposium on Stratospheric Ozone, 2–6 September 2002, Gothenburg, Sweden;
- 9th International Symposium on Remote Sensing, 24–27 September 2002, Agia Pelagia, Crete, Greece
- ENVISAT Validation Workshop, 9–13 December, 2002, Frascati, Italy;
- EGS-AGU-EUG Joint Assembly, 6–11 April 2003, Nice, France;

3. **Co-operation with other projects/networks**

   - European Commission projects and networks:
     - GATO cluster;
     - TOPOZ III (informal co-operation with co-ordinator);
     - ASSET (informal co-operation with co-ordinator);
     - VINTERSOL (informal co-operation with co-ordinator);
   - Projects with national funding:
     - (Germany) HGF Vernetzungsfonds: Generierung und Validierung von Datenprodukten aus ENVISAT-Messungen sowie deren Nutzung zur Erforschung der oberen Troposphäre und Stratosphäre;
     - (Germany: BmBF, AFO2000, 07 ATF 53) SACADA;
     - (Germany: BmBF 07 ATF 43/44) KODYACS;
     - (SPAIN) PNE-017/200C national research project;
   - ESA contracts, AO-work, and working groups
     - ”Development of an optimized algorithm for routine p, T and VMR retrieval from MIPAS limb-emission spectra”, ESTEC Contract N. 11717/95/NL/C.
     - ”INFLIC”, ESRTEX contract 15530/01/NL/SF;
     - IRAC In-flight Radiometric Accuracy Assessment of MIPAS;
     - Non-LTE study;
     - ”Development of Algorithms for the Exploitation of MIPAS Special Modes Measurement”, ESRIN Contract No 16700/02/I-L.
     - ESA ACVT (Algorithm Calibration Validation Team);
   - Miscellaneous
     - TROPOSAT (Eurotrac 2)
     - IMK contract: Noise analysis of MIPAS/ENVISAT in-flight measurements, purchase order no: 315/20228879/IMK;
     - Change #1 of contract 16150/02/NL/SF: Enhanced Analysis of MIPAS Radiometric Performance Using In-Flight Calibration Data, Investigation of signal fluctuations.

4. **Internal project web-site**: The AMIL2DA project web-site includes some internal pages for data exchange and internal communication;

5. **E-mail correspondence**: E-mail proved to be a powerful tool for fast unformalized exchange of all kinds of information;

6. A **Project Advisory Group** was been installed. This group included: C. Camy-Peyret (CNRS), Joerg Langen (ESA, ESTEC), Martine DeMaziere (BIRA), Neil Harris (Cambridge University), William Lahoz (U.K. Meteorological Office), Dirk Offermann (Wuppertal University). This group contributed by reading the reports, proposing items for the meeting agendas.

7. **Internal Communication:** Notes from the biweekly meetings of the Oxford and RAL MIPAS groups are now publicised by Oxford University on a web-site (http://www.atm.ox.ac.uk/group/mipas/meetings/) and has provided a useful means of interaction with the other AMIL2DA groups, e.g. in identifying missing January Antarctic data in the ESA distribution and tracing this to a fringe count error in the ESA processing.

1.6 Difficulties Encountered at Management and Co-ordination Level

1. **Difficulty:** The page 'Expected Project Impact' on the eTIP does not work properly under Netscape/Solaris. The most recent version of eTIP leads Netscape users into an endless loop, unless cookies and JAVAscript are activated.

   Proposed Solution: Debugging by EC; the problem has been fixed. Non-availability of this tool has caused a lot of additional effort which otherwise could have been spent for science work. It would be helpful if an automatic error message informed the user that cookies and JAVAscript have to be activated under Netscape.

2. **Difficulty:** Many parts of the eTIP are redundant with other parts of the final report, of which the eTIP formally is a section. This causes additional and unnecessary workload and effort which better could be spent for science. Keeping scientists busy by forcing then to write the same contents again and again in different formats is considered contraproductive from a scientific point of view.

   Proposed Solution: Redundant requirements in the reporting guidelines (including eTIP should be removed. EC may argue that the eTIP shall be a stand-alone document but this argument does not hold because according to the applicable reporting guidelines the TIP is only a section of the Final Report. The TIP is NOT a deliverable in its own right.

3. **Difficulty:** Cost statements were not available from all partners in time. This led to delay of submission of the cost statement by the co-ordinator to EC.

Proposed Solution: A written agreement among all participants covering also this issue might in future similar projects give the co-ordinator more authority over the participants' administrations and make him less dependent on the good-will of the administrational departments.

4. **Difficulty:** Administration on EC-side often is somewhat slow (e.g. payment; settling of the contract, contract amendment w.r.t. change of name of a participating institution)

   Proposed Solution: Reduction of overall administrative effort.

5. **Difficulty:** The reporting guidelines seem to overformalize the report and it is not understood how they should increase the readability of the report and how they should make the reviewing of the project easier.

   Proposed Solution: In Section 3 of the report a free format should be allowed. The decision how to organize this part of the report shall be left to the scientists.

6. **Difficulty:** The fact that the applicable reporting guidelines were released after the beginning of the project caused major irritation and a lot of unnecessary work.

   Proposed Solution: Any guidelines should be considered as mandatory only if they are available already when the contract is signed. It is considered a strange procedure to imply such changes of the co-ordinator's committments after signature of the contract.

Chapter 2

Executive Summary

Contract No.: EVG1-CT-1999-00015

Reporting Period: 1 July 2002 – 30 June 2003

Title: Advanced MIPAS Level 2 Data Analysis (AMIL2DA)

2.1. Objectives

Changes in atmospheric composition are important in the context of stratospheric ozone depletion, global change and related environmental problems. The Michelson Interferometer for Passive Atmospheric Sounding (MIPAS), which is a core instrument of the Envisat polar platform launched on 1 March 2001 by the European Space Agency (ESA), is a powerful tool to measure vertical profiles of trace species on a global scale. While operational data processing by ESA covers only analysis of pressure, temperature, and the mixing ratios of the species O_3, H_2O, HNO_3, CH_4, N_2O, and NO_2, MIPAS infrared spectral limb emission measurements contain information on a bulk of further species relevant to environmental problems mentioned above. Under AMIL2DA data analysis tools were generated for these supplemental species. These data analysis tools also allow a more sophisticated analysis of the key species (e.g. inclusion of a larger number of spectral data points; inclusion of additional physical processes; more flexible retrieval approaches). These analysis tools have been thoroughly tested. By application to real MIPAS data it has been shown that many additional species can be retrieved from MIPAS spectra.

The objectives left for the reporting period were the application of the data processors to real MIPAS measurement data in order to prove their robustness; charaterization of the MIPAS instrument; contribution to the validation of MIPAS data products; recommendations to ESA with respect to near-real time data analysis.

2.1 Scientific Achievements

Tools for advanced MIPAS level-2 data analysis were developed, thoroughly tested, and applied to sample MIPAS data sets. Participating groups now are in a position to analyze MIPAS data for scientific purposes with their own data processors, which are custom-tailored to the groups' particular scientific interest.

2.2 Socio-Economic Relevance and Policy Implications

After AMIL2DA participating groups have reliable MIPAS data analysis processors available and are ready for independent scientific analysis of real MIPAS data. This strengthens their position in international scientific competition.

AMIL2DA has publically stated the political and scientific need to retrieve species other than the official ESA key-species. The technical/scientific feasibility has been proven. Activities under AMIL2DA contribute largely to the overall success of the MIPAS experiment and the Envisat mission, which will make justification of further suchlike missions easier. Both industry and the scientific community would benefit from such follow-up projects.

Beyond this, AMIL2DA has strengthened the cooperation between all European research sites involved. For some participants, this project has been very important for being in the "wave" of state-of-the-art research in remote sensing of the atmosphere.

All these points apply to the overall project and can hardly be assigned to a single phase of the project. However, successful work real MIPAS measurement data, as done in the reporting period, increases the credibility and significance of the achievements of the entire project.

2.3 Conclusions

The project considerably improved the capability of the contractors to provide enhanced level-2 data from MIPAS-Envisat. Algorithms developed in an early phase of AMIL2DA were tested and prove to work reliably. Co-operation of the large consortium helped to detect some deficiencies which may have remained unnoticed without the intercomparison in the framework of this study. Activities in the last year of AMIL2DA have proven that all developments and studies based on simulated measurement data are also useful and valid for real MIPAS measurement data.

2.4 Keywords:

Envisat, MIPAS, retrieval, radiative transfer forward modeling, cross-validation

2.5 Publications: Cummulative List

Peer reviewed articles:

T. von Clarmann, T. Chidiezie Chineke, H. Fischer, B. Funke, M. García-Comas, S. Gil-López, N. Glatthor, U. Grabowski, M. Höpfner, S. Kellmann, M. Kiefer, A. Linden, M. López-Puertas, M. Á. López-Valverde, G. Mengistu Tsidu, M. Milz, T. Steck and G. P. Stiller, 2003, "Remote Sensing of the Middle Atmosphere with MIPAS", in *Remote Sensing of Clouds and the Atmosphere VII*, K. Schäfer, O. Lado-Bordowsky, A. Comerón and R. H. Picard, eds., Proc. SPIE, **4882**, 172–183, SPIE, Bellingham, WA, USA.

T. von Clarmann, M. Höpfner, B. Funke, M. López-Puertas, A. Dudhia, V. Jay, F. Schreier, M. Ridolfi, S. Ceccherini, B. J. Kerridge, J. Reburn and R. Siddans, 2003, "Modelling of atmospheric mid–infrared radiative transfer: the AMIL2DA algorithm intercomparison experiment", *J. Quant. Spectrosc. Radiat. Transfer*, **78**, 3-4, 381-407, doi:10.1016/S0022-4073(02)00262-5.

T. von Clarmann, N. Glatthor, U. Grabowski, M. Höpfner, S. Kellmann, M. Kiefer, A. Linden, G. Mengistu Tsidu, M. Milz, T. Steck, G. P. Stiller, D. Y. Wang, H. Fischer, B. Funke, S. Gil-López, and M. López-Puertas, 2003, "Retrieval of temperature and tangent altitude pointing from limb emission spectra recorded from space by the Michelson Interferometer for Passive Atmospheric Sounding (MIPAS)," J. Geophys. Res., accepted.

T. von Clarmann, S. Ceccherini, A. Doicu, A. Dudhia, B. Funke, U. Grabowski, S. Hilgers, V. Jay, A. Linden, M. López-Puertas, F.-J. Martín–Torres, V. Payne, J. Reburn, M. Ridolfi, F. Schreier, G. Schwarz, R. Siddans, and T. Steck, 2003, "A blind test retrieval experiment for infrared limb emission spectrometry", J. Geophys. Res., accepted.

A. Doicu, F. Schreier and M. Hess, 2003, "Iteratively Regularized Gauss–Newton Method for Bound–Constraint Problems in Atmospheric Remote Sensing", *Comp. Phys. Comm.*, **153** (1), pp. 59–65.

J.-M. Flaud, W. J. Lafferty, J. Orphal, M. Birk, and G. Wagner, 2003, "First high-resolution analyses of the ν_8 and $\nu_8 + \nu_9$ spectral regions of $^{35}ClONO_2$: determination of the ν_9 band center," *Mol. Phys.*, **101**, 1527-1533.

J.-M. Flaud, J. Orphal, W.J. Lafferty, M. Birk and G. Wagner, 2002, "High resolution vib-rotational analysis of the ν_3 and ν_4 spectral regions of chlorine nitrate," *J. Geophys.*

Res., **107**, D24, ACH16-1-16-9.

J.-M. Flaud, A. Perrin, J. Orphal, Q. Kou, P.-M. Flaud, Z. Dutkiewicz and C. Piccolo, 2003, "New analysis of the $\nu_5 + \nu_9 - \nu_9$ hot band of HNO_3", *J. Q. S. R. T.*, **77**, 355-364.

J.-M. Flaud, C. Piccolo, B. Carli, A. Perrin, L. H. Coudert, J.-L. Teffo, and L. R. Brown, 2003, "Molecular line parameters for the MIPAS (Michelson Interferometer for Passive Atmospheric Sounding) experiment", *J. Atmospheric and Ocean Optics*, **16**, 172-182.

J.-M. Flaud, G. Wagner, M. Birk, C. Camy-Peyret, C. Claveau, M.R. De Backer-Barilly, A. Barbe, and C. Piccolo, 2003, "Ozone absorption around 10 μm," *J. Geophys. Res.*, **108**, doi:10.1029/2002JD002755.

G. Mengistu Tsidu, T. von Clarmann, H. Fischer, N. Glatthor, U. Grabowski, M. Höpfner, M. Kiefer, S. Kellmann, A. Linden, M. Milz, T. Steck, G. P. Stiller, B. Funke, and M. López-Puertas, 2002, "Validation of non-operational MIPAS-ENVISAT data products," in *Optical Remote Sensing of the Atmosphere and Clouds III, Proc. SPIE* **4891**.

M. Milz, M. Höpfner, T. von Clarmann, U. Grabowski, T. Steck, G. P. Stiller, and H. Fischer, 2002, "Measurements of water vapor and ice clouds in the tropical UT/LS region with MIPAS/ENVISAT," submitted to Adv. Space Res.

F. Schreier and U. Böttger, 2003, "MIRART, A Line-By-Line Code for Infrared Atmospheric Radiation Computations incl. Derivatives", Atmos. Oceanic Optics **16**, pp. 262–268.

G. P. Stiller, T. Steck, M. Milz, T. von Clarmann, U. Grabowski, and H. Fischer, 2003, "Approach to the cross-validation of MIPAS and CHAMP temperature and water vapour profiles," in *First CHAMP Mission Results for Gravity, Magnetic and Atmospheric Studies*, C. Reigber, H. Lühr, and P. Schwintzer, eds., pp. 551–556, Springer–Verlag Heidelberg.

G. P. Stiller, T. v. Clarmann, T. Chidiezie Chineke, H. Fischer, B. Funke, S. Gil-López, N. Glatthor, U. Grabowski, M. Höpfner, S. Kellmann, M. Kiefer, A. Linden, M. López-Puertas, G. Mengistu Tsidu, M. Milz and T. Steck, 2003, "Early IMK/IAA MIPAS/ENVISAT results", in *Remote Sensing of Clouds and the Atmosphere VII*, K. Schäfer, O. Lado-Bordowsky, A. Comerón and R. H. Picard, Proc. SPIE, **4882**, 184-193, SPIE, Bellingham, WA, USA

G. Wagner, M. Birk, F. Schreier and J.-M. Flaud, 2002, "Spectroscopic database for ozone in the fundamental spectral regions", *J. Geophys. Res.*, **107** (D22) 4626, doi: 10.1029/2001JD000818, ACH 10-1 – 10-18.

Non refereed literature:

A. Bracher, A. Rozanov, C. von Savigny, M. von Koenig, M. Weber, K. Bramstedt, J. P. Burrows, 2003, "First validation of SCIAMACHY O3 and NO2 profiles with collocated measurements from satellite sensors HALOE, SAGE II and POAM III", *EGS-AGU-EUG Joint Assembly*, Nice, France, 6–11 April 2003, poster.

A. Bracher, M. Weber, M. von Koenig, K. Bramstedt, J. P. Burrows, 2003, "First validation of MIPAS O3, H2O, and NO2 profiles with collocated measurements from satellite sensors HALOE and SAGE II", *EGS-AGU-EUG Joint Assembly*, Nice, France, 6–11 April 2003, poster.

A. Burgess, 2003, "Retrieval of SO_2 Profiles from MIPAS below the Tropopause", *EGS-AGU-EUG Joint Assembly*, Nice, France, 6–11 April 2003, oral presentation.

T. von Clarmann, 2001, "INFLIC", *Pre-launch Workshop on the Atmospheric Chemistry Validation of Envisat (ACVE)*, Noordwijk, The Netherlands, 16–18 May 2001, oral presentation.

T. von Clarmann, 2002, "MIPAS-ENVISAT data: Beyond level 2." at *27th General Assembly of the European Geophysical Society*, Nice, France, 21-26 April 2002, oral presentation.

T. von Clarmann, 2002, "Evaluation of MIPAS satellite data." *3rd Wuppertal Springtime Seminar in Atmospheric Science*, Wuppertal, Germany, 11-22 March 2002, invited oral presentation.

T. von Clarmann, M. Birk, H. Bovensmann, A. Burgess, S. Ceccherini, A. Doicu, A. Dudhia, J.-M. Flaud, B. Funke, S. Hilgers, M. Höpfner, V. Jay, B. J. Kerridge, E. Kyrölä, A. Linden, M. López-Puertas, F.-J. Martín-Torres, G. Mengistu Tsidu, V. Payne, C. Piccolo, J. Reburn, M. Ridolfi, F. Schreier, G. Schwarz, R. Siddans, T. Steck, and D.-Y. Wang, 2003, "Advanced MIPAS-Level-2 Data Analysis (AMIL2DA)," *EGS–AGU–EUG Joint Assembly*, Nice, France, 06–11 April 2003, poster.

T. von Clarmann, H. Bovensmann, A. Dudhia, J.-M. Flaud, B. J. Kerridge, E. Kyrölä, F. J. Martín-Torres, M. Ridolfi, F. Schreier, 2000, "AMIL2DA–Advanced MIPAS level 2 data analysis", *ERS-ENVISAT Symposium*, Gothenburg, Sweden, 16–20 October 2000, poster.

T. von Clarmann, H. Fischer, B. Funke, M. García-Comas, S. Gil-López, N. Glatthor, U. Grabowski, M. Höpfner, S. Kellmann, M. Kiefer, A. Linden, M. López-Puertas, M. Á. López-Valverde, G. Mengistu Tsidu, M. Milz, T. Steck, G. P. Stiller, and D. Y. Wang,

2003, "Retrieval of temperature and pointing information from MIPAS limb emission spectra," *EGS–AGU–EUG Joint Assembly*, Nice, France, 6–11 April 2003, oral presentation.

A. Dudhia, 2002 "The Michelson Interferometer for Passive Atmospheric Sounding (MIPAS)", *Meterological Applications of Data from High Resolution Spectrometers Royal Meteorological Society Specialist Meeting*, London, UK, April 2002, oral presentation.

A. Dudhia, 2002, "AMIL2DA–Advanced MIPAS level 2 data analysis", *6th European Symposium on Stratospheric Ozone*, Gothenburg, Sweden; 2–6 September 2002, poster.

A. Dudhia, 2003, "Retrieval of Minor Species from MIPAS" *EGS–AGU–EUG Joint Assembly*, Nice, France, 6–11 April 2003, oral presentation.

J.-M. Flaud, 2002, "Infrared Laboratory Spectroscopy of O_3 and $ClONO_2$", *Symposium on High Resolution Infrared Spectroscopy*, Richland, WA USA, 2002, invited oral presentation.

J.-M. Flaud, 2002, "The HNO_3 hot bands: impact on atmospheric retrievals," *7th HITRAN database Conference*, Boston, USA, 2002, invited oral presentation.

J.-M. Flaud, 2002 "Infrared Spectroscopy and the Atmosphere", *57th Symposium on Molecular Spectroscopy*, Columbus, USA, 2002, invited oral presentation.

J.-M. Flaud, 2002 "Infrared Sensing of the Atmosphere from Satellites: Spectroscopic Needs," *International Workshop on Atmospheric Specroscopy Applications, ASA*, Moscow, Russia, 2002, invited oral presentation.

J.-M. Flaud, 2003, "FTS Laboratory Spectroscopy in Support of the MIPAS Experiment", *OSA Meeting: Fourier Transform Spectroscopy, New Methods and Applications*, Quebec, Canada, 2003, invited oral presentation.

B. Funke, F. J. Martín-Torres, M. López-Puertas, M. Höpfner, F. Hase, M. Á. López-Valverde, and M. Garcia-Comas, 2002, "A generic non-LTE population model for MIPAS-ENVISAT data analysis." *27th General Assembly of the European Geophysical Society*, Nice, France, 21-26 April 2002, oral presentation.

B. Funke, M. T. von Clarmann, H. Fischer, M. García-Comas, S. Gil-López, N. Glatthor, U. Grabowski, M. Höpfner, S. Kellmann, M. Kiefer, A. Linden, M.A. López-Puertas, López-Valverde, G. Mengistu Tsidu, M. Milz, T. Steck, G.P. Stiller and D.Y. Wang, 2003, "Sondeo remoto de la atmosfera con el interferometro MIPAS/ENVISAT: NO_x durante la ruptura del vortice de hemisferio sur en Sep./Oct. 2002," *X Congreso Nacional de Teledeteccion*, Cçceres, Spain, September 2003, oral presentation.

B. Funke, T. von Clarmann, H. Fischer, M. García-Comas, S. Gil-López, N. Glatthor, U. Grabowski, M. Höpfner, S. Kellmann, M. Kiefer, A. Linden, M. López-Puertas, M. Á. López-Valverde, G. Mengistu Tsidu, M. Milz, T. Steck, G. P. Stiller, and D. Y. Wang, 2003, "NO and CO vertical profiles derived from MIPAS/Envisat under consideration of non–LTE." *EGS–AGU–EUG Joint Assembly*, Nice, France, 6–11 April 2003, poster.

B. Funke, T. von Clarmann, H. Fischer, M. García-Comas, S. Gil-López, N. Glatthor, U. Grabowski, M. Höpfner, S. Kellmann, M. Kiefer, A. Linden, M. López-Puertas, M. Á. López-Valverde, G. Mengistu Tsidu, M. Milz, T. Steck, G. P. Stiller, and D. Y. Wang, 2003, "NO_x derived from MIPAS/Envisat in the South Hemisphere vortex split-up event in September/October 2002." *EGS–AGU–EUG Joint Assembly*, Nice, France, 6–11 April 2003, poster.

S. Gil-López, T. von Clarmann, H. Fischer, B. Funke, M. García-Comas, N. Glatthor, U. Grabowski, M. Höpfner, S. Kellmann, M. Kiefer, A. Linden, M. López-Puertas, M. Á. López-Valverde, G. Mengistu Tsidu, M. Milz, T. Steck, G. P. Stiller, and D. Y. Wang, 2003, "Stratospheric and mesospheric ozone derived from MIPAS/ENVISAT under consideration of non–LTE." *EGS–AGU–EUG Joint Assembly*, Nice, France, 6–11 April 2003, poster.

S. Gil-López, T. von Clarmann, H. Fischer, B. Funke, M. García-Comas, N. Glatthor, U. Grabowski, M. Höpfner, S. Kellmann, M. Kiefer, A. Linden, M. López-Puertas, M.A. López-Valverde, G. Mengistu Tsidu, M. Milz, T. Steck, G.P. Stiller and D.Y. Wang, 2003, "Sondeo remoto de la atmosfera con el interferometro MIPAS/ENVISAT: Il ozono estratosferico y mesosferico," *X Congreso Nacional de Teledeteccion*, Cçceres, Spain, September 2003, oral presentation.

N. Glatthor, T. von Clarmann, H. Fischer, B. Funke, U. Grabowski, M. Höpfner, S. Kellmann, M. Kiefer, A. Linden, M. Milz, T. Steck, G. P. Stiller, and D. Y. Wang, 2003, "Study of the antarctic vortex split-up in September/October 2002 by means of trace species from MIPAS/ENVISAT." *EGS–AGU–EUG Joint Assembly*, Nice, France, 6–11 April 2003, poster.

M. Höpfner, T. von Clarmann, H. Fischer, B. Funke, N. Glatthor, U. Grabowski, S. Kellmann, M. Kiefer, A. Linden, G. Mengistu Tsidu, M. Milz, T. Steck, G. P. Stiller, and D. Y. Wang, 2003, "$ClONO_2$ from MIPAS/ENVISAT during the southern hemisphere vortex split-up event in September/October 2002." *EGS–AGU–EUG Joint Assembly*, Nice, France, 06–11 April 2003, oral presentation.

M. Höpfner, T. von Clarmann, H. Fischer, B. Funke, N. Glatthor, U. Grabowski, S. Kellmann, M. Kiefer, A. Linden, G. Mengistu Tsidu, M. Milz, T. Steck, G. P. Stiller, and D. Y. Wang, 2003, "Observation of PSCs with MIPAS/ENVISAT." *EGS–AGU–EUG Joint Assembly*, Nice, France, 06–11 April 2003, poster.

V.L. Jay, A.Dudhia and C.D.Rodgers, 2001, “MIPAS Error Analysis using Spectral Signatures”, *ASSFTS10*, Ventura, California, October 2001, poster.

M. López-Puertas, T.von Clarmann, A. Dudhia, J.-M. Flaud, B. Funke, M. García-Comas, S. Gil-López, N. Glatthor, U. Grabowski, V. Jay, M. Kiefer, M.Á. López-Valverde, G. Perron, and G. Stiller, 2003, “Non-LTE studies for the validation of MIPAS/Envisat L2 products”, Proc. Envisat Validation Workshop, ESA SP-531, Noordwijk, 2003, oral presentation.

M. López-Puertas, T. von Clarmann, H. Fischer, B. Funke, M. García-Comas, S. Gil-López, N. Glatthor, U. Grabowski, M. Höpfner, S. Kellmann, M. Kiefer, A. Linden, M.A. López-Valverde, G. Mengistu Tsidu, M. Milz, T. Steck, G.P. Stiller and D.Y. Wang, 2003, “Sondeo remoto de la atmosfera con el interferometro MIPAS/ENVISAT: I Descripcion general y medidas de presion y temperatura,” *X Congreso Nacional de Teledeteccion*, Cçceres, Spain, September 2003, oral presentation.

M. López-Puertas, T. von Clarmann, H. Fischer, B. Funke, M. García-Comas, S. Gil-López, N. Glatthor, U. Grabowski, M. Höpfner, S. Kellmann, M. Kiefer, A. Linden, M. Á. López-Valverde, G. Mengistu Tsidu, M. Milz, T. Steck, G. P. Stiller, and D. Y. Wang, 2003, “A survey of the non–LTE atmospheric emissions as measured by MIPAS/Envisat.” poster presentation at *EGS–AGU–EUG Joint Assembly*, Nice, France, 6–11 April 2003, oral presentation.

M. López-Puertas, T. von Clarmann, H. Fischer, B. Funke, M. García-Comas, S. Gil-López, N. Glatthor, U. Grabowski, M. Höpfner, S. Kellmann, M. Kiefer, A. Linden, M. Á. López-Valverde, G. Mengistu Tsidu, M. Milz, T. Steck, G. P. Stiller, and D. Y. Wang, 2003, “The temperature and CO_2 abundance of the mesosphere and lower thermosphere as measured by MIPAS/Envisat.” *EGS–AGU–EUG Joint Assembly*, Nice, France, 6–11 April 2003, poster.

F. J. Martín-Torres, T. von Clarmann, B. Funke, G. P. Stiller, and M. López-Puertas, 2001, “Prospects for retrieval of O_3 and non-LTE parameters from MIPAS/ENVISAT spectra.” *26th General Assembly of the European Geophysical Society*, Nice, France, 25-30 March 2001, poster.

F. J. Martín-Torres, B. Funke, and M. López-Puertas, 2001, “Non-LTE calculations of the OH vibrational and rotational populations and implications for detection of OH Meinel bands from MIPAS/ENVISAT spectra.” *26th General Assembly of the European Geophysical Society*, Nice, France, 25-30 March 2001, oral presentation.

G. Mengistu Tsidu, T. von Clarmann, H. Fischer, B. Funke, N. Glatthor, U. Grabowski, M. Höpfner, S. Kellmann, M. Kiefer, A. Linden, M. López-Puertas, M. Milz, T. Steck, G. P. Stiller, and D. Y. Wang, 2003, ”NO_y from MIPAS/ENVISAT in the South Hemisphere vortex split-up event in September/October 2002.” *EGS–AGU–EUG Joint Assem-*

bly, Nice, France, 6–11 April 2003, poster.

M. Milz, M. Höpfner, T. von Clarmann, U. Grabowski, T. Steck, G. P. Stiller, and H. Fischer, 2002, "Measurements of water vapor and ice clouds in the tropical UT/LS region with MIPAS/ENVISAT." COSPAR, Houston, Texas, USA, 11-19 October 2002, oral presentation.

V.H. Payne, V.L. Jay and A. Dudhia, 2002, "Retrieval of CFC-12 from the MIPAS Satellite Instrument," *ERCA School*, Grenoble, France, January 2002.

F. Schreier, "The AMIL2DA Forward Model Intercomarison", oral presentation at the *Fourth International Radiative Transfer Modelling Workshop*, Bredbeck, Germany, 8-11 July 2002, poster.

F. Schreier and U. Boettger, 2002, "The Line-by-Line Infrared Atmospheric Radiation Code MIRART: Numerical and Computational Aspects," *ASA 2002 - Atmospheric Spectroscopy Application*, Moscow, August 2002, oral presentation.

T. Steck, T. von Clarmann, U. Grabowski, and M. Höpfner, 2002, "2D-retrieval for MIPAS-ENVISAT." *27th General Assembly of the European Geophysical Society*, Nice, France, 21-26 April 2002, poster.

T. Steck, T. von Clarmann, H. Fischer, B. Funke, U. Grabowski, M. Höpfner, S. Kellmann, M. Kiefer, A. Linden, M. Milz, G. P. Stiller, and D. Y. Wang, 2003, "2D-retrieval approach applied to MIPAS/ENVISAT data." *EGS–AGU–EUG Joint Assembly*, Nice, France, 6–11 April 2003, poster.

G. P. Stiller, N. Glatthor, S. Kellmann, E. Kimmich, A. Linden, M. Milz, and F. Rohrer, 2001, "Retrievability of upper tropospheric species from MIPAS/ENVISAT and their use in atmospheric modeling." *26th General Assembly of the European Geophysical Society*, Nice, France, 25-30 March 2001, oral presentation.

G. P. Stiller, T. Steck, M. Milz, T. von Clarmann, U. Grabowski, and H. Fischer, 2002, "Cross-validation of MIPAS and CHAMP temperature and water vapour profiles."*1st CHAMP Science Meeting*, Potsdam, Germany, 22-25 January 2002, poster.

G. P. Stiller, M. Höpfner, S. Kellmann, M. Milz, T. Steck, and H. Fischer, 2002, "Retrievability of upper tropospheric species and parameters from MIPAS/ENVISAT data." *EUROTRAC-2 Symposium*, Garmisch-Partenkirchen, Germany, 11–15 March 2002, poster.

G. Stiller, T. von Clarmann, N. Glatthor, U. Grabowski, M. Höpfner, M. Kiefer, and T. Steck, 2002, "SACADA: Synoptic Analysis of Chemical constituents by Advanced Data Assimilation – Cross–Validation of non–operational MIPAS and SCIAMACHY data and assimilated data products." *AFO 2000 Statusseminar 2002*, Schliersee, Ger-

many, poster.

G. P. Stiller, T. von Clarmann, H. Fischer, B. Funke, N. Glatthor, U. Grabowski, M. Höpfner, S. Kellmann, M. Kiefer, A. Linden, G. Mengistu Tsidu, M. Milz, T. Steck, and D. Y. Wang, 2003, "Retrievals of trace species in the UT/LS region from MIPAS/ENVISAT." *EGS–AGU–EUG Joint Assembly*, Nice, France, 6–11 April 2003, poster.

D. Y. Wang, T. von Clarmann, H. Fischer, B. Funke, M. García-Comas, S. Gil-López, N. Glatthor, U. Grabowski, M. Höpfner, S. Kellmann, M. Kiefer, A. Linden, M. López-Puertas, M. Á. López-Valverde, G. Mengistu Tsidu, M. Milz, T. Steck, and G. P. Stiller, 2003, "Longitudinal variations of stratospheric temperature and ozone profiles observed by MIPAS in the southern hemisphere in late september, 2002." *EGS–AGU–EUG Joint Assembly*, Nice, France, 6–11 April 2003, poster.

D. Y. Wang, T. von Clarmann, H. Fischer, B. Funke, M. García-Comas, S. Gil-López, N. Glatthor, U. Grabowski, M. Höpfner, S. Kellmann, M. Kiefer, A. Linden, M. López-Puertas, M. Á. López-Valverde, G. Mengistu Tsidu, M. Milz, T. Steck, and G. P. Stiller, 2003,"Preliminary comparisons of temperature and ozone profiles measured by MIPAS and HALOE."*EGS–AGU–EUG Joint Assembly*, Nice, France, 6–11 April 2003, poster.

Chapter 3

Detailed Report

WP 5000: Application to MIPAS data

WP 5000: Objectives

After successful validation of processors on the basis of synthetic data, the robustness of the processors should be demonstrated by application to real MIPAS data. Furthermore, contributions to the characterization of the MIPAS instrument and level 1 data (calibrated radiance spectra) should be made.

WP 5000: Methodology and scientific achievements

The retrieval processors of the participants were used to analyze some sample MIPAS measurements. This revealed some further suboptimal parameter settings of some of the processors and helped to detect some unexpected characteristics in the MIPAS radiance spectra. Details and supporting activities are discussed in details under the relevant sub-WPs.

WP 5000: Socio-economic relevance and policy implication

After this final step of processor validation, the European scientific community is ready to use their processors for science application, since the characteristics of the processors are well understood, and the characteristics of MIPAS radiance spectra and ancillary data are reasonably well understood. This allows the European MIPAS community to make valuable and timely contributions to atmospheric sciences. This strengthens the position of European research in worldwide competition. This also is advantageous for European space and remote sensing industry, because it proves the appropriateness of the technical concept behind the experiment and the quality of related engeneering.

The ability of the European Earth observation community to sciantifically analyse MIPAS radiance spectra allows to make major contributions to the research fields of ozone destruction, global change, and atmospheric pollution.

WP 5000: Discussion and conclusion

Retrieval processors developed and validated under AMIL2DA have been well characterized and are well understood such that they can now be applied to scientific analysis of MIPAS spectra. The MIPAS instrument, radiance spectra and ancillary data are reasonably well understood, such that they can be used by experts for scientific purposes already. Further aspects are discussed under related sub-workpackages.

WP 5000: Plan and objectives for the next period

Not applicable.

WP 5000: Deviation from the work plan

Due to delay of Envisat launch and subsequent delay of level-1 data delivery by ESA, rescheduling of the project has become necessary. However, thanks to tremendous effort of involved scientists, all workpackages could be finished in time.

WP 5100: Agreement on a common data set

WP 5100: Objectives

Since some of the processors of participating groups have not been designed for analysis of large data sets, a representative subset of MIPAS data had to be defined for intercomparison purposes.

WP 5100: Methodology and scientific achievements

Data set specification: MIPAS data of the orbits 504, 2081, 2082, and 2083 have been made available to the consortium. For a more detailed intercomparison, limb scans 3, 12, 20, 36, and 68 of orbit 2081 were selected. The selected scans contain no or low clouds and comprise the atmospheric states of polar summer (scan 3), polar winter (36), midlatitude day/night (12/68), and equatorial (20).

The outcoming data of WP 5100 is Deliverable D43.

WP 5100: Socio-economic relevance and policy implication

As for WP 4000.

WP 5100: Discussion and conclusion

MIPAS data of the orbits 2081, 2082, and 2083 have been used for retrieval intercomparison. A subset of these data has been defined. However, due to ambiguous counting convention in ESA data, not all participants have analysed the same data. Re-analysis of data has been performed by some participants after double-checking that all participants use the same data set.

WP 5100: Plan and objectives for the next period

Not applicable.

WP 5100: Deviation from the work plan

As for WP 5000.

WP 5200: Retrieval calculations

WP 5200: Objectives

In order to prove the robustness of their codes, IMK. Oxford University, DLR, IFAC and RAL should apply their processors to real MIPAS data as specified in WP 5100.

WP 5200: Methodology and scientific achievements

For intercomparison, profiles of temperature, H_2O, O_3, HNO_3, NO_2, CH_4 and N_2O were retrieved by the participants. Beyond this, some groups (IMK, OU, DLR) have included a considerable number of non-key species (CFC-11, CFC-12, $ClONO_2$ and N_2O_5; also investigations on retrievals of SO_2, SF_6, OCS and NH_3). Details are reported under the sub-workpackages. Several retrieval calculations had to be repeated due to ambiguous counting convention in ESA data.

WP 5200: Socio-economic relevance and policy implication

As for WP 5000.

WP 5200: Discussion and conclusion

After some final upgrades of parameter settings, all processors proved robust when applied to real MIPAS data.

WP 5200: Plan and objectives for the next period

Not applicable.

WP 5200: Deviation from the work plan

As for WP 5000.

WP 5210: Retrieval calculations, IMK

WP 5210: Objectives

In order to prove the robustness of the IMK code when applied to real MIPAS data, this processor should be applied to real MIPAS data as specified in WP 5100.

WP 5210: Methodology and scientific achievements

At IMK retrievals of the following species were performed: O_3, H_2O, HNO_3, CH_4, N_2O, NO_2, OCS, ClO, SF_6, C_2H_6, H_2O_2, $ClONO_2$, N_2O_5, NH_3, CCl_4, HOCl, CFC-11, CFC-22, HCFC-22. Results for most species are considered realistic. Beside this, at IAA, who now operate the same processor in close co-operation with IMK, O_3, NO, NO_2, CO, pressure and temperature, under consideration of non-LTE have been retrieved. The outcoming data of WP 5210 is Deliverable D45.

WP 5210: Socio-economic relevance and policy implication

As for WP 5000.

WP 5210: Discussion and conclusion

After minor upgrading with respect to frequency calibration correction, the IMK processor proves to be robust when applied to real MIPAS data. Remaining problems hint rather at irregularities in MIPAS data than inappropriate processing.

WP 5210: Plan and objectives for the next period

Not applicable.

WP 5210: Deviation from the work plan

As for WP 5000.

WP 5220: Retrieval calculations, Oxford University

WP 5220: Objectives

In order to prove the robustness of the Oxford University code when applied to real MIPAS data, this processor should be applied to real MIPAS data as specified in WP 5100.

WP 5220: Methodology and scientific achievements

To process 'real' MIPAS L1B data a prepreocessor was developed to apodise the L1B spectra, extract microwindows and construct the AILS appropriate to each microwindow.

It was also necessary to convert OPTIMO from a single profile retrieval to a sequential retrieval, and write scripts so that a complete orbit could be processed. Further code optimisations were also made to reduce CPU time.

The validation effort has mostly focussed on orbit 2081 (24Jul02), for which Level 1 data was supplied by ESTEC.

Experience with real data has identified a problem with ESA's handling of the non-linearity correction on forward and backward interferometer sweeps during L1 processing, and has been used to provide feedback to ESA for subsequent improvements.

Residuals have also shown similar spectral shift characteristics to the initial ESA retrievals. This, and comparison with preprocessor outputs with the Italian groups, has verified that the problem is with the AILS characterisation. Retrievals for the following species have been attempted: O_3, H_2O, HNO_3, CH_4, N_2O, NO_2, N_2O_5, $ClONO_2$, CFC-11, CFC-12, CFC-14, CFC-22, NH3, HCN, COF_2, OCS, SF_6, C_2H_6, HOCl, SO_2, H_2O_2, ClO and CCl_4. Particular effort has been applied to retrieving SO_2 to detect enhancement in the region of Mt Etna. The outcoming data of WP 5220 is Deliverable D46.

Additional studies have been performed on the feasibility of retrieving isotopic ratios, CO2 concentrations and joint CO volume mixing ratio and vibrational temperature profiles.

WP 5220: Socio-economic relevance and policy implication

As for WP 5000.

WP 5220: Discussion and conclusion

Retrievals were successful for the key species, CFC-11, CFC-12 and ClONO2. Results for HCN, OCS, N2O5, NH3, SF6 and SO2 were of marginal quality and further work is required on these. Other species and improved retrieval algorithms will be investigated

outside the AMIL2DA project.

The construction of a parallel preprocessor and L2 retrieval has allowed feedback to be provided to ESA as part of the MIPAS Cal/Val activities.

WP 5220: Plan and objectives for the next period

Not applicable.

WP 5220: Deviation from the work plan

As for WP 5000.

WP 5230: Retrieval calculations, DLR

WP 5230: Objectives

In order to prove the robustness of the DLR codes when applied to real MIPAS data, both the DLR-a and the DPAC processors should be applied to real MIPAS data as specified in WP 5100.

WP 5230: Methodology and scientific achievements

The following species were retrieved at DLR:

DLR-a provided retritvals of O_3, H_2O, HNO_3, CH_4, N_2O and NO_2

The **D-PAC** processor was used for the retrieval of the following profiles: temperature, pressure, line-of-sight, continuum, H_2O, O_3, NO_2, CH_4, N_2O as well as CFC-11 and CFC-12. Profiles of instrumental offsets had been tested earlier during the retrieval of balloon data. As for Envisat data, these offset profiles are not needed.

The outcoming data of WP 5230 is Deliverable D47.

WP 5230: Socio-economic relevance and policy implication

As for WP 5000.

WP 5230: Discussion and conclusion

DLR-a: The DLR-a processor gives accurate results when applied to real MIPAS data. Deviations from other results are due to the use of altitude independent microwindows. Furthermore temperature and molecular concentration retrievals were performed with a climatological pressure profile, i.e., without line-of-sight retrieval.

D-PAC: The comparison of results turned out to be highly important for the precise identification of weak points. The implementation of robust routines could only be accomplished by comparisons on a species by species basis to separate conceptual weaknesses from species-dependent and parameter selection characteristics.

WP 5230: Plan and objectives for the next period

Not applicable.

WP 5230: Deviation from the work plan

As for WP 5000.

WP 5240: Retrieval calculations, IFAC

WP 5240: Objectives

In order to prove the robustness of the IFAC code when applied to real MIPAS data, this processor was applied to real MIPAS data as specified in WP 5100.

WP 5240: Methodology and scientific achievements

The following species have been retrieved with the IFAC processor: pT, H_2O, O_3, HNO_3, CH_4, N_2O, NO_2, CFC-11, $ClONO_2$. The outcoming data of WP 5240 is Deliverable D48.

WP 5240: Socio-economic relevance and policy implication

As for WP 5000.

WP 5240: Discussion and conclusion

For the retrieval of the above species from real MIPAS data it was necessary to tune several processing setup parameters. In particular, significant performance improvements were obtained with the optimization of the convergence criteria and of the parameters controlling the evolution of the Levenberg-Marquardt damping during the retrieval iterations. With the optimized setup parameters the IFAC processor is able to reach convergence in all the considered measurement scenarios.

WP 5240: Plan and objectives for the next period

Not applicable.

WP 5240: Deviation from the work plan

As for WP 5000.

WP 5250: Retrieval calculations, RAL

WP 5250: Objectives

In order to prove the robustness of the RAL code when applied to real MIPAS data, this processor should be applied to real MIPAS data as specified in WP 5100.

WP 5250: Methodology and scientific achievements

The work at RAL was aimed at retrieving accurate H_2O and O_3 profiles from real MIPAS data, with special emphasis on the lower scan altitudes. MIPAS data acquistion and interface of the retrieval software to the MIPAS data structures were required.

Work was carried out to acquire and handle MIPAS data, including the production of code for data reading. Auxiliary data, including ECMWF meteorological analyses and MIPAS Climatology files were acquired and handling software developed.

The driver files for the forward model were upgraded to allow explicit specification of view, scan number, spectral microwindow. This allows simple specification of forward model parameters for multiple runs including spectral ranges and satellite position. The retrieval model was enhanced to make use of the new forward model options. Measurement details such as scan number, view are can now be taken from the measurement file directly. The outcoming data of WP 5250 is Deliverable D49.

WP 5250: Socio-economic relevance and policy implication

As for WP 5000.

WP 5250: Discussion and conclusion

The basic implementation of the RAL processor and its interface with MIPAS and auxiliary data operated correctly. However, a number of further refinements were shown to be desirable in terms of efficiency and the handling of data artifacts.

WP 5250: Plan and objectives for the next period

Not applicable.

WP 5250: Deviation from the work plan

As for WP 5000.

5300 Comparison of results

WP 5300: Objectives

In order to assess the reliability of results, retrieved profiles were to be intercompared for a subset of the species.

WP 5300: Methodology and scientific achievements

Retrieved vertical profiles of temperature and volume mixing ratios of key species O_3, H_2O, CH_4, N_2O, HNO_3, and N_2O as well as minor species as retrieved by the participants are intercompared, in order to better characterize the different retrieval approaches and to verify the applicability of the data processors to the use of real measurement data. Due to the fact that not all groups are able to process entire orbits and in order to concentrate the intercomparison on a significant data set, the scan numbers 3, 12, 20, 36, and 68 of orbit 2081 were selected for detailed intercomparison (see WP 5100).

The report on WP 5300 is Deliverable D51.

WP 5300: Socio-economic relevance and policy implication

As for WP 5000

WP 5300: Discussion and conclusion

The ozone results of the different groups agree well, with a few exceptions. The original IMK-RCP result suffered from wrong spectral shift assumptions. When using the retrieved spectral shift the lower values at 60 hPa and higher values at 20 hPa vanish and the IMK-RCP ozone result is much closer to the result of the other groups. The D–PAC (and less pronounced the DLR-a) result seems to underestimate ozone between 1 and 10 hPa. The standard deviations of the profiles for the different scans show values of up to 1 ppmv in the maximum of the ozone profil. This is slightly more than expected from the blind test experiment but consistent with estimated total errors.

For methane results below 30 hPa, the D–PAC values are 0.2 ppmv lower than the corresponding values of the other groups. Small oscillations can be seen in the ORM (IFAC) result and larger oscillations in the OPTIMO (Oxford) result. However, these oscillations and differences are widely consistent with the differences obtained in the blind test experiment.

In summary it can be stated that all investigated processors are able to retrieve atmospheric state parameters from MIPAS-Envisat data within explainable differences. For selected scans of orbit 2081 a detailed intercomparison is performed and in general good agreement between the results of the different groups is achieved. This is especially the

case for conditions where unexpected large systematic error sources are not present.

There are some cases where larger discrepancies between the groups have been detected: The strength of the regularization and hence the degrees of freedom plays an important role in the explanation for the differences in the results. Especially OPTIMO (Oxford) and RET2D (RAL) results tend towards stronger oscillations. In contrast to that, DLR-a (all constituents) and D–PAC (mainly temperature) tend to overconstrain their retrievals. D–PAC has already investigated this problem and will change it for future retrievals. The original IMK-RCP results for temperature and ozone were affected by a spectral calibration errors. Therefore spectral shift retrieval is performed now as a basic step ahead of the temperature, line of sight and constituent retrievals.

For water vapor, the greatest discrepancies occur at the lowest and highest altitudes. In the UTLS region water vapor is known to be highly variable and further investigation will be required to discriminate between retrieval sensitivity and artifacts. At high altitudes the error is driven by systematic errors due to non-LTE.

The largest spread in retrieved temperatures occur in the polar winter case (scan 36). It is very likely that systematic errors, especially horizontal temperature inhomogeneities, are responsible for the larger differences in the results of the different groups. This is the case not just in the temperature retrievals but also for the gases. Most of the groups soon will have 2-dimensional or tomographic retrieval algorithms available so that discrepancies due to horizontal inhomogeneities can be investigated in more detail.

A further aspect, detected by the Oxford group, is a systematic difference in calibration between forward and backward recorded spectra of channel A. The reason for the difference is the nonlinearity correction, which is part of the European Space Agency's level-1 processing chain. This systematic error term could also be a reason for oscillations in the retrieval results. However, a slightly stronger regularization reduces systematic errors, mitigates this effect and can therefore be of advantage.

WP 5300: Plan and objectives for the next period

Not applicable.

WP 5300: Deviation from the work plan

As for WP 5000.

5400 Fixing of problems

WP 5400: Objectives

In order to make retrieval processors better applicable to real MIPAS measurements, some final upgrading was foreseen under this WP.

WP 5400: Methodology and scientific achievements

See WPs 5410–5450

WP 5400: Socio-economic relevance and policy implication

As for WP 5000.

WP 5400: Discussion and conclusion

See WPs 5410–5450

WP 5400: Plan and objectives for the next period

Not applicable.

WP 5400: Deviation from the work plan

As for WP 5000.

5410 Fixing of problems, IMK

WP 5410: Objectives

In order to make the IMK retrieval processor better applicable to real MIPAS measurements, some final upgrading was to be performed.

WP 5410: Methodology and scientific achievements

The following upgrades were performed:

- The altitude dependence of regularization has been slightly changed.
- The use of ILS parameters has been improved: Now the frequency calibration correction is retrieved for each spectrum individually.
- Some microwindow selections have been revised, in particular for non-key species.
- Possible reasons for high biases in retrievals from (nominally cloud-free) spectra recorded at lowermost tangent altitudes have been investigated. Field-of-view problems, problems due to non-linearity, problems with water vapour mixing ratios and temperature profiles are likely to be excluded. Problems can easily be solved by just excluding lowermost tangent altitude from the retrieval but this is not the favored approach.

The outcoming method of WP 5410 is Deliverable D53.

WP 5410: Socio-economic relevance and policy implication

As for WP 5000.

WP 5410: Discussion and conclusion

After final upgrading of some processing parameters, the IMK processor is reliable and produces scientifically valuable results. Remaining problems are most probably due to problems in the MIPAS data rather than in the processor.

WP 5410: Plan and objectives for the next period

Not applicable.

WP 5410: Deviation from the work plan

As for WP 5000.

5420 Fixing of problems, Oxford University

WP 5420: Objectives

Upgrading of Oxford code and retrieval algorithm in order to address problems encountered processing real data and in the AMIL2DA intercomparison of results.

WP 5420: Methodology and scientific achievements

There has been some iteration with ESA who have generated different versions of Orbit 2081 L1B spectra in response to feedback on data quality. From the point of view of the Oxford processor, validation has concentrated on comparing retrievals for this particular orbit with the ESA L2 product and with the 5 profiles selected for AMIL2DA comparisons.

The main problem identified was a tendency for the Oxford retrieved profiles to oscillate with altitude (not only due to the ESA non-linearity correction, although this appeared to determine the phase of the oscillation). This was due to an intrinsic instability due to loose a priori constraints. The problem was solved by adding more regularisation via correlations in the a priori covariance matrix.

A second problem has been the sensitivity to cloud. The solution currently applied is to change the a priori continuum profile from zero to a large value when clouds are detected in the Level 1B spectrum, effectively forcing the first guess atmosphere to be optically thick and preventing any species retrieval at those tangent altitudes. Other solutions, such as removing the Level 1 data completely, may prove more robust. The outcoming method of WP 5420 is Deliverable D54.

WP 5420: Socio-economic relevance and policy implication

As for WP 5000.

WP 5420: Discussion and conclusion

Problems with the OPTIMO algorithm have been identified and solutions found. For certain species with low signal it will be necessary to modify the retrieval or preprocessing algorithm in order to average data, trading horizontal resolution for precision. This, and other developments of the Oxford processor are expected to continue beyond the end of AMIL2DA as part of other projects.

WP 5420: Plan and objectives for the next period

Not applicable.

WP 5420: Deviation from the work plan

As for WP 5000.

5430 Fixing of problems, DLR

WP 5430: Objectives

In order to make the DLR retrieval processors better applicable to real MIPAS measurements, some final upgrading was to be performed.

WP 5430: Methodology and scientific achievements

DLR-a retrieval code has been upgraded to work with analytical derivatives now available from the MIRART forward model. Furthermore a multi–parameter regularization method relying on an a posteriori criterion for selection of the weighting factors corresponding to each atmospheric parameter was implemented. Retrievals have been repeated using pressure data derived with the IMK code. Work on implementing line-of-sight retrieval is in progress.

For the D-PAC retrieval code, regularization parameters have been modified, and the subroutine for the continuum profile handling has been upgraded.

For the D-PAC processor, an improved method for retrieving profiles with bad initial pointing data has been designed and tested. Basically, improved line of sight data were generated within a single forward run to obtain a more consistent set of initial guess pointing and temperature data. Then these improved initial guess data were used within a standard retrieval sequence. Further, pure Tikhonov retrievals (instead of optimal estimation methods) were tested to exclude any potential artifacts introduced by a priori assumptions. Based on this, alternative joint and quasi-parallel retrieval techniques were compared to improve the retrieval of H_2O. The outcoming method of WP 5430 is Deliverable D55.

WP 5430: Socio-economic relevance and policy implication

As for WP 5000

WP 5430: Discussion and conclusion

Except for minor problems due to the use of climatological pressure profiles the DLR-a processor proved to be applicable to level 1–2 processing of real MIPAS data. After successful implementation of line–of–sight retrievals (soon to be completed) the DLR-a forward model and retrieval code will provide a reliable and sophisticated tool for scientific analysis of limb sounding observations, nb. MIPAS.

The successful implementation of problem fixes in the D-PAC processor showed that previously existing discrepancies have disappeared and robust retrievals can be performed with the processors. Further improvements are expected together with updated spectroscopy data.

WP 5430: Plan and objectives for the next period

Not applicable.

WP 5430: Deviation from the work plan

As for WP 5000.

5440 Fixing of problems, IFAC

WP 5440: Objectives

In order to make the IFAC retrieval processor better applicable to real MIPAS measurements, some final upgrading was to be performed.

WP 5440: Methodology and scientific achievements

In order to make the IFAC retrieval processor applicable to real MIPAS measurements it was necessary to build a pre-processing tool which is able to extract from ESA's Level 1b products the measured spectra and a set of auxiliary data required for the retrieval (e.g. pointing information, ILS definition, noise level, etc.). Furthermore, in order to be able to process real MIPAS data it was necessary to optimize several setup parameters characterizing the behavior of the retrieval procedure. The outcoming method of WP 5440 is Deliverable D56.

WP 5440: Socio-economic relevance and policy implication

As for WP 5000.

WP 5440: Discussion and conclusion

After the development of the pre-processing tool outlined above and the optimization of some setup parameters, the IFAC processor is able to successfully retrieve atmospheric profiles from real MIPAS measurements.

WP 5440: Plan and objectives for the next period

Not applicable.

WP 5440: Deviation from the work plan

As for WP 5000.

5450 Fixing of problems, RAL

WP 5450: Objectives

In order to make the IFAC retrieval processor better applicable to real MIPAS measurements, some final upgrading was to be performed.

WP 5450: Methodology and scientific achievements

The forward model was enhanced to allow generation and re-use of absorption coefficient files. These store absorption coefficients and associated derivatives and their use has produced a significant decrease in calculation time for real, iterative retrieval calculations.

The code can now also be run in a mode which scales the retrieved products to allow for widely differing values of weighting functions. This is particularly relevant for retrieval of instrument parameters in conjunction with mixing ratio profiles where values may differ by many orders of magnitude. The outcoming method of WP 5450 is Deliverable D57.

WP 5450: Socio-economic relevance and policy implication

As for WP 5000.

WP 5450: Discussion and conclusion

With the improvements indicated the RAL processor is able to produce scientifically valuable results. Remaining problems probably indicate artifacts in the current version of the MIPAS data rather than issues with processor.

WP 5450: Plan and objectives for the next period

Not applicable.

WP 5450: Deviation from the work plan

As for WP 5000.

5500 Analysis of residuals w.r.t. particular problems

WP 5500: Objectives

Often residuals (measured minus calculated spectra) carry information on either sub-optimal parameter settings of the retrieval code or on instrument malfunction. Systematic analysis of residuals should help to detect some problems.

WP 5500: Methodology and scientific achievements

Residual and Error Correlation (REC) Analysis has been developed under this project as a retrieval diagnostic tool. It provides a useful statistical tool for correlating the large amount of information contained in the residual spectra from retrievals with expected signatures from known error terms, such as instrument calibration problems or missing/incorrectly modelled contaminant gases. The analysis of Non-LTE from the residuals spectra suggests than Non-LTE is, in general, in accordance with predictions except for two cases, the NO_2, for which NLTE is much smaller than anticipated, and for CH_4, which seems to be larger than predicted by a factor of 2.

WP 5500: Socio-economic relevance and policy implication

As for WP 5000.

WP 5500: Discussion and conclusion

The REC analysis is particularly suited to large volumes of data which produce statistically significant features in the average residuals, although it has also been applied to the relatively small datasets generated by the different groups for this project.

Particular problems identified in the ESA retrieval, and consequently many of those in the AMIL2DA project which make use of similar L1B and auxiliary data, are

1. Spectral shift $\pm$ 0.001 cm^{-1}, varying linearly across the MIPAS spectrum, also varying with altitude.

2. The apodized instrument line shape is too wide by a few percent.

3. Problems in radiometric gain in early L1B data.

4. Poor characterisation of atmospheric NH_3 and COF_2 climatology.

5. Significant improvement in ESA data after November algorithm/setting modifications

The REC analysis has proved a useful tool for quick error diagnosis and will now be incorporated in ESA's routine MIPAS monitoring activities.

IFAC analysis condirmed item 1. They found that the spectral shift detected by the residual error correlation analysis and by their analysis carried-out in WP 6000 is visually detectable on spectral residuals averaged over a whole orbit of measurements.

Beyond this, IMK found that often their retrievals at lower altitudes are, due to H_2O lines, not properly caught in the fits. Thorough description of H_2O lines either by simultaneous retrieval or by proper use of volume mixing ratio information retrieved in a prior step is recommended. Further details are discussed under WPs 5510–5560
The behaviour of the retrieval processors w.r.t. fit residuals is understood. Some unexpected features were detected in the calibrated measured radiance spectra.

WP 5500: Plan and objectives for the next period

Not applicable.

WP 5500: Deviation from the work plan

As for WP 5000.

5510 Non-LTE effects

WP 5510: Objectives

Modelling of non-local thermodynamic equilibrium within the radiative transfer calculations causes additional effort and thus is avoided in the routine data analysis by selection of spectral microwindows which are free of non-LTE, or, where non-LTE is at least not the predominant error source. However, this pre-flight assessment of non-LTE relies on climatological vibrational temperatures, which may not be appropriate for the actual atmospheric condition. Therefore, possible non-LTE effects not appropriately considered in the level-2 processing should be detected by analysis of the fit residuals.

WP 5510: Methodology and scientific achievements

First, the residuals of the retrievals have been analysed also with respect to non-LTE by using the REC analysis carried out by Oxford University. The residuals spectra were correlated to the NLTE-LTE differences spectra to find NLTE effects in real data. The results are described in Deliverables D59, D60, D61, D62.

Beyond this, non-LTE retrievals have been carried out at IAA. In these cases the non-LTE populations, e.g. vibrational temperatures, were computed for the actual retrieved pressure-temperature and species abundances retrieved directly from the spectra. The NLTE retrievals were carried out for the major operational products, eg, p-T, ozone, water vapour, methane and NO_2. In these retrievals (except for NO_2) the current information (e.g., prior to MIPAS measurements) was included. In case of NO_2, a previous retrieval of non-LTE parameters (carried out under another project), was included. The report on WP 5510 are Deliverables D59, D60, D61, D62 and D70. subsection*WP 5510: Socio-economic relevance and policy implication As for WP 5000.

WP 5510: Discussion and conclusion

The analysis of NLTE from the residuals spectra suggests than NLTE is, in general, in accordance with predictions except for two cases, the NO_2, for which NLTE is much smaller than anticipated, and for CH_4, which seems to be larger than predicted by a factor of 2.

The main conclusions on the NLTE retrievals are detailed in WP 5511 below.

The comparison between MIPAS O_3 and NO_2 with those measured by GOMOS and SCIAMACHY shows that NLTE-LTE retrieved MIPAS abundance differences were much smaller than the differences between the abundances measured by MIPAS and the other instruments. NLTE was found then not to be the likely candidate that could explain the found MIPAS/GOMOS and MIPAS/SCIAMACHY differences.

The analysis of NLTE in the day/night spectra show, in general, the major expected NLTE features. Exceptions are NO_2, for which the NLTE effects seem to be significantly smaller than predicted, and CH_4, for which NLTE seems to be larger than theoretically predicted. Furthermore, this analysis have also revealed the existence of many first detected NLTE emissions, as well as more clear and nitty determinations of some previously detected NLTE features. These new detected emissions, however, do not affect the retrievals of most species, since they are located out of the microwindows normally used for the species retrievals.

WP 5510: Plan and objectives for the next period

Not applicable.

WP 5510: Deviation from the work plan

Retrievals under consideration of non-LTE is a more complete and comprehensive way of analysing non-LTE than just to analyse the residuals. This approach of higher sophistication had not been foreseen at the beginning of the study since it was not clear if the tools necessary for this task would be available in time.

For scheduling issues, the same deviations apply which were mentioned under WP 5000.

5511 Non-LTE effects: MIPAS data

WP 5511: Objectives

Analysis of MIPAS best fit residuals should help to detect possible inappropriate treatment of non-LTE in the processors.

WP 5511: Methodology and scientific achievements

Beyond the REC analysis of residuals, which includes the assessment of non-LTE, non-LTE effects were analysed by the superior method of carrying out retrievals under consideration of non-LTE. The report on WP 5511 is Deliverable D60.

WP 5511: Socio-economic relevance and policy implication

As for WP 5000.

WP 5511: Discussion and conclusion

The analysis of non-LTE from the residuals spectra suggests than non-LTE is, in general, in accordance with predictions except for two cases, the NO_2, for which non-LTE is much smaller than anticipated, and for CH_4, which seems to be larger than predicted by a factor of 2.

The main conclusions on the NLTE retrievals are:

- Non-LTE retrievals for temperature, O_3, H_2O and CH_4 for orbit #2081 show that non-LTE errors are small below about 50 km. There can be however, significant errors (underpredictions) for considering LTE in the retrievals of temperature for polar-winter like atmospheric conditions (cold stratopause and warm lower mesosphere) above about 50 km.

- The non-LTE retrievals in O_3 show that non-LTE effects are small ($\leq$5%) below 50 km but can be significant (5–15%) between 50 and 60 km, particularly in the daytime and polar winter conditions.

- The non-LTE retrievals for H_2O show that non-LTE is negligible below about 55 km, but can be significant above, in the daytime and polar winter conditions, reaching differences of up to –30% at 60 km. They can also induce differences of about –10% at 20-35 km at daytime.

- Non-LTE in CH_4 is negligible except above 50 km at daytime, where they can induce errors of about –15%. The residual analysis and the upper atmosphere measurements suggest that they might be even larger.

- The non-LTE chemical excitation rate of NO_2 seems to be significantly smaller than predicted (at least a factor of 10 smaller). Non-LTE retrievals in NO_2 show that non-LTE effects are small ($\leq$5%) below $\sim$50 km but can be large (50%) between 50 and 60 km when we have a warm lower mesosphere, e.g., at polar winter conditions.
- Non-LTE effects are sometimes linked with the *a priori* profiles and the number of measurements (altitudes) included in the retrieval. Care should be taken to distinguish direct non-LTE effects from those induced by using different *a priori* profiles and the number of measurements (altitudes) included in the retrieval.

WP 5511: Plan and objectives for the next period

Not applicable.

WP 5511: Deviation from the work plan

As for WP 5000 and 5510.

5512 Non-LTE effects: GOMOS, SCIAMACHY

WP 5512: Objectives

While MIPAS measurements are affected by non-LTE, GOMOS and SCIAMACHY measurements because of their different technique are considered free of non-LTE effects. Therefore, these measurements can be used to detect possible non-LTE induced retrieval errors in MIPAS retrieved profiles of atmospheric state parameters by comparison with the other Envisat instruments GOMOS and SCIAMACHY.

WP 5512: Methodology and scientific achievements

All the vertical profiles of retrieved species measured by GOMOS and SCIAMACHY, i.e., O_3 and NO_2, were compared with MIPAS. The report on WP 5512 is Deliverable D61.

WP 5512: Socio-economic relevance and policy implication

As for WP 5000.

WP 5512: Discussion and conclusion

The comparison between MIPAS O_3 and NO_2 with those measured by GOMOS and SCIAMACHY shows that non-LTE–LTE retrieved MIPAS abundance differences were much smaller than the differences between the abundances measured by MIPAS and the other instruments. Non-LTE was found then not to be the likely candidate that could explain the found MIPAS/GOMOS and MIPAS/SCIAMACHY differences.

WP 5512: Plan and objectives for the next period

Not applicable.

WP 5512: Deviation from the work plan

Unfortunately, only a very limited number of profiles was available from the GOMOS and SCIAMACHY instruments.

For scheduling issues, the same deviations apply which were mentioned under WP 5000.

5513 Non-LTE effects: Day/night spectra

WP 5513: Objectives

Non-LTE effects in the atmosphere show remarkable diurnal changes. Therefore, comparison of daytime and nighttime MIPAS spectra should help to detect further non-LTE effects.

WP 5513: Methodology and scientific achievements

A comparison between co-added spectra at daytime and nighttime was undertaken for orbits #504 and 2081 (nominal mode) and for those taken at higher altitudes (1748-1752). Non-LTE effects were analysed for most of the bands of the atmospheric species, including CO_2, O_3, H_2O, CH_4, NO_2, NO, CO and OH. The detailed results and figures are shown in Deliverable D62. The major conclusions are listed below.

WP 5513: Socio-economic relevance and policy implication

As for WP 5000.

WP 5513: Discussion and conclusion

The analysis of non-LTE in the day/night spectra show, in general, the major expected non-LTE features. Exceptions are NO_2, for which the non-LTE effects seem to be significantly smaller than predicted, and CH_4, for which non-LTE seems to be larger than theoretically predicted. Furthermore, this analysis have also revealed the existence of many first detected non-LTE emissions, as well as more clear and nitty determinations of some previously detected non-LTE features. These new detected emissions, however, do not affect the retrievals of most species, since they are located out of the microwindows normally used for the species retrievals.

WP 5513: Plan and objectives for the next period

Not applicable.

WP 5513: Deviation from the work plan

As for WP 5000.

5520 Spectroscopic data insufficiencies

WP 5520: Objectives

Accurate forward modelling of spectral radiances relies on reliable spectroscopic input data. All errors and deficiencies of spectroscopic data directly map onto the modeled spectra and thus also on the retrieved atmospheric state parameters. The objective of this WP was to provide complementary spectroscopic data for species and bands where such deficiencies were identified.

WP 5520: Methodology and scientific achievements

Nitric acid absolute intensities: In a previous effort (WP2600) the spectral parameters of the hot band $\nu_5 + \nu_9 - \nu_9$ (HIT24-19) were improved. However simulations of the MIPAS spectra using these data showed that there is an inconsistency between the spectral parameters of this hot band and those of the cold bands absorbing in the same spectral region, namely ν_5 (HIT18-14) and $2\nu_9$ (HIT21-14). A careful analysis, for different altitudes and sequences of the MIPAS microwindow covering the spectral domain 885.1-888.1 cm^{-1}, which contains this hot band, showed that either the hot band intensity is too weak by about 13 % or that the cold band intensities (which were those of HITRAN2K) are too large by the same amount.

In parallel new measurements of HNO_3 line intensities were recently performed at JPL [R.A. Toth, L.R. Brown and E.A. Cohen, Line strengths of nitric acid from 850 to 920 cm^{-1}, J. Mol. Spectrosc., 218, 151-168 (2003)] and Table 6.4 presents a synthesis of available intensity measurements for the 11.2 μm spectral region of HNO_3.

Several comments can be made:

- the total absorption as derived from HITRAN2K is in good agreement with the value of Giver et al.. This could be expected since the cold bands of HITRAN2K were calibrated in absolute using the Giver's value.

- the total absorption measured in ref. [5] is about 14% lower than the HITRAN2K value.

- the hot band Q-branch intensities measured during WP2600 and in [R.A. Toth, L.R. Brown and E.A. Cohen, Line strengths of nitric acid from 850 to 920 cm^{-1}, J. Mol. Spectrosc., 218, 151-168 (2003)] are in good agreement.

Then, if one assumes that the HNO_3 hot band Q-branch has been properly measured, the last two points demonstrate that the cold band intensities given in HITRAN2K are too high by about 14%, confirming what was found when analyzing the MIPAS spectra. Accordingly a new database has been generated multiplying the line intensities of the bands

Table 3.1: Comparison of measured HNO_3 intensities in the 11.2 μm spectral region

REFERENCES	TOTAL ABSORPTION	HOT BAND Q-BRANCH between 885.418 and 885.437 cm^{-1}
Goldman et al. [1]	585	
Giver et al. [2]	630	
Massie et al. [3]	483	
Hjorth et al. [4]	541	
Average	560 (10%)	
HITRAN2K	637	
Toth et al. [5]	560 (5%)	
WP2600		2.05
Toth et al. [5]		2.1

The intensities are in units of cm/atm^{-2}.

1. A. Goldman, T.G. Kyle, and F.S. Bonomo, Statistical band model parameters and integrated intensities for the 5.9 micron, and 7.5 μm, and 11.3 μm bands of HNO_3 vapour, Appl. Opt. 10, 65-73 (1971).

2. L.P. Giver, F.P.J. Valero, D. Goorvitch, and F.S. Bonomo, Nitric-acid band intensities and band-model parameters from 610 to 1760 cm^{-1}, J. Opt. Soc. Am. B1, 715-722 (1984).

3. S.T. Massie, A. Goldman, D.G. Murcray, and J.C. Gille, Approximate absorption cross sections of F12, F11, $ClONO_2$, N_2O_5, HNO_3, CCl_4, CF_4, F21, F113, F114, and HNO_4, Appl. Opt. 24, 3426-3427 (1985).

4. J. Hjorth, G. Ottobrini, F. Cappellani, and G. Restelli, A Fourier-transform infrared study of the rate-constant of the homogeneous gas-phase reaction N_2O_5 + H_2O and determination of absolute infrared band intensities of N_2O_5 and HNO_3, J. Phys. Chem. 91, 1565-1568 (1987).

5. R.A. Toth, L.R. Brown and E.A. Cohen, Line strengths of nitric acid from 850 to 920 cm^{-1}, J. Mol. Spectrosc., 218, 151-168 (2003)

ν_5 (HIT18-14), $2\nu_9$ (HIT21-14), ν_3 (HIT27-14) and ν_4 (HIT17-14)[1] by the factor 0.879. A HNO_3 retrieval has been performed with this new data.

It is essential to notice that, if it improves noticeably the RMS of the retrievals and hence their precision, this change leads to a systematic increase of the HNO_3 abundances of about 13%.

[1]The intensities of these bands have to be multiplied by the same factor as for ν_5 and $2\nu_9$ since their absolute intensities were calibrated against those of these latter bands.

Nitrogen dioxide line widths:

Recently a number of studies have dealt with the line widths of the NO_2 molecule. In particular A. C. Vandaele et al. [. A.C. Vandaele, C. Hermans, S. Fally, M. Carleer, M.-F. Merienne, A. Jenouvrier and R. Colin, Äbsorption cross-section of NO_2: Simulation of temperature and pressure effects", J.Q.S.R.T. (in press)] have performed an overview and a comparison of various papers in order to derive the temperature and pressure dependence of the NO_2 absorption features in the 13200-42000 cm^{-1} range. Comparing a number of experimental results they recommend the values:

$$\gamma_{air}(296K) = 0.080(3)\ cm^{-1}/atm,\ n = 0.8(2)$$

These values are to be compared:

- to the values given in HITRAN96 or HITRAN2K:

  $$\gamma_{air}(296K) = 0.067\ cm^{-1}/atm,\ n = 0.5$$

- or to the values given in HITRAN01:

  $$\gamma_{air}(296K) = 0.0707^{a}\ cm^{-1}/atm,\ n = 0.97^{b}$$

  (^{a} Mean value calculated from all individual values of [V. Dana, J.-Y. Mandin, M.-Y. Allout, A. Perrin, L. Regalia, A. Barbe and X. Thomas, 'Broadening parameters of NO_2 lines in the 3.4μm spectral region', J.Q.R.S.T., 57, 445-457 (1997)]
  ^{b} value derived from ref. [V. Malathy Devi, B. Fridovich, G. D. Jones, D. G. S. Snyder, P. P. Das, J.-M. Flaud, C. Camy-Peyret, and K. Narahari Rao, 'Tunable diode laser spectroscopy of NO_2 at 6.2 μm,' J. Mol. Spectrosc. 93, 179-195 (1982); V. Malathy Devi, B. Fridovich, G. D. Jones, D. G. S. Snyder and A. Neuendorffer, 'Temperature dependence of the widths of N_2-broadened lines of the ν_3 band of $^{14}N^{16}O_2$,' Appl. Opt. 21, 1537-1538 (1982); R. D. May and C. R. Webster, 'Laboratory measurements of NO_2 line parameters near 1600 cm^{-1} for the interpretation of stratospheric spectra,' Geophys. Res. Lett. 17, 2157-2160 (1990)].

- or to the values derived from UV spectra in ref. [S. Voigt, J. Orphal and J.P. Burrows, 'The temperature and pressure dependence of the absorption cross-sections of NO_2 in the 250-800 nm region measured by Fourier transform spectroscopy', J. Photochemistry and Photobiology A (in press)]:

  $$\gamma_{air}(296K) = 0.134(10)\ cm^{-1}/atm,\ n = 1.03(80)$$

  noticing that the authors recognize in their paper that the value obtained for γ_{air} is questionable because of line-mixing and resolution problems. Given these results and the errors associated we suggest, until new experimental or theoretical results are available, to use in the MIPAS database:

$$\gamma_{air}\text{air}(296\text{K}) = 0.074/0.71^{*}\ \gamma_{air}\text{air}(\text{HITRAN01}),\ n = 0.97$$

Also instead of no value, HITRAN01 gives a value of 0.095 cm^{-1}/atm for the self broadening coefficient. This seems reasonable and has been introduced in the MIPAS database. The outcoming data of WP 5520 is Deliverable D63.

WP 5520: Socio-economic relevance and policy implication

As for WP 5000.

WP 5520: Discussion and conclusion

The spectroscopic database which now is available for MIPAS is considered the most accurate and most comprehensive wordlwide available.

WP 5520: Plan and objectives for the next period

Not applicable.

WP 5520: Deviation from the work plan

As for WP 5000.

5530 Characterisation of applied microwindows

WP 5530: Objectives

Some of the microwindows used for MIPAS data analysis may be inappropriate and lead to increased fit residuals and/or systematic retrieval errrors. This was to be investigated.

WP 5530: Methodology and scientific achievements

REC analyses were generated for the residuals supplied by the various groups from the AMIL2DA intercomparison retrievals for orbit 2081. Furthermore, visual inspection of residuals was used to identify inappropriate microwindows.

The IMK-processor has testwise been run with the operational ESA microwindow set and proved to be quite robust w.r.t. the microwindow selection. The report on WP 5530 is Deliverable D64.

WP 5530: Socio-economic relevance and policy implication

As for WP 5000.

WP 5530: Discussion and conclusion

Although large residual signatures have been found for various error components, these are generally consistent with problems in the ESA L1 or auxiliary data rather than intrinsic to particular microwindows.

WP 5530: Plan and objectives for the next period

Not applicable.

WP 5530: Deviation from the work plan

As for WP 5000.

5540 Unexpected instrumental behaviour

WP 5540: Objectives

Unexpected behaviour of the MIPAS instrument (including the instrument-related part of the data processing chain, i.e. calibration, non-linearity correction etc.) may cause large fit residuals and/or systematic retrieval errors. The objective of this workpackage was to identify such unexpected instrumental behaviour.

WP 5540: Methodology and scientific achievements

- In order to detect pointing errors of the MIPAS instrument, independent line of sight retrievals were performed which revealed major errors in the ESA-provided pointing data. These pointing errors could be assigned to the use of inappropriate target stars used as reference by the star tracker system and a malfunction of the Envisat orbit and attitude control system.
- Systematic errors were found between forward and reverse sweeps in the p,T-retrieval. Since adjacent tangent heights in a limb scan are comprised of alternating forward and reverse sweeps, even small radiometric errors are magnified by the retrieval algorithm (profile oscillations). The cause was linked to the outputs of the work concerning non-linearity correction.
- It turned out the non-linearity characterisation during the commissioning phase did not lead to satisfactory non-linearity correction. Thus, we proposed to use the on-ground characterisation data which were unfortunately identical for forward and reverse interferometer sweeps but still much better regarding radiometric accuracy. The photon flux, which ist an input to the non-linearity correction, is estimated from the maximum - minimum of the interferogram ADC (analog to digital converter) counts. Since forward and reverse sweeps are slightly differently digitised, the ADC max-min values for forward and reverse sweeps also differ. This leads to about 0.8 % different radiance levels of forward and reverse spectra after non-linearity correction. It was checked that the forward and reverse spectra before non-linearity correction differed by only 0.1 %. After we identified the origin the BOMEM company in charge of the level 1 processor produced an algorithm which compensated for the forward-reverse difference in sampling. Meanwhile, we have introduced new sets of non-linearity correction factors applying a new characterisation method developed by us and funded by ESA where the forward-reverse difference in radiance is decreased to 0.2 % without compensating. This was achieved by producing different sets of non-linearity correction curves for forward and reverse sweeps, as already implemented in the standard level 1 processing.
- Radiometric gains were found to increase slowly with time, then drop to the initial value when warming up the focal plane unit. Ratios of radiometric gains approximated by ratios of CBB spectra measured after and before warming of the focal plane unit show distinct spectral signatures which coincide with the absorption

spectrum of water ice at low temperature (URL: www.strw.leidenuniv.nl/schutte/database.html), spectrum of ice at 80 K). This is due the outgassing of water vapor from various surfaces of ENVISAT and deposition of ice on cold surfaces in the focal plane unit which was remove by warming up. The Gain change is rather large (up to 50%) and from the spectroscopic ice data and the gain change a thickness of 0.4 μm was estimated. Whereas channels A and C are heavily affected, channels B and D show minor changes, only. The detectors associated with the complementary interferometer output labeled with "2" are more affected. Furthermore, channel C has even more ice formation.

- Up to date no extended investigation of phase errors is available. As for the on-ground measurements the instrument shows an excellent phase stability. For some examples a different route was taken for assessing phase errors. Scene, gain, and offset spectra were phase corrected prior to radiometric calibration. The calibrated scene showed only marginal differences to the standard product. The standard product is derived using a complex gain. Any phase error should influence the radiance spectra as well as yielding non-zero imaginary part. The phase correction before calibration avoids phase errors introduced by instrument drifts.

- It was found that periodic oscillations of the spectral intensity occurred which were attributed to microvibrations of an unknown source. These microvibrations were already present when the instrument was tested on-ground but unfortunately were only detected recently within this study. The microvibrations have several radiometric impacts: a) up to 1% intensity error varying with time, b) ghost lines error varying with time, c) signal in the imaginary part of the calibrated scene varying with time, previously leading to errors in the reproted NESR. The last problem has been solved by modification of the level 1 processing.

- In-flight characterization measurement IF4 contains CBB interferograms for different CBB temperatures. The photoconductive channels A1, A2, AB and B were corrected with the old non-linearity correction factors. 300 forward sweeps for all channels for CBB and DS for the temperatures 229.7, 234.9, 239.6, 246.4 K were averaged and radiometric gains formed. The averaging removes the fluctuations caused by microvibrations. Gains were ratioed for each channel against the gain for 246.6 K. The maximum difference of gain ratios for CBB=229.5 K and 246.5 K from 1 was found in channels A1 (0.7%) and C (0.4%), both for the largest temperature contrast and can be attributed to water ice contamination over the 15 orbits of the measurement duration. Beside this the ratios deviate from 1 within 0.3%. Due to the very non-linear relation of blackbody temperature and spectral radiance substantial temperature errors outside specifications would have caused larger differences. Furthermore, this indicates the validity of the old non-linearity correction factors within the given brightness temperature range. However, a deteriorated blackbody emissivity differing significantly from 1 cannot be detected unless the radiation reflected into the field of view of the instrument due to a deteriorated blackbody surface is significant when compared to the blackbody radiance. The

imaginary part of the ratios showed differences up to 0.3% which is quite small and can be expressed as phase variations over the 15 orbits where this data were taken.

See also under REC analysis, WP5500. The report on WP 5540 is Deliverable D65.

WP 5540: Socio-economic relevance and policy implication

As for WP 5000

WP 5540: Discussion and conclusion

Major instrumental deficiencies have been detected, which, when undetected, could lead to major retrieval errors. This shows, that independent quality monitoring of ESA data products is essential. Some further details on this are also discussed under WP 6000.

WP 5540: Plan and objectives for the next period

Not applicable.

WP 5540: Deviation from the work plan

As for WP 5000.

5550 Inappropriate a priori data

WP 5550: Objectives

Inappropriate a priori data can cause poor retrievals and large residuals. It should be checked if this had happened in the MIPAS retrievals under AMIL2DA.

WP 5550: Methodology and scientific achievements

No evidence of inappropriate a priori data has been found. The report on WP 5550 is Deliverable D66.

WP 5550: Socio-economic relevance and policy implication

As for main WP 5000

WP 5550: Discussion and conclusion

A priori data used seem to be appropriate.

WP 5550: Plan and objectives for the next period

Not applicable.

WP 5550: Deviation from the work plan

None.

5560 Other explanations for residuals

WP 5560: Objectives

Residuals in best fit spectra can hint at systematic retrieval errors beyond those assessed with the correlation analysis. Therefore, analysis of suspicious residuals is an important step in the quality control of retrievals.

WP 5560: Methodology and scientific achievements

No evidence of further kind of residuals has been found. The report on WP 5560 is Deliverable D67.

WP 5560: Socio-economic relevance and policy implication

As for WP 5000.

WP 5560: Discussion and conclusion

The fact that no significant unexplained residuals have been found, does not imply that there are no further errors. It just means, that all errors in spectra or a priori assumption are compensated by the retrieval parameters.

WP 5560: Plan and objectives for the next period

Not applicable.

WP 5560: Deviation from the work plan

As for WP 5000.

5600 Comparison to external data

WP 5600: Objectives

MIPAS retrievals should be validated by comparison to data from other instruments.

WP 5600: Methodology and scientific achievements

MIPAS retrievals were compared to retrievals from GOMOS, SCIAMACHY, as well as non-Envisat measurements and model results. Further details are reported under WPs 5610–5630. The report on WP 5600 is Deliverable D69.

WP 5600: Socio-economic relevance and policy implication

As for WP 5000.

WP 5600: Discussion and conclusion

Results are discussed under WPs 5610–5630.

WP 5600: Plan and objectives for the next period

Not applicable.

WP 5600: Deviation from the work plan

As for WP 5000.

5610 Comparison to GOMOS data

WP 5610: Objectives

MIPAS retrievals should be validated by comparison to data from GOMOS.

WP 5610: Methodology and scientific achievements

The comparison of GOMOS and MIPAS were performed by individual, direct comparisons of profiles requiring stringent spatial and temporal collocation requirements and by a statistical study with a more relaxed temporal collocation. Because of small number of overlapping data periods from these two instruments at this stage of the general validation period only 14 individual collocations were found. The statistical comparison was based on 100 collocations. Because of immature state of retrievals of both instruments, the comparison did not consider the different vertical resolutions of these two instruments neither the individual error estimates were used in the comparisons. The constituents compared were O_3, NO_2 and H_2O. The vertical grid of MIPAS was used and GOMOS measurements were interpolated to this grid.
The report on WP 5610 is Deliverable D70.

WP 5610: Socio-economic relevance and policy implication

As for WP 5000.

WP 5610: Discussion and conclusion

In this work we compared GOMOS and MIPAS measurements for O_3, NO_2 and H_2O using limited data sets measured during the polar vortex split in 2002. Ozone profiles from these two instruments show reasonable agreement when compared individually using stringent collocation requirements. Also the statistical comparison with relaxed collocation shows a promising agreement.

For NO_2 the individual comparisons are made difficult because of large oscillations in the GOMOS profiles. The statistical comparison may indicate a bias between GOMOS and MIPAS.

The comparison of H2O profiles showed large differences. It must be noted that retrieval schemes for both instruments are not yet optimized. In GOMOS retrievals we expect that a Tikhonov smoothing will be deployed in vertical profiles which would alleviate comparisons. The IMK processing employs already a Tikhonov smoothing. It is evident that much more data are needed for conclusive conclusions. MIPAS-GOMOS comparisons will be continued in near future.

WP 5610: Plan and objectives for the next period

Not applicable.

WP 5610: Deviation from the work plan

None.

5620 Comparison to SCIAMACHY data

WP 5620: Objectives

Since both atmospheric instruments at ENVISAT, MIPAS and SCIAMACHY, measure a few trace gases which are the same, many coincidences which are very close together in time and space can be found. Therefore a cross validation between the two data sets should enable a good statistical analyses of comparisons and enable to look for zonal and seasonal peculiarities.

WP 5620: Methodology and scientific achievements

The SCIAMACHY instrument is an UV/Vis/NIR grating spectrometer covering the spectral range from 220 - 2380 nm with a moderate spectral resolution of 0.2 - 1.5 nm. The instrument measures atmospheric radiance from scattered, reflected and transmitted sunlight, extraterrestrial solar irradiance and lunar radiance in the three geometries nadir, limb and occultation and achieves global coverage within 6 days at the equator. SCIAMACHY limb measurements are made from 0-100 km with a vertical resolution of around 2.6 km. The horizontal resolution in azimuth direction is 240 km (120 km min.) by a swath of 960 km and in flight direction 400 km. At the IUP O_3 profiles from SCIAMACHY limb measurements are retrieved from all available Level_0 and Level_1 data with a solar zenith angle (SZA) $< 90°$. The retrieval uses 3 wavelengths of the O_3 Chappuis bands with optimal estimation and tangent heights are systematically corrected by -2km to compensate for an offset in the instrument's limb pointing.

At the IUP NO_2 profiles from SCIAMACHY limb measurements are retrieved from all available Lv1 data. The retrieval uses the spectrum within 420 - 490 nm and a ratio of limb measurements at different tangent heights, with the 45 km tangent height as a reference. With optimal estimation the vertical profile is retrieved using measured and modeled limb radiances with all corrections from pre-fit routine applied, weighting functions from RTM and a priori information. These SCIAMACHY NO_2 profiles are sensitive for the altitudes from 15 to 40 km. O_3 and NO_2 products from September 20 and 23, 2002 from both instruments were compared to each other. The sample of collocations was limited to the availability of MIPAS Level_1 data to the IMK and of SCIAMACHY Level_0 and Level_1 (for NO_2 only) data to the IUP. Collocated SCIAMACHY and MIPAS O_3 and NO_2 profiles were identified where measurements of the two satellite instruments were taken within the same or next orbit and using a 650 km collocation radius between the tangent point of the MIPAS measurement and the SCIAMACHY measurement. All collocated measurements were from the Southern Hemisphere and some of them were within, at the edge or outside of the polar vortex. Therefore, in order to avoid to compare collocated measurements from different airmasses, the potential vorticity (PV) data (given from the UKMO dataset) at 475 K were checked for the time and place of each collocated measurements. Only collocations were both measurements were within ($<$ -40 PVU), at the edge ($<$30 PVU to $>$-40 PVU) or outside the polar vortex ($>$ -30 PVU) have been

included in the comparisons.

Additionally, results for MIPAS/Envisat retrieved by the University of Oxford (OXF), Rutherford Appleton Laboratory (RAL) and the Instituto de Astrofisica de Andalucia (IAA) have been used for the comparison. These retrievals have been performed using different retrieval codes and retrieval approaches.

WP 5620: Socio-economic relevance and policy implication

As for WP 5000.

WP 5620: Discussion and conclusion

Out of the total of 25 collocations for O_3 profile measurements, at 15 collocation pairs both measurements were outside the polar vortex and at 6 both were inside the polar vortex. For the NO_2 comparisons, at 3 collocation pairs both measurements were outside the polar vortex and at 2 both were inside the polar vortex.

O_3 cross validation: The O_3 results for two selected collocations retrieved by SCIAMACHY-IUP and available MIPAS results of IMK, OXF, RAL, and IAA, where both coincidences were outside the polar vortex, are discussed in more detail. The comparisons of collocations where both measurements are outside the polar vortex look fairly good, but SCIAMACHY values are mostly lower than MIPAS. The statistical analyses gives at 18 - 48 km a mean relative deviation of SCIAMACHY-IUP to MIPAS-IMK with -15 - +1% (+/- 10 - 20%). Inside the polar vortex, the profile structure deviates quite a lot between the instruments, but the overall range of O_3 values are still comparable between 23 to $>$ 40 km. A double peak structure which is recognizable in all MIPAS retrievals cannot be resolved by SCIAMACHY. It seems that SCIAMACHY cannot resolve fine profile structures. One possible reason is the swath width with about 960 km perpendicular to the viewing direction which is significantly wider than the horizontal field of view of MIPAS which is about 30 km. The statistical analyses gives at 23 - 48 km a mean relative deviation of SCIAMACHY to MIPAS with -10 - +15% (+/- 10 - 20%).

NO_2 cross validation: Six collocations of SCIAMACHY and MIPAS NO_2 retrievals were selected for comparison. For both instruments only measurements above 15 km were considered for the retrieval. For these collocations only MIPAS-retrievals by IMK were available. MIPAS retrievals were performed under LTE and non-LTE conditions. The results of the comparisons show large deviations for the collocations. The IMK NO_2 results generally have the maximum at too low altitudes. The maximum is expected to be at around 30 km. While the results for SCIAMACHY peak in this region, the MIPAS results peak between 20 and 25 km. One reason is the retrieval set-up with too strong regularisation for tangent altitudes below 25 km which forces the retrieval result towards the a priori profile. Since the a priori profile used general shows larger values than the

result, the profile is forced to higher number densities and the maximum moves to lower altitudes. The retrieval scheme is currently being modified and improved and will be

WP 5620: Plan and objectives for the next period

Not applicable.

WP 5620: Deviation from the work plan

As for WP 5000.

WP 5630 Comparison to further external validation data

WP 5630: Objectives

MIPAS retrievals should be validated by comparison to data from external experiments.

WP 5630: Methodology and scientific achievements

The MIPAS-measured temperatures on 24 July and 20-27 September of 2002 are compared with those observed by a number of other satellites, including HALOE (Halogen Occultation Experiment) Version 19 L2 data, SABER (Sounding of the Atmosphere using Broadband Emission Radiometry) (Version 1.01 data), and UKMO (United Kingdom Meteorological Office) Stratospheric Assimilated Data (taken from BADC). The UKMO data are produced by analyzing a heterogeneous mixture of operational meteorological observations, including data from NOAA polar orbiters in addition to conventional meteorological observations such as radiosonde data.

Furthermore ozone profiles retrieved from GOME (Global Ozone Monitoring Experiment) measurements collocated with MIPAS measurements are compared. GOME is onboard ERS-2, which is on the same orbit as Envisat but with a delay of several minutes. Thus several collocations are available.

For the comparison individual paired-profile comparisons are conducted for those measurements with latitude and longitude differences smaller than 5 and 10 degrees, respectively. The time differences between the paired profiles are required to be less than 1 hour for the MIPAS/SABER and MIPAS/UKMO, but are allowed to be as large as 12 hours for MIPAS/HALOE due to the sampling characteristics of HALOE.

The paired profiles from SABER, HALOE, UKMO between 5 and 70 km are then interpolated to a common altitude grid as that used by the MIPAS-IMK data.

WP 5630: Socio-economic relevance and policy implication

As for WP 5000.

WP 5630: Discussion and conclusion

Total 208 MIPAS temperature profiles measured at different locations and seasons are compared with other satellite observations. The MIPAS data show general consistencies with those of the correlative HALOE, SABER and UKMO measurements on profile-by-profile basis.

The MIPAS temperatures exhibit reasonable agreements with those of the three other satellite measurements. For solstitial measuremnets on 24 July, the MIPAS temperatures

below 30 km are generally hotter than those of UKMO, but colder than those of SABER, with the differences less than 1 K and 2 K with respect to UKMO and SABER, respectively. At upper heights between 30 and 55 km, both HALOE and SABER are colder than MIPAS by 2-3 K, while UKMO hotter by 3-5 K. Larger deviations of 10-20 K are found above 60 km, where the upper boundary of the MIPAS observations is reached. The mean differences on 24 July of 2002 indicate that the MIPAS temperatures are colder than SABER by 2 K below 30 km (no HALOE data are available in the low altitudes), but hotter than both HALOE and SABER by 2-3 K at upper heights between 30 and 55 km. The discrepancies at the upper heights could be understood by the known cold bias of SABER data.

Due to missing collocations of MIPAS and HALOE and reprocessing of the SABER data only comparisons of MIPAS and UKMO are presented for the days in September. As a consequence of the coincidence requirement MIPAS/UKMO collocations is available on 20,21,23,26, and 27 September. Between 10 and 30 km, the daily mean differences are of about $\pm$(1-3) K, with larger magnitudes at the lowest and highest levels, and with apparent day-to-day variations. The resultant differences of the five days tend to be zero in this height region, suggesting no apparent systematical deviations between MIPAS and UKMO measurements. At upper heights above 30 km, the discrepancies generally increase with increasing height, with UKMO hotter than MIPAS by 10 -20 K at the upper boundary of UKMO and MIPAS measurements around 60 km. It is known that the UKMO temperatures are constrained and have a significant warm bias in the lower mesosphere. To further examine the statistical consistency between MIPAS and UKMO data, we compare the zonal mean differences between the correlative MIPAS and UKMO measurements. The zonal means of the differences between available correlative MIPAS and UKMO measurements revealed large discrepancies of maximum 6-8 K to occur around 25 km at higher latitudes of 60°S south, with MIPAS generally hotter than UKMO. This could be due to the deviations between the MIPAS observations and the current UKMO assimilation model, which may not fully reflect the unprecedented event. More discussions about possible mechanism can be found in Deliverable D72.

Ozone retrievals from GOME and MIPAS have been compared for three collocations. Both instruments reproduce the maximum and the results look good. The altitude of the maximum is consistent for all MIPAS retrievals and the GOME profile. As the MIPAS results were obtained using different retrieval approaches and constraints the distribution varies, particularly in the maximum region. The IMK results seem to have lower maximum values than the others. For the observed cases the maximum of the GOME ozone profile shows slightly larger values than the MIPAS retrievals. Takeing into account the assumed random errors for MIPAS, MIPAS and GOMOS agree quite good.

WP 5630: Plan and objectives for the next period

Not applicable.

WP 5630: Deviation from the work plan

As for WP 5000.

6000 Reference Algorithm qualification

WP 6000: Objectives

The objective of this WP was the characterization the results of the IROE-R processor with respect to their accuracy and their variability as a function of the behavior of some instrumental parameters.

WP 6000: Methodology and scientific achievements

The functionalities inplemented in the IROE-I processor were exploited in this WP to re-process some MIPAS data sets with the aim of characterizing the accuracy of the retreived profiles with respect to some instrumental parameters that are assumed to be known in the ESA Level 2 processing chain. In particular, the following instrumental aspects were considered:

- Adequacy of the ILS shape as modelled in Level 1b processing,
- Frequency and intensity calibrations,
- Altitude dependence of the residual (uncorrected) intrumental offset.

The report on WP 6000 is Deliverable D73.

WP 6000: Socio-economic relevance and policy implication

As for WP 5000.

WP 6000: Discussion and conclusion

The analyses carried-out under this WP have highlighted a frequency shift error in MIPAS measured spectra. A correction scheme was activated in Level 2 processor to correct the frequency scale of Level 1b spectra allowing to improve the retrieval accuracy. A recommendation was issued to improve the frequency calibration scheme implemented in MIPAS Level 1b processor (which did not properly allow for detectors non-linearity).

The retrieved intrument offset was found to be generally smaller than the measurement noise therefore, fitting of the residual instrument offset is an operation that could be avoided in routine retrievals.

WP 6000: Plan and objectives for the next period

Not applicable.

WP 6000: Deviation from the work plan

None.

Chapter 4

Technological Implementation Plan

The Technical Implementation Plan is accessible via http://etip.cordis.lu/

Chapter 5

Executive Summary

Contract No.: EVG1-CT-1999-00015
Reporting Period: 1 July 2000 - 30 June 2003
Title: Advanced MIPAS Level 2 Data Analysis (AMIL2DA)

5.1 Objectives

Changes in atmospheric composition are important in the context of stratospheric ozone depletion, global change and related environmental problems. The Michelson Interferometer for Passive Atmospheric Sounding (MIPAS), which is a core instrument of the Envisat polar platform launched on 1 March 2001 by the European Space Agency (ESA), is a powerful tool to measure vertical profiles of trace species on a global scale. While operational data processing by ESA covers only analysis of pressure, temperature, and the mixing ratios of the species O_3, H_2O, HNO_3, CH_4, N_2O, and NO_2, MIPAS infrared spectral limb emission measurements contain information on a bulk of further species relevant to environmental problems mentioned above. The main objective of AMIL2DA was to fill this gap by development and validation of complementary data processors. This includes: the development and adaption of the data analysis codes to the MIPAS requirements; cross-comparison of radiative transfer models involved, since all forward modelling errors map to the retrieved atmospheric state parameters; a blind test retrieval experiment on the basis of synthetically simulated measurements, in order to detect and remove potential deficiencies in the data analysis processors of the consortium; intercomparison of real data retrievals carried out with these data processors; detection of deficiencies during these three steps of processor validation and upgrading of related processors; characterization of the MIPAS instrument and the processing schemes by various means as well as validation of the data with other instruments.

5.2 Scientific Achievements

Tools for advanced MIPAS level-2 data analysis were developed, thoroughly tested, and applied to sample MIPAS data sets. Participating groups now are in a position to analyze MIPAS data for scientific purposes with their own data processors, which are custom-tailored to the groups' particular scientific interest.

5.3 Main Deliverables

The main deliverables were validated and cross-checked methods for the direct and inverse solution of the radiative transfer problem (D15-19, D21–25, D35–39, D53–D57) as well as spectroscopic data (D20, D63).

5.4 Socio-economic Relevance and Policy Implications

After AMIL2DA participating groups have reliable MIPAS data analysis processors available and are ready for independent scientific analysis of real MIPAS data. This strengthens their position in international scientific competition. AMIL2DA has publically stated the political and scientific need to retrieve species other than the official ESA key-species. The technical/scientific feasibility has been proven. Activities under AMIL2DA contribute largely to the overall success of the MIPAS experiment and the Envisat mission, which will make justification of further suchlike missions easier. Both industry and the scientific community would benefit from such follow-up projects. Beyond this, AMIL2DA has strengthened the cooperation between all European research sites involved.

5.5 Conclusions

The project considerably improved the capability of the contractors to provide enhanced level-2 data from MIPAS-Envisat. Algorithms have been developed and tested and prove to work reliably. Co-operation of the large consortium helped to detect some deficiencies which may have remained unnoticed without the intercomparison in the framework of this study. The participants now are in a good position to make valuable scientific contributions to atmospheric research on the basis of MIPAS data.

5.6 Dissemination of Results

Methods and results were published in peer-reviewed articles and at scientific conferences. Spectroscopic data and one of the algorithms are available to the public via internet. Data processors are used to generate data which are distributed in the scientific community on the basis of co-operation contracts within the framework of follow-up projects.

5.7 Keywords:

Envisat, MIPAS, retrieval, radiative transfer forward modeling, cross-validation

Chapter 6

Detailed Report

6.1 Background

The Michelson Interferometer for Passive Atmospheric Sounding (MIPAS) on the Envisat earth observation satellite developed by the European Space Agency (ESA) provides vertical profiles of atmospheric species relevant to several mostly inter-linked problems in ozone chemistry and global change. Routine data analysis under ESA responsibility covers only six species (H_2O, O_3, N_2O, CH_4, HNO_3, NO_2) as well as pressure and temperature. The MIPAS data, however, contains much more information of other atmospheric trace species of very high scientific value. Thus, the exploitation of MIPAS data with respect to the retrieval of many more scientifically interesting species such as the complete nitrogene family, chlorine source gases and reservoirs, greenhouse gases, ozone precursors, aerosols etc as well as the analysis of the six key species by means of data processors of higher sophistication than the operational ESA code are of high interest for better understanding of the ozone-chemistry and global change. The main goal of AMIL2DA project is to fill this gap and to ensure quality and intercomparability of these independently generated value-added data products, which are generated by innovative data analysis and retrieval approaches developed by participating groups. The basic strategy to achieve this was to leave the diversity of MIPAS data processors rather than to generate an all-purpose standardized code.

6.2 Scientific/Technological and Socio-Economic Objectives

A major objective of AMIL2DA was the development and adaption of the data analysis codes to the MIPAS requirements. The next step was to validate these data processors. The first objective in the framework of processor validation was cross-comparison of radiative transfer models involved, since all forward modelling errors map to the retrieved atmospheric state parameters. The second objective was a blind test retrieval experiment on the basis of synthetically simulated measurements, in order to detect and remove po-

tential deficiencies in the data analysis processors of the consortium. The third objective was intercomparison of real data retrievals carried out with these data processors. Detection of deficiencies during these three steps of processor validation led to upgrading of related processors. Further activities of AMIL2DA included a characterization of the MIPAS instrument and the processing schemes by various means as well as validation of the data with other instruments.

On the socio-economic side, the objectives were to strengthen the position of involved groups in the scientific community, to get the best possible benefit from the Envisat mission and the MIPAS experiment, and to place participating groups in a position such that they are well prepared to tackle scientific problems related to global change on the basis of MIPAS data. Furthermore, it was attempted to prove the benefits of MIPAS in order to justify a potential follow-up mission of similar kind, which would be desirable both from scientific and economic point of view, in particular because this strengthens the position of European space industry in international competition.

6.3 Applied Methodology, Scientific Achievements, and Main Deliverables

6.3.1 General Outline

The basic strategy of AMIL2DA was to leave the diversity of retrieval codes rather than to generate an all-purpose standardized code. The work was organized as follows: The first step was to adapt the processors of involved groups to MIPAS requirements. The second step was to cross-validate radiative transfer forward models, which are a key part of each data processor. The third step was to validate the retrieval processor on the basis of synthetic measurements. The fourth step was to prove the robustness of the data processors by application to real measurement data. Further activities included characterization of MIPAS spectra and validation of data products.

6.3.2 Processor Development and Adaption

The processor work is organized in three parts, (a) the modeling of radiative transfer through the Earth's atmosphere; (b) the solution of the inverse problem, i.e. the retrieval of geophysical parameters from measured MIPAS spectra (level-2 processing); and (c) processor work of a more generic type, e.g. user environments, diagnostic tools etc. The methods developed are major deliverables of this project (D15–D19).

The IMK Data Processor

The Karlsruhe Optimized and Precise Radiative Transfer Algorithm (KOPRA) and the Retrieval Control Program (RCP) were available at the beginning of the project. How-

ever, during AMIL2DA many details had to be refined in order to increase accuracy and computational efficiency of the codes. These activities included, (I.) on the side of forward modeling (KOPRA): (a) The forward model KOPRA was extended in order to support calculation of OH signatures; (b) the interface between the forward model and the inversion tool was improved; (c) the input data structure of the forward model was reorganized in order to support non-local thermodynamic equilibrium retrieval; (d) alternative line-mixing routines were included; (e) the CKD2.4 water-vapor continuum was included in the KOPRA forward model; (f) a Mie model was implemented in the KOPRA forward model; (g) the forward model KOPRA was extended in order to support 3-D input fields of atmospheric state parameters; (h) a further KOPRA update made possible the simultaneous modeling of various polar stratospheric cloud types. (II.) On the side of solution of the inverse problem (RCP): (a) Matrix inversion was accelerated by use of specific inversion tools which are custom tailored to the hardware in use at IMK; (b) the Levenberg-Marquardt damping was included in the retrieval code; (c) convergence criteria were refined; (d) data interfaces between the forward radiative transfer code and the retrieval code were upgraded, in particular with respect to derivatives involving continuum emission; (e) the retrieval code was upgraded such that it supports a user-defined retrieval grid; (f) the Tikhonov-regularization tool was upgraded in order to support also non-equidistant altitude grids; (g) the inversion tool was upgraded in order to support retrieval of elevation angles and calibration offset; (h) the internal data structure with respect to isotopic species was improved; (i) the hydrostatic constraint was applied to the inversion tool; (j) the interface between the forward model and the inversion tool were upgraded in order to make possible retrieval of observation geometry in terms of elevation as well as instrument line shape parameters. (III.) On the side of data bases, further routines, and user environment: (a) Microwindow databases were created for some non-key species; (b) spectral microwindows for data analysis for polar atmospheres were generated; (c) some diagnostic tools were provided; (d) processing parameters and internal thresholds were tuned; (e) the design of the graphical user interface of the retrieval processor were completed; (f) a generic non-LTE model for generation of vibrational temperature data, which was developed at IAA, has been implemented in the processor.

The Oxford University Data Processor

Oxford had the mature stand-alone MIPAS Reference Forward Model (RFM) at the start of the study so the main objective was to develop a retrieval code (OPTIMO) using this as the internal forward model. There were also some minor modifications and bug-fixes to the RFM itself as a result of this study. Actions under AMIL2DA included (I.) on the side of forward radiative transfer modelling (RFM): (a) The handling of non-LTE calculations was improved; (b) the efficiency of Jacobian calculations was improved; (c) horizontal gradients of state parameters were included; (d) Voigt lineshape calculations were improved; (e) the Oxford forward model RFM was modified to handle GEISA as well as HITRAN spectroscopic data; (f) the RFM (Forward model) was extended to handle new cross-sectional data released with HITRAN 2000 (new format and additional HFC species); (II.) With respect to the solution of the inverse problem (OPTIMO): The

OPTIMO retrieval algorithm has been coded according to specifications detailed in the Retrieval Strategy Documentation. With respect to data bases, further routines, and user environment: (a) The RFM web-page http://www.atm.ox.ac.uk/RFM/ was updated to include some simple IDL procedures for RFM data analysis. (b) the MWMAKE (Microwindow selection) program was extended to handle variable viewing geometry for error analysis of different MIPAS scan patterns. Also it was modified for evaluating low-spectral resolution (0.1 cm^{-1}) mode; (c) analysis of Residual Spectra: A new technique was developed for a quantitative analysis of error components in residual spectra.

The DLR Data Processors

Two totally independent retrieval processors are available at DLR. One of them is a processor using the MIRART radiative transfer forward model, and a multi-purpose retrieval processor, henceforth labelled DLR-a. These codes where upgraded in order to cope with MIPAS measurements. The other processor is the D-PAC processor, which uses the IMK forward model KOPRA, but a distinct implementation for the inversion. Also this processor was upgraded within AMIL2DA in order to cope better with MIPAS measurements.

Activities for the DLR-a processor included, (I.) on the side of forward radiative transfer modelling (MIRART): (a) The DLR forward model MIRART has been redesigned and analytical derivatives (gas densities or VMR) have been implemented by means of algorithmic differentiation; (b) the field of view convolution for an arbitrary field of view has been implemented in MIRART; (c) line shift implemented in MIRART; (d) GEISA databank implemented in MIRART; (e) in addition to the AMIL2DA forward model intercomparison MIRART has been extensively intercompared with several microwave line-by-line codes for limb-, up-, and down-looking geometries in the framework of the Third International Radiative Transfer Modelling Workshop (Bredbeck, October 2001) organized by the University of Bremen. (II.) With respect to the solution of the inverse problem: (a) Documentation of the DLR-a retrieval code (Tikhonov code) has been thoroughly extended; (b) a bound–constraint version of the iteratively regularized Gauss–Newton method has been developed; (c) The retrieval code has been verified using various simulated scan patterns. These tests aimed at validating all internal interpolation steps; (d) a multiple microwindow mode (altitude independent) was implemented in the DLR-a processor. (III.) With respect to data bases, further routines, and user environment: The output routine for the generation of results has been finalized. This output routine includes a visualization tool allowing a check-out of results prior to delivery.

Activities for the D-PAC processor included, (I.) on the side of forward radiative transfer modelling: Since the IMK forward KOPRA is used in the D-PAC processor, forward modelling related work was restricted to clarification of data interfaces and testing. In order to verify the existing data handling and analysis tools of the D-PAC processor, a series of transmittance tests involving a N_2O transition at 1274.6166 cm^{-1} was conducted. The tests had been compiled by IMK and aimed at the verification of Voigt line shape modelling: when Lorentz dominated, under Lorentz Doppler balance, when

Doppler dominated, and with infinitesimal field-of-view. The results were in agreement with calculations performed at IMK and verified the maturity and usefulness of the existing and updated data analysis tools of the D-PAC processor. (II.) With respect to the solution of the inverse problem: (a) The D-PAC processor functions have been extended to use of pre-selected sweeps within each scan; (b) interfaces for the ingestion of balloon data have been written and tested. This allows us to compare synthetic test data with realistic experiment data. (c) The D-PAC retrieval software was provided with another option to allow trace gas profile retrievals based on basis functions instead of height grids. First retrieval tests with ozone profiles revealed that a limited number of basis function coefficients is fully sufficient for a reliable trace gas profile representation. As a consequence, the memory requirements of the Jacobians used during a retrieval can be reduced considerably. (d) Multi-scale experiments were prepared for the retrieval of CFCs from broad band emissions, where some emission features might be treated with reduced spectral resolution. Detailed results are expected during the next weeks. (III.) With respect to data bases, further routines, and user environment: (a) The final computer configuration was selected; (b) the software was transferred and AMIL2DA test runs were performed within the final configuration; (c) a local profile database for initial guesses, a priori data and interfering species was installed; (d) numerical and graphical tools for quality measures and convergence tests have been implemented and tested; (e) visualization routines were adapted to final computer configuration; (f) test tools analyzing the behaviour of each microwindow have been completed; (g) the software was embedded within the in-house archiving and cataloguing system.

The IFAC Data Processor

The operational ESA processor used for near-real time Level 2 MIPAS data analysis is based on algorithms prototyped at IFAC: the OFM (Optimized Forward Model) and the ORM (Optimized Retrieval Model). The objective of the IFAC contribution to this AMIL2DA workpackage was twofold: First, to have the ESA-used algorithms available as a reference, and second, to implement possible improvements for the operational processing. Activities included, (I.), with respect to forward radiative transfer modelling (OFM): (a) The model was improved to allow for pressure-shift, self-broadening and line-mixing; (b) additional output interfaces have been created in the forward model in order to generate the data to be intercompared within AMIL2DA which are not standard products of the OFM; (c) a tool for selection of lines contributing significantly within a given spectral interval has been implemented; (d) the forward model has been modified in order to cope with chemical species for which only a database of cross-sections is available; (e) the forward model has been modified to allow for the horizontal variability of the atmosphere; (f) the forward model has been modified to include the capability of simulating broad spectral intervals. With respect to (II.) the solution of the inverse problem (ORM): (a) The option of retrieving the following instrument parameters was introduced in the retrieval model: height-dependent offset calibration, ILS broadening parameter, frequency shift, intensity calibration; (b) the retrieval model has been modified in order to cope with chemical species for which only a database of cross-sections is available. With respect

to (III.) data bases, further routines, and user environment: (a) Several visualization tools have been implemented; (b) additional output interfaces have been created in the forward model in order to generate the data to be intercompared which are not standard product of the IFAC forward model.

The RAL Data Processor

Major parts of the coding of the radiative transfer model and the retrieval algorithm were performed under AMIL2DA, since codes available at the beginning of the project were not applicable to MIPAS. These include, (I) with respect to forward radiative transfer modelling (FM2D): (a) The forward model FM2D was developed. This includes the adaption of the RAL in-house forward model capable of handling horizontal variations in the line of sight for operation in the IR, with a view to comparison with the MIPAS Reference Forward Model; (b) the RAL forward model has been adapted for use at mid-infrared frequencies; (c) mid-infrared spectral data, relevant to MIPAS has been obtained; (d) a strategy for rapid modelling of far-line wing contributions to absorption coefficient has been developed, based on the MIPAS RFM approach; (e) an improved numerical integration scheme has been implemented; (f) a more advanced continuum modelling has been achieved by inclusion of the Clough-Kneizys-Davies formulation for H_2O, CO_2 and O_2; (g) self-broadening was implemented for all species; (h) pressure shift has been included; (i) efficient modelling of 1-D radiative transfer has been embedded in the 2-D model, such that the previous 1-D model now is redundant; (j) an extra option for direct output of transmission, not only absorption coefficients, has been provided; (k) rapid convolution routines (in C) have been implemented. (II.) With respect to the solution of the inverse problem (RET2D): (a) A 2-dimensional retrieval code was developed and implemented for use at infrared wavelengths by adaptation of the RAL mm-wave retrieval scheme; (b) the handling of multiple microwindows was developed for MIPAS data analysis. (III.) With respect to data bases, further routines, and user environment: (a) Criteria for selection of spectral ranges suitable for sounding H_2O and O_3 in the upper troposphere and lower stratosphere were defined; (b) the Oxford University (OU) Reference Forward Model (RFM) has been installed on RAL processors for reference purposes; (c) the spectral data input option has been enhanced; now it allows the same input format as the MIPAS RFM; (d) an option to switch between RAL code and MIPAS RFM code using same drivers has been provided.

Spectroscopic Data

Accurate modelling of radiative transfer through the atmosphere requires accurate spectroscopic input data, because all errors in these data map directly onto the calculated spectra and thus to the retrieved geophysical state parameters. While large databases of spectroscopic transitions of atmospheric species had been available even at the beginning of AMIL2DA (e.g. HITRAN), the reliability of these data had to be reviewed, and for some species and bands, updates were necessary. This includes: **Ozone:** Spectroscopic parameters (positions, intensities, widths) of the ozone ($^{16}O_3$) ν_1 and ν_3 bands in the 10

micron region were improved. **HNO_3:** The HNO_3 hot band $\nu_5 + \nu_9$ - ν_9 located around 885 cm^{-1} has been improved. In particular it has been shown that the shape of this band as well as its intensity are not properly modelled in the 2000 version of the spectroscopic atmospheric databases. **HOCl:** New spectroscopic data have been made available. The spectral interval spanned by the data is adapted to the spectral domain covered by the MIPAS experiment, namely 600-2500 cm^{-1}. **NO_2:** New spectroscopic data have been made available. The spectral interval spanned by the data is adapted to the spectral domain covered by the MIPAS experiment, namely 600-2500 cm^{-1}. **$ClONO_2$:** However, some supplementary effort was spent on the modelling of the ν_4 band of $ClONO_2$ by a line-by line calculation. This spectroscopic database is a major deliverable of AMIL2DA

6.3.3 Cross-check of Forward Models

Since any radiative transfer forward model errors map directly to retrieved atmospheric state parameters, thorough testing of these forward models is essential for building up confidence in the overall data processing chain. Since in the AMIL2DA consortium several independent forward models are used, the approach of cross-comparison has been chosen to prove the reliability of forward models.

A test scenario has been defined, distributed via internet, discussed, and finally frozen. Forward calculations have been performed. Resulting spectra have been intercompared, and the findings have been documented in the related report. Explanations have been found for most detected differences. Where necessary, solutions have been identified and implemented. The overall performance of the codes is good.

Definition of Test Scenario

Test cases were defined for which spectra were to be calculated with all forward models used in the consortium. The set of test cases should be limited in order to avoid unnecessary work while it should be complete in order to detect as many as possible of the weaknesses of the code. The test cases were set up in an order starting from quite simple scenarios (single transition cell transmission calculations), proceeding towards more realistic cases (atmospheric limb radiance calculations under consideration of instrument line shape and field of view, refraction, line coupling, non-local thermodynamic equilibrium (non-LTE), water vapour continuum, chi-factors etc.). This approach was chosen in order to better be able to trace back differences in calculated spectra. Test cases are summarized in Tables 6.1 and 6.2.

Generation of Vibrational Temperatures

For non-LTE radiative transfer calculations, vertical profiles of vibrational temperatures are needed as input quantity. Since test calculations contained non-LTE scenarios, vibrational temperatures for the atmospheres defined there were needed. Therefore, profiles

Table 6.1: Cell Transmittance Test Cases

Test Id. /	Spectral Region cm^{-1}	Cell Length m	Species	VMR ppmv	p hPa	T K	Continua	Chi Factor	Line Mixing	ILS
1	1270.0–1280.0	5.0	N_2O[1]	100	1013.25	296	/	/	/	/
2	1274.2–1275.0	5.0	N_2O[1]	100	20.0	296	/	/	/	/
3	1274.2–1275.0	20.	N_2O[1]	100	2.0	296	/	/	/	/
4	1274.2–1275.0	20.	N_2O[1]	100	2.0	296	/	/	/	yes[2]
5	1274.2–1275.0	20.	N_2O[1]	100	2.0	296	/	/	/	yes[3]
6	1274.2–1275.0	20.	N_2O[1]	100	2.0	296	/	/	/	yes[4]
7	1270.0–1280.0	5.	N_2O[1]	100	1013.25	250	/	/	/	/
8	1274.2–1275.0	5.	N_2O[1]	100	20.0	250	/	/	/	/
9	1274.2–1275.0	20.	N_2O[1]	100	2.0	250	/	/	/	/
10	1830.0–1840.0	50.0	NO N_2O O_3	$5. \times 10^2$ $5. \times 10^5$ $1. \times 10^5$	20.0	250	/	/	/	/
11	2390.0–2500.0	10^6	CO_2	355	250	296	/	yes	/	/
12	2390.0–2500.0	10^6	CO_2	355	250	250	/	yes	/	/
13	715.0–725.0	50.0	CO_2	355	250	250	/	yes[5]	yes	/
14	715.0–725.0	50.0	CO_2	355	50	250	/	yes[5]	yes	/
15	738.0–744.0	500.0	CO_2	355	250	250	/	yes[5]	yes	/
16	738.0–744.0	1000.0	CO_2	355	50	250	/	yes[5]	yes	/
17	1600.0–1610.0	100.0	H_2O	1000	250	250	yes	/	/	/

[1] only one transition at 1274.6166 cm^{-1} to be considered.
[2] unapodized instrument line shape
[3] apodized instrument line shape
[4] apodized simplified (pretabulated) instrument line shape
[5] chi–factor may not be active in this microwindow under consideration of line mixing.

of vibrational temperatures have been calculated with the IAA non-LTE models for all important bands of all relevant species for various climatological conditions. Within this project the Generic RAdiative traNsfer AnD non-LTE population Algorithm (GRANADA) was developed and applied to most of the species. The model was extended and improved to previous version of vibrational temperatures in many aspects: 1) use of physically consistent reference atmospheres; 2) small deviations from LTE in the stratosphere were removed; 3) a better estimation of the upwelling tropospheric flux; 4) new models for O_3, NO, N_2O; 5) added OH; 6) thorough intercomparison with other non-LTE models; 7) extension in the number of vibrational levels included for many molecules; and 8) updates in the non-LTE parameters for many species. This exhaustive dataset was made accessible to the consortium via the AMIL2DA web-site.

Table 6.2: Atmospheric Radiance Test Cases

Test Id.	Spectral Region cm^{-1}	tangent altitude km	Species Considered	FOV	ILS	Continua	Line Mixing	non LTE
18[1]	1215.0–1217.0	15	H_2O, CO_2, O_3 N_2O, CH_4	/	/	yes	/	/
19[2]	1215.0–1217.0	15	H_2O, CO_2, O_3 N_2O, CH_4	/	/	yes	/	/
20	1215.0–1217.0	40	H_2O, CO_2, O_3 N_2O, CH_4	yes	yes	yes	/	/
21	1215.0–1217.0	15	H_2O, CO_2, O_3 N_2O, CH_4	yes	yes	yes	/	/
22	790.0–794.0	15	CO_2, O_3	/	/	/	yes	/
23	790.0–794.0	15	CO_2, O_3	yes	yes	/	yes	/
24	920.0–940.0	15	CO_2, O_3, CFC-12	/	/	/	yes	/
25	920.0–940.0	15	CO_2, O_3, CFC-12	yes	yes	/	yes	/
26	1600.0–1610.0	10	H_2O, N_2O, CH_4 O_2, NO_2	yes	yes	yes	/	/
27	675.5–676.5	100	CO_2, O_3	yes	yes	yes	/	/
28	675.5–676.5	100	CO_2, O_3	yes	yes	yes	/	yes
29	967.0–968.0	100	CO_2, O_3	yes	yes	yes	/	/
30	967.0–968.0	100	CO_2, O_3	yes	yes	yes	/	yes

[1] standardized altitude grid of 1 km used for integration of radiative transfer equation.
[2] default altitude grid used for integration of radiative transfer equation.

Comparison of Radiance Spectra

Participating groups calculated spectra for the defined scenarios with their radiative transfer forward models. These spectra then were intercompared in order to detect and understand deficiencies in the radiative transfer codes. Possible reasons for differences were discussed and validated by additional test calculations. As main reasons for differences were identified: Different implementation of the Voigt algorithm; different handling of far wings of lines; different gridding for integration of the radiative transfer equation and field of view integration; different specification of the algorithms. Some did not support non-LTE, line coupling, presure shift, refraction. Sample spectra are shown in Figs. 6.1–6.3.3.

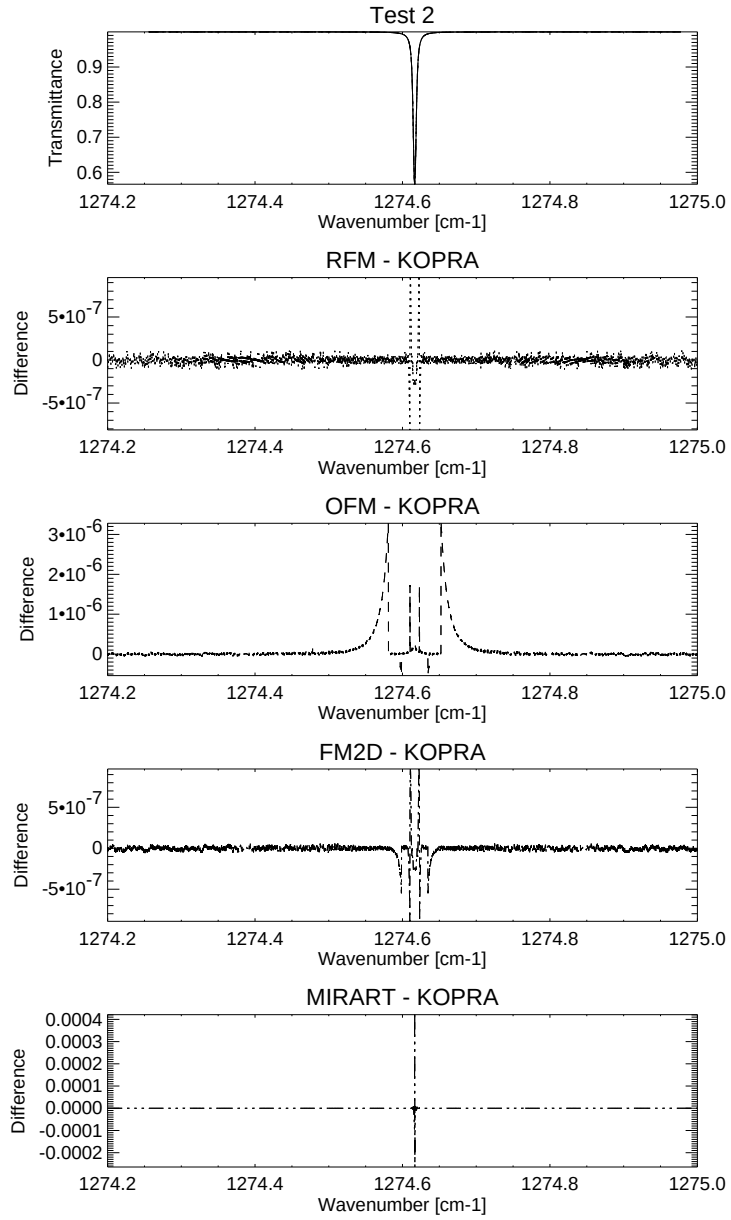

Figure 6.1: Single line transmission spectra (test case 2). The uppermost panel shows the spectra, whereas the other panels show difference spectra with respect to KOPRA. Differences between the spectra are so small that they are not resolved in the uppermost panel, which indeed includes all five spectra under investigation.

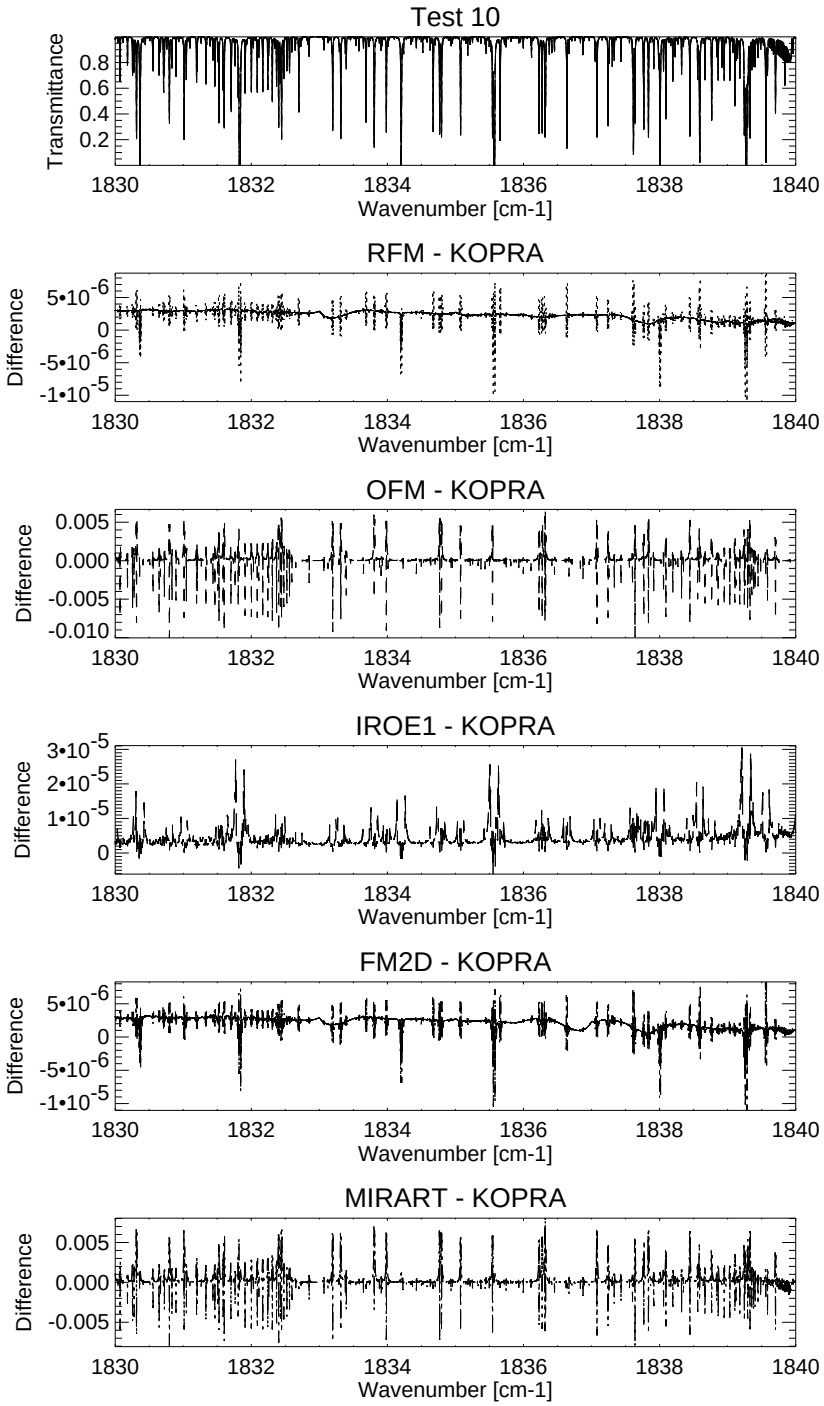

Figure 6.2: Multi-transition transmittance spectra (test case 10). The uppermost panel contains the spectra, whereas the other panels show difference spectra with respect to KOPRA. Differences between spectra are so small that they are not resolved in the uppermost panel. Continuum-like differences are attributed to different treatment of the far wings of lines.

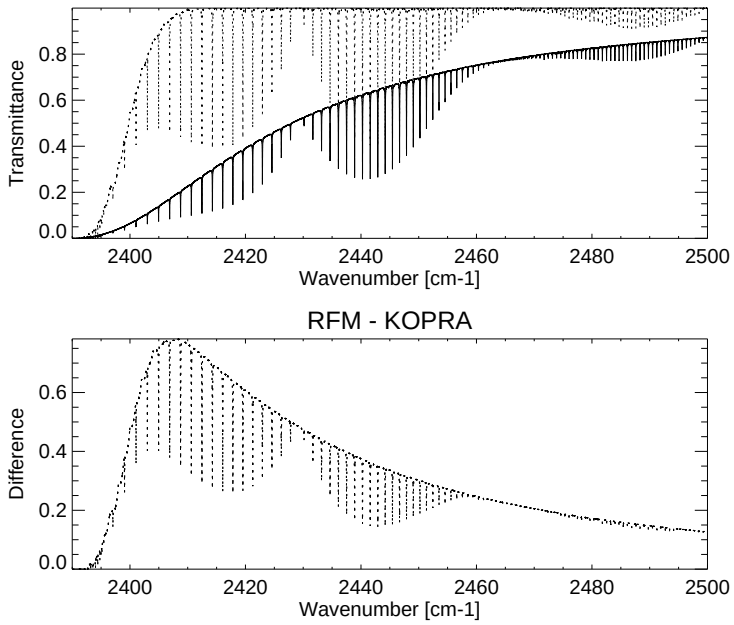

Figure 6.3: Transmittance difference between RFM (dotted line) and KOPRA (solid line) in the 4.3 μm-region. Differences are attributed to different line rejection criteria. The test scenario is as for test case 11 except that no chi-factor has been applied. Differences are attributed to different line rejection criteria.

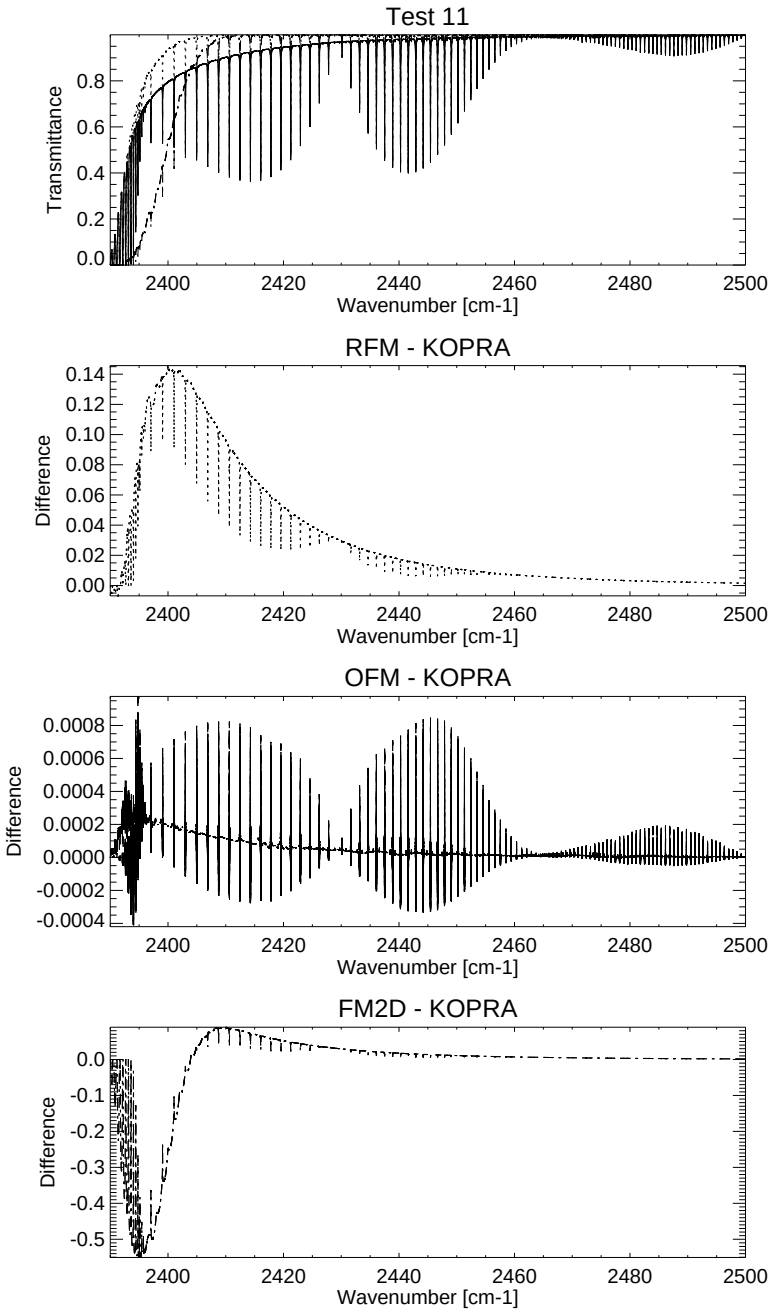

Figure 6.4: Chi-factor (test case 11). The uppermost panel shows the transmittance spectra, whereas the other panels show difference spectra with respect to KOPRA. Again, differences are attributed to different line rejection criteria, while there is no evidence of any chi-factor related problems.

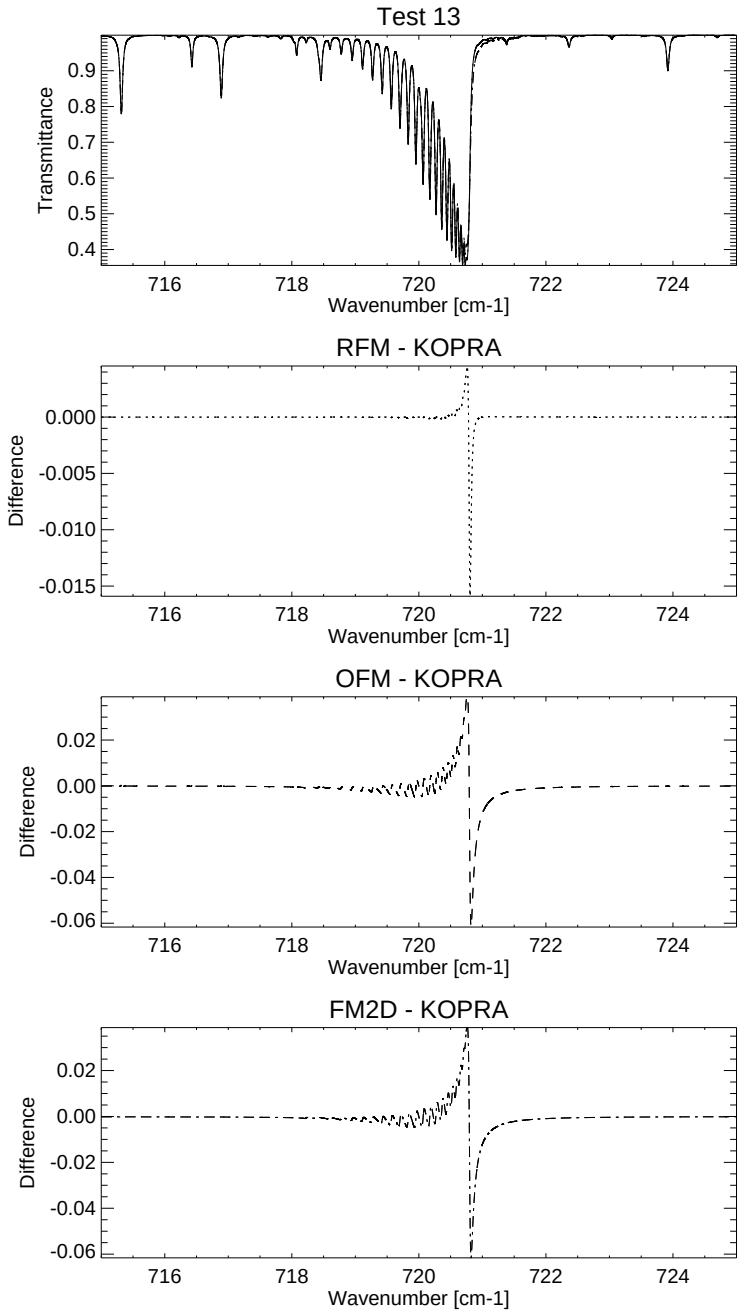

Figure 6.5: Q–branch line coupling (test case 13). The uppermost panel shows the transmittance spectra, whereas the other panels show difference spectra with respect to KOPRA. Differences between spectra are so small that they are hardly resolved in the uppermost panel. Neither OFM nor FM2D support line-coupling, which explains the difference. Differences between RFM and KOPRA are attributed to different line-coupling implementations (direct diagonalization versus Rosenkranz approximatuion).

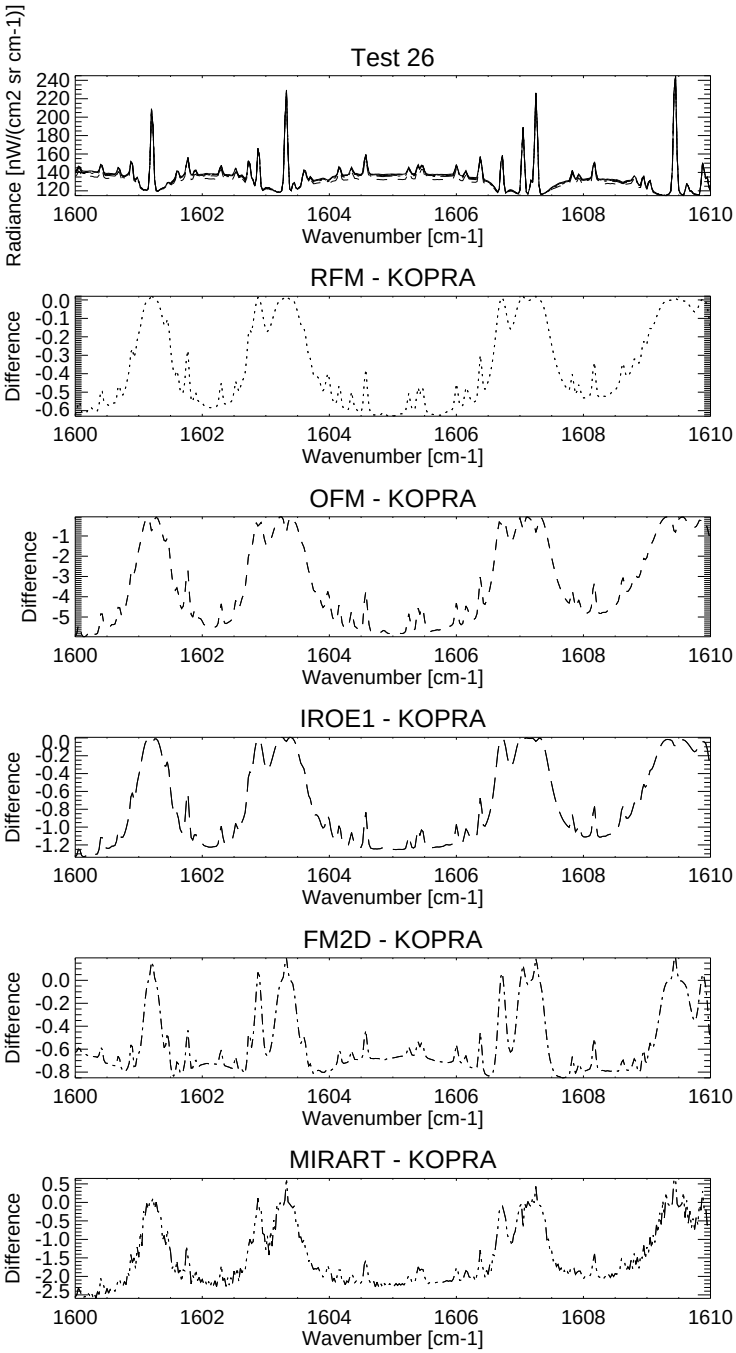

Figure 6.6: Water vapour continuum (test case 26). The uppermost panel are radiance spectra (KOPRA: solid; RFM: dotted; OFM: dashed; IROE1: long dash; FM2D: dashed–dotted (overlaid with RFM); MIRART: dashed doubledotted). The other panels show difference spectra with respect to KOPRA. Differences are attributed to the use of different versions of the CKD water vapour continuum.

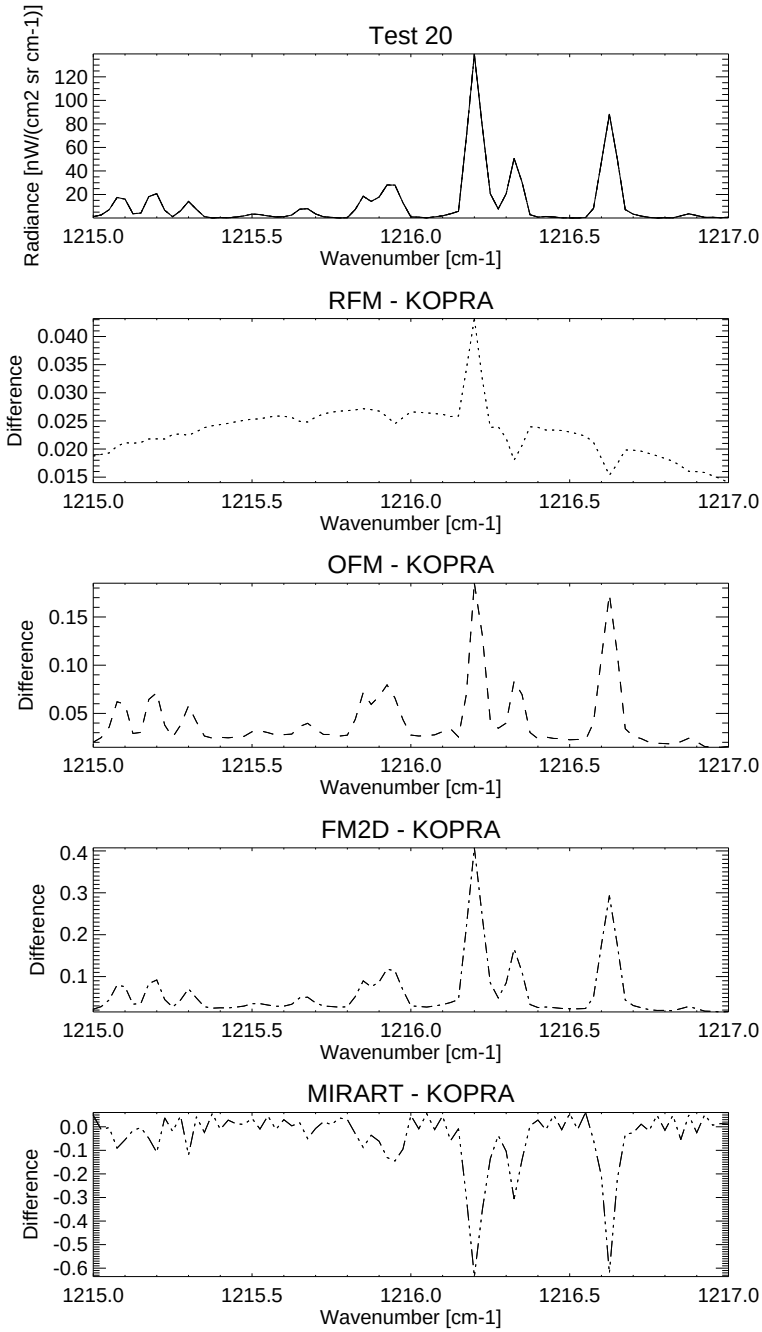

Figure 6.7: FOV-convolved radiance spectra (test case 20). The uppermost panel shows the spectra for all codes (not distinguishable from each other), whereas the other panels show difference spectra with respect to KOPRA. Differences are explained by different numerical integration of spectral radiances over the instrument field of view.

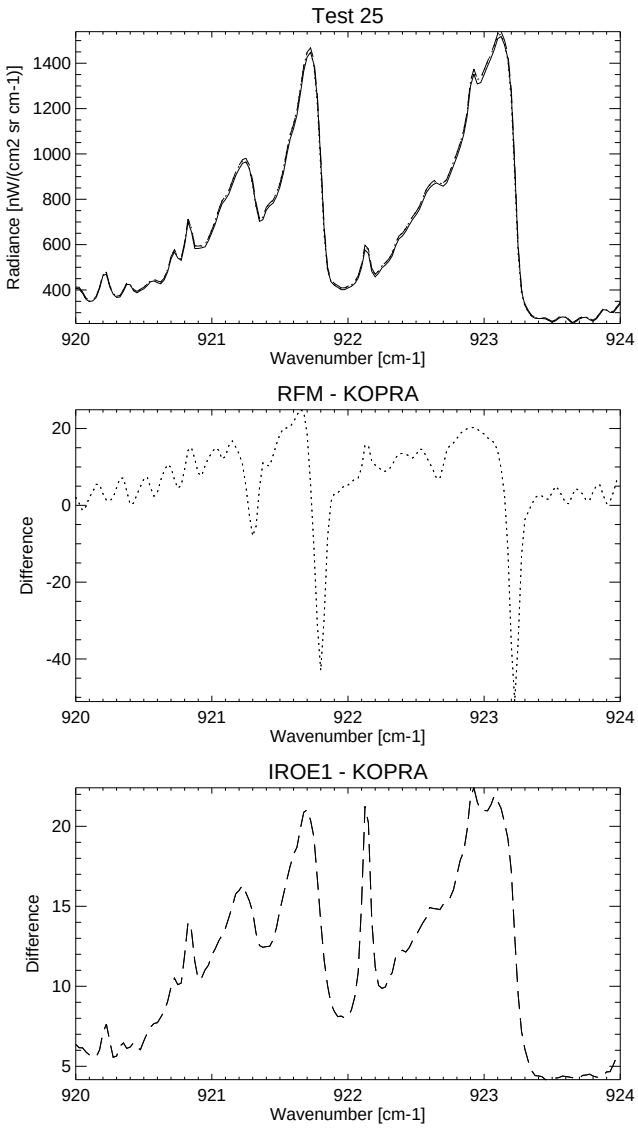

Figure 6.8: Emission spectra of CFC-12 (test case 25). The uppermost panel includes the spectra (KOPRA: solid; RFM: dotted; IROE1: long dashes). The other panels show difference spectra with respect to KOPRA. Differences are explained by different interpolation approaches of absorption cross sections in pressure and temperature.

Fixing of Radiative Transfer Modelling Problems

Some differences in calculated spectra hinted at deficiencies in the related radiative transfer models. These were removed.

KOPRA: A problem in KOPRA was discovered with respect to self broadening. When the HITRAN parameter for self-broadened halfwidth was set to zero (i.e. unknown). The code was changed in a sense that it is now set equal to the air-broadened halfwidth (which should never be zero in HITRAN). Problems with numerical accuracy of field-of-view discretization appeared in the exercises where instrumental field-of-view is taken into account. It became clear that five pencil beams (as originally used) were not enough to get good comparisons with models using higher discretization. Setting this number to 17 solved the problem. (This is a change in a parameter of the KOPRA input file and no changes in the program itself were necessary).

The **RFM** was already a well-developed and validated code at the start of the project so major changes or improvements were not foreseen. In the event one or two minor improvements were made and some relatively obscure bugs associated with previously untried combinations of options were detected and fixed.

Some differences in **MIRART** spectra hinted at a different sign convention used for field-of-view convolution, which then was removed.

With respect to the **ORM**, self-broadening of spectral lines was included; pressure shift was included; the H_2O continuum model was updated from CKD 2.1 to CKD 2.4; CO_2 Q-branch line-mixing has been implemented using the approach of Hartmann and the calculation can be done exploiting either the full relaxation operator or the first order approximation (less time consuming); a functionality was added that allows to include in the calculations the emission of heavy molecules (e.g. N_2O_5, $ClONO_2$, CFCs etc.) that is characterized by broad spectral features simulated by means of pre-tabulated absorption cross-sections.

No major problems were found with the **FM2D**. Tests indicated that the set-up of the forward model was not optimal for some cases. In particular, the number of atmospheric levels in the atmospheric model and the number of monochromatic pencil beams used in the calculation were shown to be important. The set-ups were adjusted accordingly.

6.3.4 Blind-test on Basis of Synthetic Data

Spectra for realistic conditions were generated at IAA and superimposed with realistic measurement errors. These spectra were distributed among the consortium. Information on the atmospheric state and part of the instrument parameters was kept secret. Participating institutions tried to retrieve the state of the atmosphere from these spectra. Deviations

of the retrieved vertical profiles of state parameters from the reference profiles hinted at problems with the related retrieval codes, which then were removed.

For the polar summer test scenario (80^oN latitude, 12.00 h local time, 70^o SZA), a set of self-consistent atmospheric parameters has been generated by means of a chemical transport model. Some additional gravity-wave like vertical structure has been added to the temperature profile. For these set of state parameters, a complete set of vibrational temperatures has been generated. These data were used for radiative transfer forward calculations for the MIPAS observation geometry. Resulting spectra were superimposed with noise and zero-offset calibration error. These synthetic measurements spectra were distributed among the consortium along with some ancillary data (nominal measurement geometry, geolocation time of measurement, instrument specification etc.), while some relevant instrument state parameters and all atmospheric state parameters (actual instrument pointing, zero offset calibration) were kept secret (with one exception, see below).

Two such sets of measurements were distributed: In blind test 1 (BT1), the temperature profile and actual instrument pointing in terms of tangent altitude was known to the consortium, while in blind test 2 (BT2) these quantities were unknown to the participants. This was done in order to give those groups an opportunity to participate, whose data processor was not specified for temperature and tangent altitude retrieval but who relied on ESA-provided temperatures and tangent altitudes.

Blind Test Retrievals

IMK, Oxford University, DLR, IFAC, and RAL tried to retrieve the most possible amount of information on atmospheric state parameters from the synthetic measurements spectra. Comparison of the retrieved data with the reference data made then the particular strengths and weaknesses of the various retrieval processors visible.

IMK: Tangent altitudes as well as vertical profiles of temperature, O_3, HNO_3, NO_2, H_2O, N_2O, CH_4, CFC-11, CFC-12, HCFC-22, $ClONO_2$, N_2O_5, and NO were retrieved with the IMK-RCP. The functionality of the IMK-RCP allows retrieval of key-species and species beyond key species. However, some tuning of the processing parameters, particularly strength of regularization, had become necessary. The following characteristics of the IMK-RCP retrievals were found: LOS: In spite of a bad temperature/pressure a priori profile chosen in this study, the knowledge of the absolute line of sight information is improved by a factor of two with respect to the a priori. Relative line-of-sight errors are in the order of a few tens of meters above 30 km altitude but increase towards larger values below. Temperature is retrieved nicely by the IMK code. While the overall structure of the profile is well recovered without smearing out any relevant features, no oscillations in the retrieval are visible. O_3: BT1 retrievals match with the reference profile nicely, while some overshooting of the upper of the two maxima of the profile is evident in BT2. HNO_3: In BT1 the profile is well recovered except for a minor dip near the VMR max-

imum. In BT2, the retrieval tends to oscillate around the reference profile near its peak. NO_2: In BT1 the peak is slightly overestimated, while in BT2 the profile seems to be shifted slightly towards higher altitudes. H_2O: In BT1 the profile is well recovered, except for minor oscillations and the hygropause, which is not fully resolved. In BT2 the oscillations are amplified in the higher atmosphere but the hygropause is better resolved. N_2O: is well retrieved both in BT1 and BT2. Some deviations at the lowermost end of the profiles are fully explained by the estimated errors. CH_4: is well retrieved both in BT1 and BT2 except for the lower end of the profiles. CFC-11: The IMK CFC-retrievals show some oscillations, which are within the estimated noise error. These are induced by the inappropriate a priori profile shape, which is conserved within some of its segments by first order Tikhonov regularization. The reference profile is recovered nicely by the IMK CFC-11 retrieval between 13 and 20 km. CFC-12: Some oscillations of similar type as for CFC-11 have been found. HCFC-22: retrievals show some oscillations around the reference profiles, of similar nature as for CFC-11 and CFC-12. They seem to be caused by the segmental mapping of the a priori profile shape on to the retrieval. $ClONO_2$: The retrieval is largely dominated by the initial guess, since there is so small amount of $ClONO_2$ in the reference atmosphere that there is only weak $ClONO_2$ signal. N_2O_5: There is such a small amount of N_2O_5 in the reference atmosphere that the profile is difficult to retrieve. The mixing ratio peak at 25 km is recovered by the IMK retrieval. Around 40 km spectra do not contain much information such that the result is dominated by the initial guess. Some negative overshooting at 20 km appears to be either some error correlation with other altitudes or with continuum.

Oxford University: performed retrievals of: Temperature, relative tangent altitudes, O_3, HNO_3, H_2O, CH_4, N_2O, NO_2, CFC-11, CFC-12, $ClONO_2$, and N_2O_5. Also at Oxford University microwindows for CFC-12 global retrieval have been selected and applied to the blind test data. The retrieved profile is in reasonable agreement with the reference profile, but there are discrepancies at lower altitudes. Also the Oxford University group has selected microwindows for CFC-11 global retrieval and applied them to the blind test data. The retrieval underestimates the CFC-11 concentrations at lower altitudes, but the difference from the true profile is within the error bars. On the whole, the reference profile is recovered well. Also for CFC-11 there seems to be a correlation of retrieval errors between IMK and Oxford results. For possible explanation, see the CFC-12 section. Also Oxford University group has selected microwindows for $ClONO_2$ global retrieval and has applied them to the blind test data. The maximum in the reference profile has not been captured well in the retrieval. This could be due to systematic error contributions in this altitude region. An attempt to select global microwindows for N_2O_5 retrieval suggested not enough signal/noise for a useful retrieval, but repeating the test confined to mid-latitude night-time retrieval scenario was more successful. The N_2O_5 retrieval was not very successful. The difficulties are probably due to a very low signal to noise ratio for N_2O_5.

The following data products were retrieved with the **DLR-a** processor (BT1 only): O_3, HNO_3, CH_4, N_2O, NO_2. The ozone profile is reasonably well retrieved. Mixing ratios

below 22 km are overestimated. The HNO_3 profile is reasonably well retrieved. Mixing ratios below 25 km are underestimated. The NO_2 profile is retrieved within the estimated error margin. CH_4 is almost perfectly retrieved; errors seem to be overestimated. N_2O is reasonably well retrieved; errors at lower altitudes seem to be overestimated.

The following data products were retrieved with the **D-PAC** processor: Temperature, H_2O, O_3, HNO_3, CH_4, N_2O, NO_2. There are large LOS fluctuations which could be removed by an upgraded processor setup. Temperature is reasonably well retrieved, with some evidence of mapping of LOS errors to the temperature profile. Retrieved O_3 fits almost perfectly to the reference profile. Retrieved HNO_3 fits well to the reference profile. While the general shape of the NO_2 retrieval coincides with the reference profile, some oscillations in the retrieval hint at a too weak regularization. H_2O is well retrieved for all stratospheric altitudes. CH_4 is well retrieved in the stratosphere, but there are some problems at lowermost altitudes.

The following data products were retrieved with the **IFAC**: Temperature, relative tangent altitudes, H_2O, O_3, HNO_3, CH_4, N_2O, NO_2 (all species both for BT1 and BT2). Relative tangent altitudes are underestimated below 25 km and overestimated above 40 km. Temperature is well retrieved. The O_3 and NO_2-retrievals (BT1 and BT2) recover the reference profile within the estimated error margin. The maximum of the HNO_3 profile is slightly underestimated in BT1 but not in BT2. Stratospheric H_2O (BT1 and BT2) is well retrieved, but there are problems to resolve the hygropause (as with most of the other processors). N_2O (BT1 and BT2) is almost perfectly retrieved. CH_4 (BT1) is reasonably well retrieved, but there seems to be an instability at the lower end of the profile, which is more pronounced in BT2 than in BT1. NO_2 is reasonably well retrieved.

The **RAL** processor should be used to retrieve the accurate H_2O and O_3 profiles with special emphasis on the upper troposphere/lower stratosphere region. Comparison of the retrieved data with the reference data should then make visible the particular strengths and weaknesses of this retrieval processor. For real data retrievals, it is envisaged that external information on temperature, pressure and pointing, such as ECMWF analyses combined with standard MIPAS pressure/temperature products, will be employed and so no temperature/pressure/pointing retrieval tests were carried out for the RAL processor. H_2O and O_3 profiles have been retrieved simultaneously, with joint fitting of some further contaminant species including CO_2, N_2O, CH_4, NO_2 and HNO_3. After some upgrading of the processor and optimized setting of the processing parameters, good retrievals of ozone and water vapour were obtained for blind test BT1. The structure in the ozone profile is well recovered. At the lower altitudes the water vapour retrieval shows small deviations from the reference indicating the difficulty in determining H_2O mixing ratios in this region of rapidly changing concentrations.

Comparison of the different groups' retrievals was based on visual inspection of retrieved profiles versus reference profiles. In order to assess the significance of deviations, the ratio of empirical over predicted sum of variances was calculated. Normalized retrieval

errors (as proxy of chi square) are listed in Table 6.3. These are unity when the deviation of the retrieval from the reference profile is consistent with the estimated retrieval error. Results are shown in Figs. 6.9–6.15.

Table 6.3: Normalized retrieval errors

	IMK-RCP	OPTIMO	DLR-a	D-PAC	ORM	RET2D
O_3 (BT1)	1.42	4.52	2.83	0.76	0.96	4.20
HNO_3 (BT1)	2.21	4.90	3.72	215.4	13.2	
NO_2 (BT1)	0.98	1.27	1.01	52.6	5.18	
H_2O (BT1)[a]	3.19	82.5		2469.		5.11
H_2O (BT1)[b]	0.64	1.12		3.17	1.62	1.63
CH_4 (BT1)	0.74	2.01	0.70	3.06	0.75	
N_2O (BT1)	2.11	3.09	1.04	1.25	1.22	
O_3 (BT2)	1.60	1.10			1.27	
HNO_3 (BT2)	8.10	31.9			3.07	
NO_2 (BT2)	1.29	4.77			6.20	
H_2O (BT2)[a]	0.99	9.31				
H_2O (BT1)[b]	0.87	1.65			1.62	
CH_4 (BT2)	0.65	1.97			0.91	
N_2O (BT2)	0.56	1.43			0.62	

[a] with consideration of tropospheric values
[b] without consideration of tropospheric values

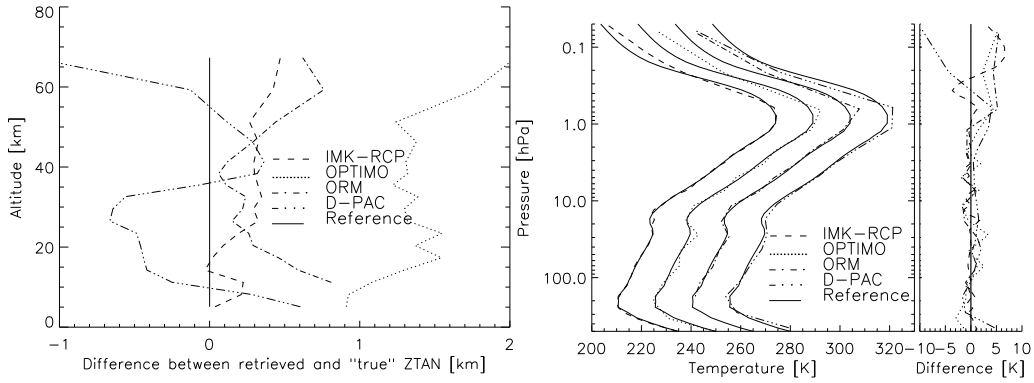

Figure 6.9: Results of blind test line of sight retrievals (left figure) and temperature retrievals (right figure) .Temperature results of different processors are shifted horizontally by 10 K each for clearer representation. In the right panel of the right figure the differences between the retrieved profiles and the reference profile are shown.

Lessons learned from the blind test study were at **IMK**: Joint retrieval of CH_4 and N_2O turned out to be more accurate and more efficient than sequential single retrievals. A continuum constraint in the wavenumber domain was found to stabilize the retrievals. The

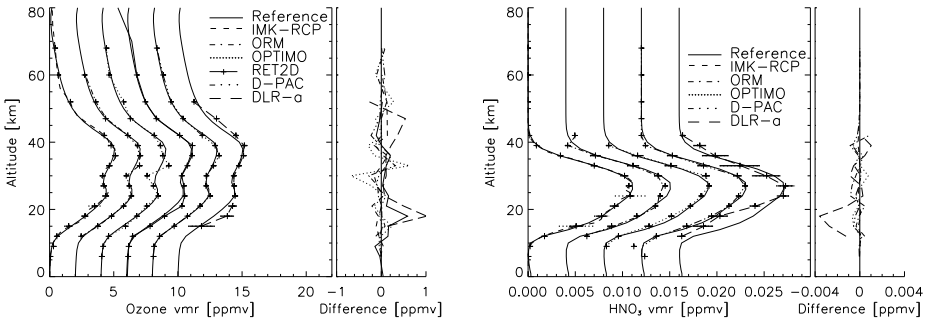

Figure 6.10: Retrieved ozone and HNO_3 profiles, BT1. Error bars for random error (solid line) and systematic errors (dotted line) are included. Results of different processors are shifted horizontally by 2 ppmv (O_3) and 0.004 ppmv (HNO_3) each for clearer representation. In the right panels the differences between the retrieved profiles and the reference profile are shown.

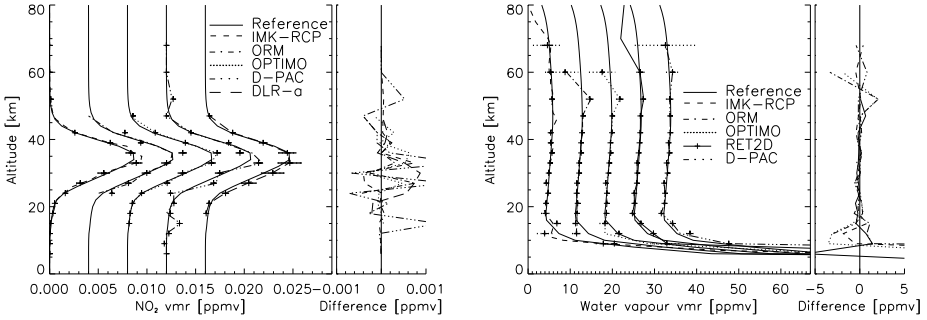

Figure 6.11: Retrieved NO_2 and H_2O, BT1. Results of different processors are shifted horizontally by 0.004 ppmv (NO_2) and 7.0 ppmv (H_2O) each for clearer representation.

NO_2 microwindow selection was changed in order to achieve better performance at stratospheric altitudes. The altitude dependence of regularization parameters was optimized.

At **Oxford University**, the BT1 spectra (known pointing) were used during the blind-test to refine the handling of the a priori pointing information. After the input profiles were known, an additional retrieval level was added to OPTIMO above the top of the measurement range in order to constrain the high altitude column. The blind test results indicated no serious problems with the retrieval, although oscillations in profiles and some difficulty handling continuum were evident. Solutions for these problems were deferred until more experience was gained with real data.

The following upgrades were performed for the **DLR-a** processor: The regularization parameter selection was simplified by using an approximate scheme for localizing the corner of the L–curve. The use of a bound–constraint algorithm was found to improve the

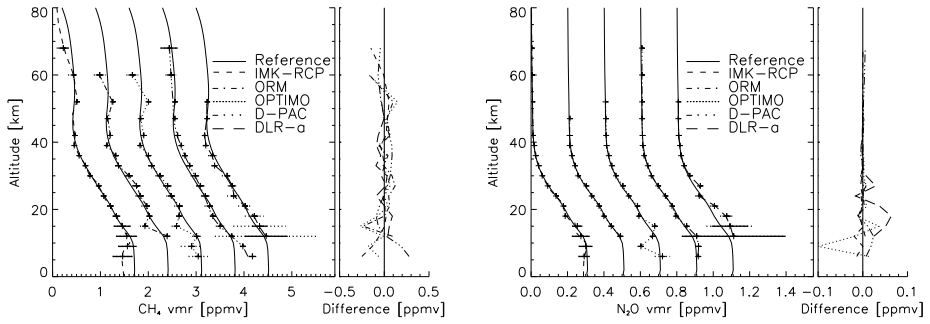

Figure 6.12: Retrieved CH_4 and N_2O, BT1. Results of different processors are shifted horizontally by 0.7 ppmv (CH_4) and 0.2 ppmv (N_2O) each for clearer representation.

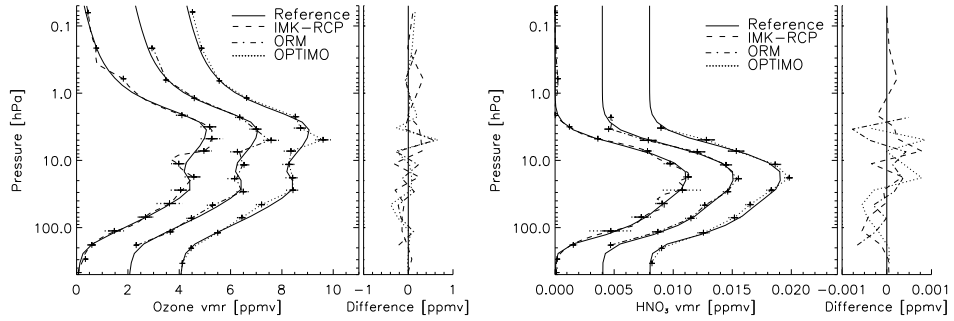

Figure 6.13: Retrieved ozone and HNO_3 profiles, BT2. Results of different processors are shifted horizontally by 2 ppmv (O_3) and 0.004 ppmv (HNO_3) each for clearer representation.

retrievals.

The following upgrades were performed for the **D-PAC** processor: Common agreements of how to identify selected scans within orbit data were found; identification of scans with significant pointing offsets; Introduction of pre-retrievals generating consistent initial guess profiles; improved parameter selections providing mostly stable profile retrievals; selection of sweeps affected by clouds and retrieval of partial scans together with appropriate handling of regularisation matrices; Provision of additional test interfaces and analysis tools.

The intercomparison work did not highlight dramatic deficiencies of the IROE-R (**IFAC**) processor in terms of accuracy. Therefore it was decided to update the algorithm and to develop tools in order to allow for a quantification and possibly for a correction of the errors associated to both some instrument-related parameters and some assumptions adopted in the ESA's Level 2 algorithm. The "improved" version of the IROE-R code, named IROE-I (-I=improved), does not represent an improvement in terms of retrieval

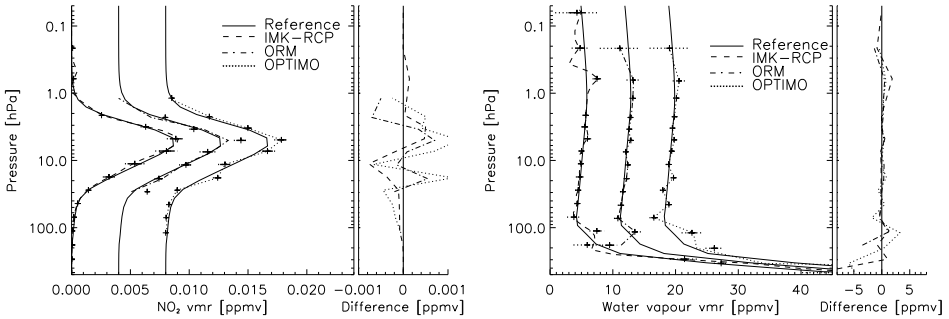

Figure 6.14: Retrieved NO_2 and H_2O, BT2. Results of different processors are shifted horizontally by 0.004 ppmv (NO_2) and 7.0 ppmv (H_2O) each for clearer representation.

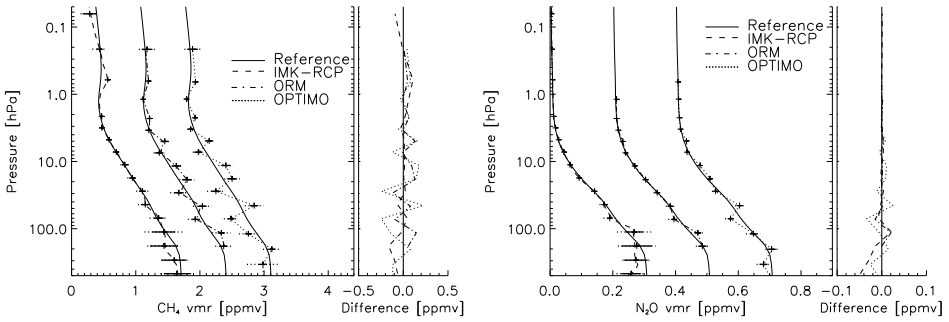

Figure 6.15: Retrieved CH_4 and N_2O, BT2. Results of different processors are shifted horizontally by 0.7 ppmv (CH_4) and 0.2 ppmv (N_2O) each for clearer representation.

accuracy, however it includes some diagnostic functionalities allowing to characterise the residuals of the IROE-R and to check the behaviour of some instrument-related parameters derived in Level 1b processing and assumed as known in the Level 2 chain. Compared to the IROE-R, the IROE-I code includes now, as new functionalities, the option to retrieve from the analyzed spectra the following instrument-related parameters: ILS broadening, frequency shift, intensity calibration, height- and altitude- dependent instrumental offset. An additional functionality of the IROE-I processor is the capability of retrieving further species beyond the key ones that can be retrieved by the IROE-R processor. The discrepancies between the profiles retrieved by the IROE-R processor and the other processors considered in the study were analyzed and compared with the various retrieval error components. These discrepancies were found to be mostly consistent with the applicable retrieval error. For the cases in which the observed discrepancies exceed the retrieval error a possible explanation was searched and, whenever possible, it was supported with further test calculations.

Early comparisons indicated an artifact in minimisation routines of the **RAL** processor often leading to large, unrealistic oscillations in the retrieved products. The problem was

addressed and corrected.

Standardized Calculation of Retrieval Errors

A generalized approach on error assessment was developed, which allowed comparison of retrieval errors of different processors. The method used was to adapt the Oxford MIPAS microwindow selection algorithm to handle the various microwindows, forward model and retrieval assumptions (e.g. sequence, joint-retrievals) used by the different groups in order to provide a uniform error analysis.

On the basis of standardized perturbance spectra and Jacobians, the mapping of both random and systematic errors onto the retrieved state parameters was calculated for the individual microwindow selections and retrieval altitude ranges on the basis of standardized assumptions on primary error sources. The following sources of error were considered: noise, uncertainties in atmospheric state parameters (abundances of contaminant species and temperature, horizontal gradients of atmospheric state parameters), modeling errors (non-local thermodynamic equilibrium, line-mixing, spectroscopic data), and instrument parameters (gain and frequency calibration errors, pointing). According to the particular application, additional datasets were generated, where only the subset of error sources relevant to the actual application were considered (e.g. for the blind test, where horizontal gradients were not applicable).

Estimated standardized retrieval errors allowed to judge if deviations of retrievals from the reference profiles are significant or if they can be explained by assumed uncertainties in ancillary parameters. These analyses also provide information on which systematic are likely to be significant (and, equally importantly, insignificant) when validating the retrievals of each group.

6.3.5 Application to MIPAS Data

After successful validation of processors on the basis of synthetic data, the robustness of the processors was demonstrated by application to real MIPAS data. Furthermore, contributions to the characterization of the MIPAS instrument and level 1 data (calibrated radiance spectra) were made.

MIPAS data of the orbits 504, 2081, 2082, and 2083 have been made available to the consortium. For a more detailed intercomparison, limb scans 3, 12, 20, 36, and 68 of orbit 2081 were selected. The selected scans contain no or low clouds and comprise the atmospheric states of polar summer (scan 3), polar winter (36), midlatitude day/night (12/68), and equatorial (20).

For intercomparison, profiles of temperature, H_2O, O_3, HNO_3, NO_2, CH_4 and N_2O were retrieved by the participants. Beyond this, some groups (IMK, OU, DLR) have included a considerable number of non-key species (CFC-11, CFC-12, $ClONO_2$ and N_2O_5; also investigations on retrievals of SO_2, SF_6, OCS and NH_3).

At **IMK** retrievals of the following species were performed: O_3, H_2O, HNO_3, CH_4, N_2O, NO_2, OCS, ClO, SF_6, C_2H_6, H_2O_2, $ClONO_2$, N_2O_5, NH_3, CCl_4, HOCl, CFC-11, CFC-22, HCFC-22. Results for most species are considered realistic. Beside this, at IAA, who now operate the same processor in close co-operation with IMK, O_3, NO, NO_2, CO, pressure and temperature, under consideration of non-LTE have been retrieved. After minor upgrading with respect to frequency calibration correction, the IMK processor proves to be robust when applied to real MIPAS data. Remaining problems hint rather at irregularities in MIPAS data than inappropriate processing.

At **Oxford University**, it was also necessary to convert OPTIMO from a single profile retrieval to a sequential retrieval, and write scripts so that a complete orbit could be processed. Further code optimisations were also made to reduce CPU time. The validation effort has mostly focussed on orbit 2081 (24Jul02), for which Level 1 data was supplied by ESTEC. Experience with real data has identified a problem with ESA's handling of the non-linearity correction on forward and backward interferometer sweeps during L1 processing, and has been used to provide feedback to ESA for subsequent improvements. Residuals have also shown similar spectral shift characteristics to the initial ESA retrievals. This, and comparison with preprocessor outputs with the Italian groups, has verified that the problem is with the AILS characterisation. Retrievals for the following species have been attempted: O_3, H_2O, HNO_3, CH_4, N_2O, NO_2, N_2O_5, $ClONO_2$, CFC-11, CFC-12, CFC-14, CFC-22, NH3, HCN, COF_2, OCS, SF_6, C_2H_6, HOCl, SO_2, H_2O_2, ClO and CCl_4. Particular effort has been applied to retrieving SO_2 to detect enhancement in the region of Mt Etna. Additional studies have been performed on the feasibility of retrieving isotopic ratios, CO_2 concentrations and joint CO volume mixing ratio and vibrational temperature profiles.

DLR-a provided retrievals of O_3, H_2O, HNO_3, CH_4, N_2O and NO_2. The DLR-a processor gives accurate results when applied to real MIPAS data. Deviations from other results are due to the use of altitude independent microwindows. Furthermore temperature and molecular concentration retrievals were performed with a climatological pressure profile, i.e., without line-of-sight retrieval.

The **D-PAC** processor was used for the retrieval of the following profiles: temperature, pressure, line-of-sight, continuum, H_2O, O_3, NO_2, CH_4, N_2O as well as CFC-11 and CFC-12. Profiles of instrumental offsets had been tested earlier during the retrieval of balloon data. As for Envisat data, these offset profiles are not needed. The comparison of results turned out to be highly important for the precise identification of weak points. The implementation of robust routines could only be accomplished by comparisons on a species by species basis to separate conceptual weaknesses from species-dependent and

parameter selection characteristics.

The following species have been retrieved with the **IFAC** processor: p, T, H_2O, O_3, HNO_3, CH_4, N_2O, NO_2, CFC-11, $ClONO_2$. For the retrieval of the above species from real MIPAS data it was necessary to tune several processing setup parameters. In particular, significant performance improvements were obtained with the optimization of the convergence criteria and of the parameters controlling the evolution of the Levenberg-Marquardt damping during the retrieval iterations. With the optimized setup parameters the IFAC processor is able to reach convergence in all the considered measurement scenarios.

The work at **RAL** was aimed at retrieving accurate H_2O and O_3 profiles from real MIPAS data, with special emphasis on the lower scan altitudes. MIPAS data acquistion and interface of the retrieval software to the MIPAS data structures were required. Work was carried out to acquire and handle MIPAS data, including the production of code for data reading. Auxiliary data, including ECMWF meteorological analyses and MIPAS Climatology files were acquired and handling software developed. The driver files for the forward model were upgraded to allow explicit specification of view, scan number, spectral microwindow. This allows simple specification of forward model parameters for multiple runs including spectral ranges and satellite position. The retrieval model was enhanced to make use of the new forward model options. Measurement details such as scan number can now be taken from the measurement file directly.

Comparison of Results

Retrieved vertical profiles of temperature and volume mixing ratios of key species O_3, H_2O, CH_4, N_2O, HNO_3, and N_2O as well as minor species as retrieved by the participants are intercompared, in order to better characterize the different retrieval approaches and to verify the applicability of the data processors to the use of real measurement data. Due to the fact that not all groups are able to process entire orbits and in order to concentrate the intercomparison on a significant data set, the scan numbers 3, 12, 20, 36, and 68 of orbit 2081 were selected for detailed intercomparison.

In the following intercomparison two example cases from orbit 2081 and scan 12 (mid-latitude conditions) are shown. The ozone results of the different groups are depicted in Figure 6.16 (left plot). Good agreement between the groups is found, with a few exceptions. The original IMK-RCP result suffered from wrong spectral shift assumptions (dashed line). When using the retrieved spectral shift the lower values at 60 hPa and higher values at 20 hPa vanish and the IMK-RCP ozone result is much closer to the result of the other groups (red line in Figure 6.16 left). The D–PAC (and less pronounced the DLR-a) result seems to underestimate ozone between 1 and 10 hPa. The standard deviations of the profiles for the different scans show values of up to 1 ppmv in the maximum of the ozone profile (Figure 6.16 middle). This is slightly more than expected from the

blind test experiment but consistent with estimated total errors.

Methane results are shown in Figure 6.16 right. Below 30 hPa the D–PAC values is 0.2 ppmv lower than the corresponding values of the other groups. Small oscillations can be seen in the ORM (IFAC) result and larger oscillations in the OPTIMO (Oxford) result. However, these oscillations and differences are widely consistent with the differences obtained in the blind test experiment.

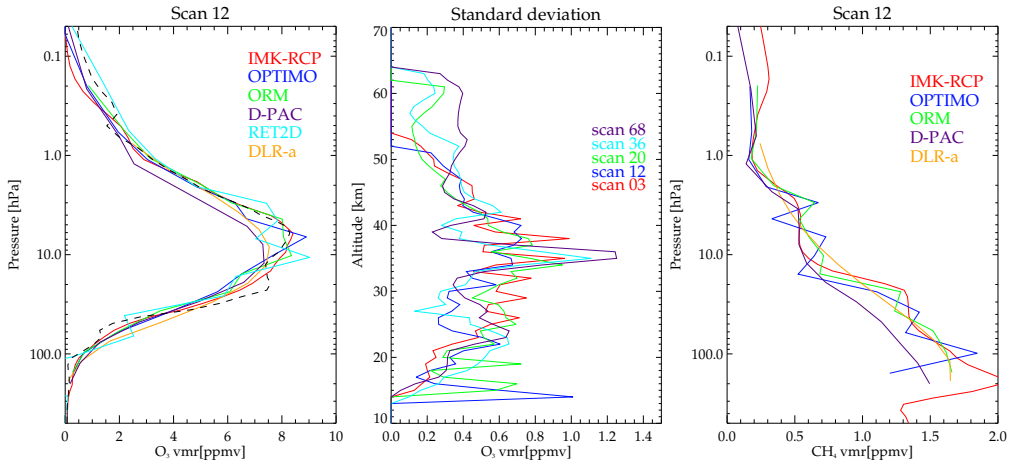

Figure 6.16: Left: Ozone and methane results for scan 12 (midlatitude conditions). Dashed line show the IMK-RCP ozone retrieval without a preceding spectral shift retrieval. Middle: Standard deviation of the different ozone results for the five selected scans. Right: Methane results for scan 12 (midlatitude conditions).

In summary it can be stated that all investigated processors are able to retrieve atmospheric state parameters from MIPAS-Envisat data within explainable differences. For selected scans of orbit 2081 a detailed intercomparison is performed and in general good agreement between the results of the different groups is achieved. This is especially the case for conditions where unexpected large systematic error sources are not present.

There are some cases where larger discrepancies between the groups have been detected: The strength of the regularization and hence the degrees of freedom play an important role in the explanation of the differences in the results. Especially OPTIMO (Oxford) and RET2D (RAL) results tend towards stronger oscillations. In contrast to that DLR-a (all constituents) and D–PAC (mainly temperature) tend to overconstrain their retrievals. D–PAC has already investigated this problem and will change it for future retrievals. The original IMK-RCP results for temperature and ozone were affected by spectral calibration errors. Therefore spectral shift retrieval is performed now as a basic step ahead of the temperature, line of sight and constituent retrievals.

For water vapor, the greatest discrepancies occur at the lowest and highest altitudes. In

the UTLS region water vapor is known to be highly variable and further investigation will be required to discriminate between retrieval sensitivity and artifacts. At high altitudes the error is driven by systematic errors due to non-LTE.

The largest spread in retrieved temperatures occur in the polar winter case (scan 36). It is very likely that systematic errors, especially horizontal temperature inhomogeneities, are responsible for the larger differences in the results of the different groups. This is the case not just in the temperature retrievals but also for the gases. Most of the groups soon will have 2-dimensional or tomographic retrieval algorithms available so that discrepancies due to horizontal inhomogeneities can be investigated in more detail.

A further aspect, detected by the Oxford group, is a systematic difference in calibration between forward and backward recorded spectra of channel A. The reason for the difference is the nonlinearity correction, which is part of the European Space Agency's level-1 processing chain. This systematic error term could also be a reason for oscillations in the retrieval results. However, a slightly stronger regularization reduces systematic errors, mitigates this effect and can therefore be of advantage.

Fixing of Problems

In order to make the **IMK** retrieval processor better applicable to real MIPAS measurements, some final upgrading was to be performed: The altitude dependence of regularization has been slightly changed. The use of ILS parameters has been improved: Now the frequency calibration correction is retrieved for each spectrum individually. Some microwindow selections have been revised, in particular for non-key species. Possible reasons for high biases in retrievals from (nominally cloud-free) spectra recorded at lowermost tangent altitudes have been investigated. Field-of-view problems, problems due to non-linearity, problems with water vapour mixing ratios and temperature profiles are likely to be excluded. Problems can easily be solved by just excluding lowermost tangent altitude from the retrieval but this is not the favored approach.

There has been some iteration between **Oxford University** and ESA who have generated different versions of Orbit 2081 L1B spectra in response to feedback on data quality. From the point of view of the Oxford processor, validation has concentrated on comparing retrievals for this particular orbit with the ESA L2 product and with the 5 profiles selected for AMIL2DA comparisons. The main problem identified was a tendency for the Oxford retrieved profiles to oscillate with altitude (not only due to the ESA non-linearity correction, although this appeared to determine the phase of the oscillation). This was due to an intrinsic instability due to loose a priori constraints. The problem was solved by adding more regularisation via correlations in the a priori covariance matrix. A second problem has been the sensitivity to cloud. The solution currently applied is to change the a priori continuum profile from zero to a large value when clouds are detected in the Level 1B spectrum, effectively forcing the first guess atmosphere to be optically thick and prevent-

ing any species retrieval at those tangent altitudes. Other solutions, such as removing the Level 1 data completely, may prove more robust.

The **DLR-a** retrieval code has been upgraded to work with analytical derivatives now available from the MIRART forward model. Furthermore a multi–parameter regularization method relying on an a posteriori criterion for selection of the weighting factors corresponding to each atmospheric parameter was implemented. Retrievals have been repeated using pressure data derived with the IMK code. Work on implementing line-of-sight retrieval is in progress.

For the **D-PAC** retrieval code, regularization parameters have been modified, and the subroutine for the continuum profile handling has been upgraded. For the D-PAC processor, an improved method for retrieving profiles with bad initial pointing data has been designed and tested. Basically, improved line of sight data were generated within a single forward run to obtain a more consistent set of initial guess pointing and temperature data. Then these improved initial guess data were used within a standard retrieval sequence. Further, pure Tikhonov retrievals (instead of optimal estimation methods) were tested to exclude any potential artifacts introduced by a priori assumptions. Based on this, alternative joint and quasi-parallel retrieval techniques were compared to improve the retrieval of H_2O.

In order to make the **IFAC** retrieval processor applicable to real MIPAS measurements it was necessary to build a pre-processing tool which is able to extract from ESA's Level 1b products the measured spectra and a set of auxiliary data required for the retrieval (e.g. pointing information, ILS definition, noise level, etc.). Furthermore, in order to be able to process real MIPAS data it was necessary to optimize several setup parameters characterizing the behavior of the retrieval procedure.

The **RAL** forward model was enhanced to allow generation and re-use of absorption coefficient files. These store absorption coefficients and associated derivatives and their use has produced a significant decrease in calculation time for real, iterative retrieval calculations. The code can now also be run in a mode which scales the retrieved products to allow for widely differing values of weighting functions. This is particularly relevant for retrieval of instrument parameters in conjunction with mixing ratio profiles where values may differ by many orders of magnitude.

MIPAS Instrument and Retrieval Characterization

Often residuals (measured minus calculated spectra) carry information on either suboptimal parameter settings of the retrieval code or on instrument malfunction. Systematic analysis of residuals should help to detect some problems. Residual and Error Correlation (REC) Analysis has been developed under this project as a retrieval diagnostic tool. It provides a useful statistical tool for correlating the large amount of information con-

tained in the residual spectra from retrievals with expected signatures from known error terms, such as instrument calibration problems or missing/incorrectly modelled contaminant gases. The analysis of non-LTE from the residuals spectra suggests than non-LTE is, in general, in accordance with predictions except for two cases, the NO_2, for which NLTE is much smaller than anticipated, and for CH_4, which seems to be larger than predicted by a factor of 2. Particular problems identified in the ESA retrieval, and consequently many of those in the AMIL2DA project which make use of similar L1B and auxiliary data, are spectral shift $\pm$ 0.001 cm^{-1}, varying linearly across the MIPAS spectrum, also varying with altitude; the apodized instrument line shape is too wide by a few percent; problems in radiometric gain in early L1B data; poor characterisation of atmospheric NH_3 and COF_2 climatology; significant improvement in ESA data after November algorithm/setting modifications. IFAC analysis confirmed that the spectral shift detected by the residual error correlation analysis and by their analysis carried-out in WP 6000 is visually detectable on spectral residuals averaged over a whole orbit of measurements. Beyond this, IMK found that often their retrievals at lower altitudes are, due to H_2O lines, not properly caught in the fits. Thorough description of H_2O lines either by simultaneous retrieval or by proper use of volume mixing ratio information retrieved in a prior step is recommended.

Non-local Thermodynamic Equilibrium

Modelling of non-local thermodynamic equilibrium within the radiative transfer calculations causes additional effort and thus is avoided in the routine data analysis by selection of spectral microwindows which are free of non-LTE, or, where non-LTE is at least not the predominant error source. However, this pre-flight assessment of non-LTE relies on climatological vibrational temperatures, which may not be appropriate for the actual atmospheric condition. Therefore, possible non-LTE effects not appropriately considered in the level-2 processing were analysed in the fit residuals.

Beyond this, non-LTE retrievals were carried out at IAA. In these cases the non-LTE populations, e.g. vibrational temperatures, were computed for the actual retrieved pressure-temperature and species abundances retrieved directly from the spectra. The NLTE retrievals were carried out for the major operational products, eg, p-T, ozone, water vapour, methane and NO_2. In these retrievals (except for NO_2) the current information (e.g., prior to MIPAS measurements) was included. In case of NO_2, a previous retrieval of non-LTE parameters (carried out under another project), was included. The analysis of NLTE from the residuals spectra suggests than NLTE is, in general, in accordance with predictions except for two cases, the NO_2, for which NLTE is much smaller than anticipated, and for CH_4, which seems to be larger than predicted by a factor of 2.

The comparison between MIPAS O_3 and NO_2 with those measured by GOMOS and SCIAMACHY shows that NLTE-LTE retrieved MIPAS abundance differences were much smaller than the differences between the abundances measured by MIPAS and the other instruments. NLTE was found then not to be the likely candidate that could explain the

found MIPAS/GOMOS and MIPAS/SCIAMACHY differences.

The analysis of NLTE in the day/night spectra show, in general, the major expected NLTE features. Exceptions are NO_2, for which the NLTE effects seem to be significantly smaller than predicted, and CH_4, for which NLTE seems to be larger than theoretically predicted. Furthermore, this analysis have also revealed the existence of many first detected NLTE emissions, as well as more clear and nitty determinations of some previously detected NLTE features. These new detected emissions, however, do not affect the retrievals of most species, since they are located out of the microwindows normally used for the species retrievals.

The main conclusions on the NLTE retrievals are: Non-LTE retrievals for temperature, O_3, H_2O and CH_4 for orbit #2081 show that non-LTE errors are small below about 50 km. There can be however, significant errors (underpredictions) for considering LTE in the retrievals of temperature for polar-winter like atmospheric conditions (cold stratopause and warm lower mesosphere) above about 50 km. The non-LTE retrievals in O_3 show that non-LTE effects are small ($\leq$5%) below 50 km but can be significant (5–15%) between 50 and 60 km, particularly in the daytime and polar winter conditions. The non-LTE retrievals for H_2O show that non-LTE is negligible below about 55 km, but can be significant above, in the daytime and polar winter conditions, reaching differences of up to –30% at 60 km. They can also induce differences of about –10% at 20-35 km at daytime. Non-LTE in CH_4 is negligible except above 50 km at daytime, where they can induce errors of about –15%. The residual analysis and the upper atmosphere measurements suggest that they might be even larger. The non-LTE chemical excitation rate of NO_2 seems to be significantly smaller than predicted (at least a factor of 10 smaller). Non-LTE retrievals in NO_2 show that non-LTE effects are small ($\leq$5%) below $\sim$50 km but can be large (50%) between 50 and 60 km when we have a warm lower mesosphere, e.g., at polar winter conditions. Non-LTE effects are sometimes linked with the *a priori* profiles and the number of measurements (altitudes) included in the retrieval. Care should be taken to distinguish direct non-LTE effects from those induced by using different *a priori* profiles and the number of measurements (altitudes) included in the retrieval.

While MIPAS measurements are affected by non-LTE, GOMOS and SCIAMACHY measurements because of their different technique are considered free of non-LTE effects. Therefore, these measurements can be used to detect possible non-LTE induced retrieval errors in MIPAS retrieved profiles of atmospheric state parameters by comparison with the other Envisat instruments GOMOS and SCIAMACHY. The comparison between MIPAS O_3 and NO_2 with those measured by GOMOS and SCIAMACHY shows that non-LTE–LTE retrieved MIPAS abundance differences were much smaller than the differences between the abundances measured by MIPAS and the other instruments. Non-LTE was found then not to be the likely candidate that could explain the found MIPAS/GOMOS and MIPAS/SCIAMACHY differences.

Non-LTE effects in the atmosphere show remarkable diurnal changes. Therefore, compar-

ison of daytime and nighttime MIPAS spectra helped to detect further non-LTE effects. A comparison between co-added spectra at daytime and nighttime was undertaken for orbits #504 and 2081 (nominal mode) and for those taken at higher altitudes (1748-1752). Non-LTE effects were analysed for most of the bands of the atmospheric species, including CO_2, O_3, H_2O, CH_4, NO_2, NO, CO and OH. The detailed results and figures are shown in Deliverable D62. The major conclusions are listed below. The analysis of non-LTE in the day/night spectra show, in general, the major expected non-LTE features. Exceptions are NO_2, for which the non-LTE effects seem to be significantly smaller than predicted, and CH_4, for which non-LTE seems to be larger than theoretically predicted. Furthermore, this analysis have also revealed the existence of many first detected non-LTE emissions, as well as more clear and nitty determinations of some previously detected non-LTE features. These new detected emissions, however, do not affect the retrievals of most species, since they are located out of the microwindows normally used for the species retrievals.

Spectroscopic Data Insufficiencies

Nitric acid absolute intensities: In a previous effort (WP2600) the spectral parameters of the hot band $\nu_5 + \nu_9 - \nu_9$ (HIT24-19) were improved. However simulations of the MIPAS spectra using these data showed that there is an inconsistency between the spectral parameters of this hot band and those of the cold bands absorbing in the same spectral region, namely ν_5 (HIT18-14) and $2\nu_9$ (HIT21-14). A careful analysis, for different altitudes and sequences of the MIPAS microwindow covering the spectral domain 885.1-888.1 cm^{-1}, which contains this hot band, showed that either the hot band intensity is too weak by about 13 % or that the cold band intensities (which were those of HITRAN2K) are too large by the same amount.

In parallel new measurements of HNO_3 line intensities were recently performed at JPL [R.A. Toth, L.R. Brown and E.A. Cohen, Line strengths of nitric acid from 850 to 920 cm^{-1}, J. Mol. Spectrosc., 218, 151-168 (2003)] and Table 6.4 presents a synthesis of available intensity measurements for the 11.2 μm spectral region of HNO_3.

Several comments can be made: The total absorption as derived from HITRAN2K is in good agreement with the value of Giver et al.. This could be expected since the cold bands of HITRAN2K were calibrated in absolute using the Giver's value. The total absorption measured in ref. [5] is about 14% lower than the HITRAN2K value. The hot band Q-branch intensities measured during WP2600 and in [R.A. Toth, L.R. Brown and E.A. Cohen, Line strengths of nitric acid from 850 to 920 cm^{-1}, J. Mol. Spectrosc., 218, 151-168 (2003)] are in good agreement. Then, if one assumes that the HNO_3 hot band Q-branch has been properly measured, the last two points demonstrate that the cold band intensities given in HITRAN2K are too high by about 14%, confirming what was found when analyzing the MIPAS spectra. Accordingly a new database has been generated multiplying the line intensities of the bands ν_5 (HIT18-14), $2\nu_9$ (HIT21-14), ν_3 (HIT27-14) and ν_4 (HIT17-14)[1] by the factor 0.879. A HNO_3 retrieval has been performed with this

[1]The intensities of these bands have to be multiplied by the same factor as for ν_5 and $2\nu_9$ since their

Table 6.4: Comparison of measured HNO_3 intensities in the 11.2 μm spectral region

REFERENCES	TOTAL ABSORPTION	HOT BAND Q-BRANCH between 885.418 and 885.437 cm^{-1}
Goldman et al. [1]	585	
Giver et al. [2]	630	
Massie et al. [3]	483	
Hjorth et al. [4]	541	
Average	560 (10%)	
HITRAN2K	637	
Toth et al. [5]	560 (5%)	
WP2600		2.05
Toth et al. [5]		2.1

The intensities are in units of cm/atm^{-2}.

1. A. Goldman, T.G. Kyle, and F.S. Bonomo, Statistical band model parameters and integrated intensities for the 5.9 micron, and 7.5 μm, and 11.3 μm bands of HNO_3 vapour, Appl. Opt. 10, 65-73 (1971).

2. L.P. Giver, F.P.J. Valero, D. Goorvitch, and F.S. Bonomo, Nitric-acid band intensities and band-model parameters from 610 to 1760 cm^{-1}, J. Opt. Soc. Am. B1, 715-722 (1984).

3. S.T. Massie, A. Goldman, D.G. Murcray, and J.C. Gille, Approximate absorption cross sections of F12, F11, $ClONO_2$, N_2O_5, HNO_3, CCl_4, CF_4, F21, F113, F114, and HNO_4, Appl. Opt. 24, 3426-3427 (1985).

4. J. Hjorth, G. Ottobrini, F. Cappellani, and G. Restelli, A Fourier-transform infrared study of the rate-constant of the homogeneous gas-phase reaction N_2O_5 + H_2O and determination of absolute infrared band intensities of N_2O_5 and HNO_3, J. Phys. Chem. 91, 1565-1568 (1987).

5. R.A. Toth, L.R. Brown and E.A. Cohen, Line strengths of nitric acid from 850 to 920 cm^{-1}, J. Mol. Spectrosc., 218, 151-168 (2003)

new data.

It is essential to notice that, if it improves noticeably the RMS of the retrievals and hence their precision, this change leads to a systematic increase of the HNO_3 abundances of about 13%.

Nitrogen dioxide line widths: Recently a number of studies have dealt with the line widths of the NO_2 molecule. In particular A. C. Vandaele et al. [A.C. Vandaele, C. Hermans, S. Fally, M. Carleer, M.-F. Merienne, A. Jenouvrier and R. Colin, "Absorption cross-section of NO_2: Simulation of temperature and pressure effects", J.Q.S.R.T. (in press)] have performed an overview and a comparison of various papers in order to derive

absolute intensities were calibrated against those of these latter bands.

the temperature and pressure dependence of the NO_2 absorption features in the 13200-42000 cm^{-1} range. Comparing a number of experimental results they recommend the values:

$$\gamma_{air}(296K) = 0.080(3)\ cm^{-1}/atm,\ n = 0.8(2)$$

These values are to be compared to the values given in HITRAN96 or HITRAN2K:

$$\gamma_{air}(296K) = 0.067\ cm^{-1}/atm,\ n = 0.5$$

or to the values given in HITRAN01:

$$\gamma_{air}(296K) = 0.0707^{a}\ cm^{-1}/atm,\ n = 0.97^{b}$$

(^{a} Mean value calculated from all individual values of [V. Dana, J.-Y. Mandin, M.-Y. Allout, A. Perrin, L. Regalia, A. Barbe and X. Thomas, 'Broadening parameters of NO_2 lines in the 3.4μm spectral region', J.Q.R.S.T., 57, 445-457 (1997)]
^{b} value derived from ref. [V. Malathy Devi, B. Fridovich, G. D. Jones, D. G. S. Snyder, P. P. Das, J.-M. Flaud, C. Camy-Peyret, and K. Narahari Rao, 'Tunable diode laser spectroscopy of NO_2 at 6.2 μm,' J. Mol. Spectrosc. 93, 179-195 (1982); V. Malathy Devi, B. Fridovich, G. D. Jones, D. G. S. Snyder and A. Neuendorffer, 'Temperature dependence of the widths of N_2-broadened lines of the ν_3 band of $^{14}N^{16}O_2$,' Appl. Opt. 21, 1537-1538 (1982); R. D. May and C. R. Webster, 'Laboratory measurements of NO_2 line parameters near 1600 cm^{-1} for the interpretation of stratospheric spectra,' Geophys. Res. Lett. 17, 2157-2160 (1990)].

or to the values derived from UV spectra in ref. [S. Voigt, J. Orphal and J.P. Burrows, The temperature and pressure dependence of the absorption cross-sections of NO_2 in the 250-800 nm region measured by Fourier transform spectroscopy', J. Photochemistry and Photobiology A (in press)]:

$$\gamma_{air}(296K) = 0.134(10)\ cm^{-1}/atm,\ n = 1.03(80)$$

noticing that the authors recognize in their paper that the value obtained for γ_{air} is questionable because of line-mixing and resolution problems. Given these results and the errors associated we suggest, until new experimental or theoretical results are available, to use in the MIPAS database:

$$\gamma_{air}\text{air}(296K) = 0.074/0.71^{*}\ \gamma_{air}\text{air}(\text{HITRAN01}),\ n = 0.97$$

Also instead of no value, HITRAN01 gives a value of 0.095 cm^{-1}/atm for the self broadening coefficient. This seems reasonable and has been introduced in the MIPAS database.

Unexpected Instrumental Behaviour

In order to detect pointing errors of the MIPAS instrument, independent line of sight retrievals were performed which revealed major errors in the ESA-provided pointing data. These pointing errors could be assigned to the use of inappropriate target stars used as reference by the star tracker system and a malfunction of the Envisat orbit and attitude control system.

Systematic errors were found between forward and reverse sweeps in the p,T-retrieval. Since adjacent tangent heights in a limb scan are comprised of alternating forward and reverse sweeps, even small radiometric errors are magnified by the retrieval algorithm (profile oscillations). The cause was linked to the outputs of the work concerning non-linearity correction.

It turned out the non-linearity characterisation during the commissioning phase did not lead to satisfactory non-linearity correction. Thus, we proposed to use the on-ground characterisation data which were unfortunately identical for forward and reverse interferometer sweeps but still much better regarding radiometric accuracy. The photon flux, which ist an input to the non-linearity correction, is estimated from the maximum - minimum of the interferogram ADC (analog to digital converter) counts. Since forward and reverse sweeps are slightly differently digitised, the ADC max-min values for forward and reverse sweeps also differ. This leads to about 0.8 % different radiance levels of forward and reverse spectra after non-linearity correction. It was checked that the forward and reverse spectra before non-linearity correction differed by only 0.1 %. After we identified the origin the BOMEM company in charge of the level 1 processor produced an algorithm which compensated for the forward-reverse difference in sampling. Meanwhile, we have introduced new sets of non-linearity correction factors applying a new characterisation method developed by us and funded by ESA where the forward-reverse difference in radiance is decreased to 0.2 % without compensating. This was achieved by producing different sets of non-linearity correction curves for forward and reverse sweeps, as already implemented in the standard level 1 processing.

Radiometric gains were found to increase slowly with time, then drop to the initial value when warming up the focal plane unit. Ratios of radiometric gains approximated by ratios of CBB spectra measured after and before warming of the focal plane unit show distinct spectral signatures which coincide with the absorption spectrum of water ice at low temperature (URL: www.strw.leidenuniv.nl/schutte/database.html), spectrum of ice at 80 K). This is due the outgassing of water vapor from various surfaces of ENVISAT and deposition of ice on cold surfaces in the focal plane unit which was remove by warming up. The Gain change is rather large (up to 50%) and from the spectroscopic ice data and the gain change a thickness of 0.4 μm was estimated. Whereas channels A and C are heavily affected, channels B and D show minor changes, only. The detectors associated with the complementary interferometer output labeled with ”2” are more affected. Furthermore, channel C has even more ice formation.

Up to date no extended investigation of phase errors is available. As for the on-ground measurements the instrument shows an excellent phase stability. For some examples a different route was taken for assessing phase errors. Scene, gain, and offset spectra were phase corrected prior to radiometric calibration. The calibrated scene showed only marginal differences to the standard product. The standard product is derived using a complex gain. Any phase error should influence the radiance spectra as well as yielding non-zero imaginary part. The phase correction before calibration avoids phase errors introduced by instrument drifts.

It was found that periodic oscillations of the spectral intensity occurred which were attributed to microvibrations of an unknown source. These microvibrations were already present when the instrument was tested on-ground but unfortunately were only detected recently within this study. The microvibrations have several radiometric impacts: a) up to 1% intensity error varying with time, b) ghost lines error varying with time, c) signal in the imaginary part of the calibrated scene varying with time, previously leading to errors in the reproted NESR. The last problem has been solved by modification of the level 1 processing.

In-flight characterization measurement IF4 contains CBB interferograms for different CBB temperatures. The photoconductive channels A1, A2, AB and B were corrected with the old non-linearity correction factors. 300 forward sweeps for all channels for CBB and DS for the temperatures 229.7, 234.9, 239.6, 246.4 K were averaged and radiometric gains formed. The averaging removes the fluctuations caused by microvibrations. Gains were ratioed for each channel against the gain for 246.6 K. The maximum difference of gain ratios for CBB=229.5 K and 246.5 K from 1 was found in channels A1 (0.7%) and C (0.4%), both for the largest temperature contrast and can be attributed to water ice contamination over the 15 orbits of the measurement duration. Beside this the ratios deviate from 1 within 0.3%. Due to the very non-linear relation of blackbody temperature and spectral radiance substantial temperature errors outside specifications would have caused larger differences. Furthermore, this indicates the validity of the old non-linearity correction factors within the given brightness temperature range. However, a deteriorated blackbody emissivity differing significantly from 1 cannot be detected unless the radiation reflected into the field of view of the instrument due to a deteriorated blackbody surface is significant when compared to the blackbody radiance. The imaginary part of the ratios showed differences up to 0.3% which is quite small and can be expressed as phase variations over the 15 orbits where this data were taken.

Comparison MIPAS–GOMOS

The comparison of GOMOS and MIPAS were performed by individual, direct comparisons of profiles requiring stringent spatial and temporal collocation requirements and by a statistical study with a more relaxed temporal collocation. Because of small number of

overlapping data periods from these two instruments at this stage of the general validation period only 14 individual collocations were found. The statistical comparison was based on 100 collocations. Because of immature state of retrievals of both instruments, the comparison did not consider the different vertical resolutions of these two instruments neither the individual error estimates were used in the comparisons. The constituents compared were O_3, NO_2 and H_2O. The vertical grid of MIPAS was used and GOMOS measurements were interpolated to this grid.
In this work we compared GOMOS and MIPAS measurements for O_3, NO_2 and H_2O using limited data sets measured during the polar vortex split in 2002. Ozone profiles from these two instruments show reasonable agreement when compared individually using stringent collocation requirements. Also the statistical comparison with relaxed collocation shows a promising agreement. The mean difference for the subset of 100 collocations is shown in Fig. 6.17, left.

For NO_2 the individual comparisons are made difficult because of large oscillations in the GOMOS profiles. The statistical comparison may indicate a bias between GOMOS and MIPAS. For NO_2 the difference and standard deviation is shown in Fig. 6.17, right.

The comparison of H_2O profiles showed large differences. It must be noted that retrieval schemes for both instruments are not yet optimized. In GOMOS retrievals we expect that a Tikhonov smoothing will be deployed in vertical profiles which would alleviate comparisons. The IMK processing employs already a Tikhonov smoothing. It is evident that much more data are needed for conclusive conclusions. MIPAS-GOMOS comparisons will be continued in near future.

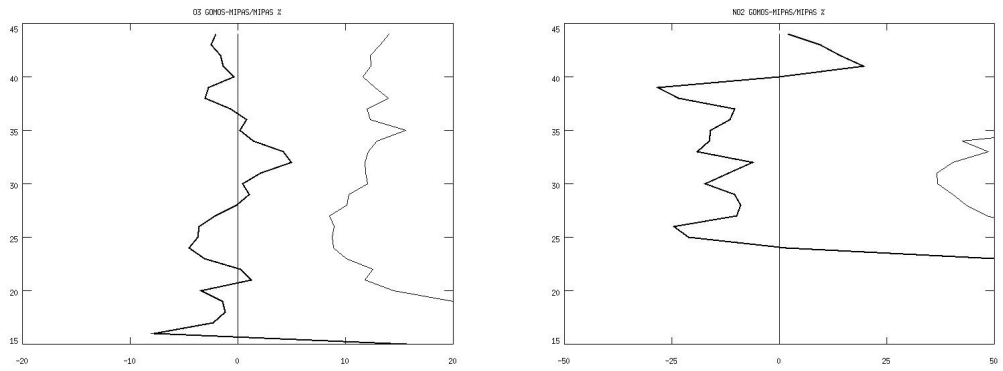

Figure 6.17: Relative mean difference (GOMOS-MIPAS)/MIPAS for Ozone (left panel) and NO_2 (right) (bold lines). Additionally the standard deviations of the differences are plotted (weak lines)

Comparison MIPAS–SCIAMACHY

The SCIAMACHY instrument is an UV/Vis/NIR grating spectrometer covering the spectral range from 220 - 2380 nm with a moderate spectral resolution of 0.2 - 1.5 nm. The

instrument measures atmospheric radiance from scattered, reflected and transmitted sunlight, extraterrestrial solar irradiance and lunar radiance in the three geometries nadir, limb and occultation and achieves global coverage within 6 days at the equator. SCIAMACHY limb measurements are made from 0-100 km with a vertical resolution of around 2.6 km. The horizontal resolution in azimuth direction is 240 km (120 km min.) by a swath of 960 km and in flight direction 400 km. At the IUP O_3 profiles from SCIAMACHY limb measurements are retrieved from all available Level_0 and Level_1 data with a solar zenith angle (SZA) $< 90°$. The retrieval uses 3 wavelengths of the O_3 Chappuis bands with optimal estimation and tangent heights are systematically corrected by -2km to compensate for an offset in the instrument's limb pointing.

At the IUP NO_2 profiles from SCIAMACHY limb measurements are retrieved from all available Lv1 data. The retrieval uses the spectrum within 420 - 490 nm and a ratio of limb measurements at different tangent heights, with the 45 km tangent height as a reference. With optimal estimation the vertical profile is retrieved using measured and modeled limb radiances with all corrections from pre-fit routine applied, weighting functions from RTM and a priori information. These SCIAMACHY NO_2 profiles are sensitive for the altitudes from 15 to 40 km. O_3 and NO_2 products from 20. and 23.09.02 from both instruments were compared to eachother. The sample of collocations was limited to the availability of MIPAS Level_1 data to the IMK and of SCIAMACHY Level_0 and Level_1 (for NO_2 only) data to the IUP. Collocated SCIAMACHY and MIPAS O_3 and NO_2 profiles were identified where measurements of the two satellite instruments were taken within the same or next orbit and using a 650 km collocation radius between the tangent point of the MIPAS measurement and the SCIAMACHY measurement. All collocated measurements were from the Southern Hemisphere and some of them were within, at the edge or outside of the polar vortex. Therefore, in order to avoid to compare collocated measurements from different airmasses, the potential vorticity (PV) data (given from the UKMO dataset) at 475 K were checked for the time and place of each collocated measurements. Only collocations were both measurements were within ($<$ -40 PVU), at the edge ($<$30 PVU to $>$-40 PVU) or outside the polar vortex ($>$ -30 PVU) have been included in the comparisons.

Additionally, results for MIPAS/Envisat retrieved by the University of Oxford (OXF), Rutherford Appleton Laboratory (RAL) and the Instituto de Astrofisica de Andalucia (IAA) have been used for the comparison. These retrievals have been performed using different retrieval codes and retrieval approaches.

Out of the total of 25 collocations for O_3 profile measurements, at 15 collocation pairs both measurements were outside the polar vortex and at 6 both were inside the polar vortex. For the NO_2 comparisons, at 3 collocation pairs both measurements were outside the polar vortex and at 2 both were inside the polar vortex.

O_3 cross validation: The O_3 results for two selected collocations retrieved by SCIAMACHY-IUP and available MIPAS results of IMK, OXF, RAL, and IAA, where

both coincidences were outside the polar vortex, are shown in Fig. (6.18). The comparisons (Fig. 6.18) of collocations where both measurements are outside the polar vortex look fairly good, but SCIAMACHY values are mostly lower than MIPAS. The statistical analyses (Fig. 6.19, left) gives at 18 - 48 km a mean relative deviation of SCIAMACHY-IUP to MIPAS-IMK with -15 - +1% (+/- 10 - 20%). Inside the polar vortex, the profile structure deviates quite a lot between the instruments, but the overall range of O_3 values are still comparable between 23 to $>$ 40 km (Fig. 6.20). The double peak structure which is recognizable in all MIPAS retrievals cannot be resolved by SCIAMACHY. It seems that SCIAMACHY cannot resolve fine profile structures. One possible reason is the swath width with about 960 km perpendicular to the viewing direction which is significantly wider than the horizontal field of view of MIPAS which is about 30 km. The statistical analyses (Fig. 6.19, right) gives at 23 - 48 km a mean relative deviation of SCIAMACHY to MIPAS with -10 - +15% (+/- 10 - 20%).

NO_2 cross validation: Six collocations of SCIAMACHY and MIPAS NO_2 retrievals were selected for comparison. For both instruments only measurements above 15 km were considered for the retrieval. For these collocations only MIPAS-retrievals by IMK were available. MIPAS retrievals were performed under LTE and non-LTE conditions. The results of the comparisons show large deviations for the collocations. Two of six collocations are shown in Fig. (6.21). The IMK NO_2 results generally have the maximum at too low altitudes. The maximum is expected to be at around 30 km. While the results for SCIAMACHY peak in this region, the MIPAS results peak between 20 and 25 km. One reason is the retrieval set-up with too strong regularisation for tangent altitudes below 25 km which forces the retrieval result towards the a priori profile. Since the a priori profile used general shows larger values than the result, the profile is forced to higher number densities and the maximum moves to lower altitudes. The retrieval scheme is currently being modified and improved and will be used for reprocessing of the data.

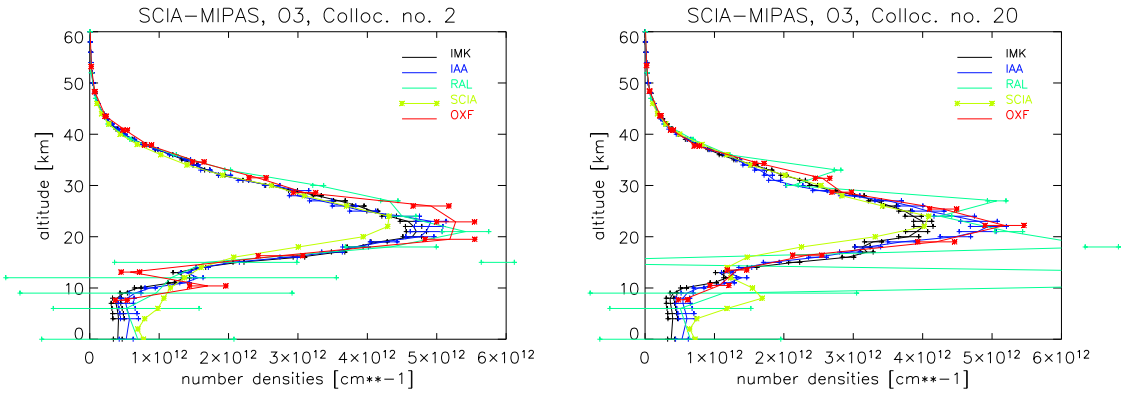

Figure 6.18: Ozone number density profiles for collocations outside the vortex. Results for SCIAMACHY from IUP (SCIA, yellow), for MIPAS from IMK (black), IAA (blue), OXF (red) and RAL (green).

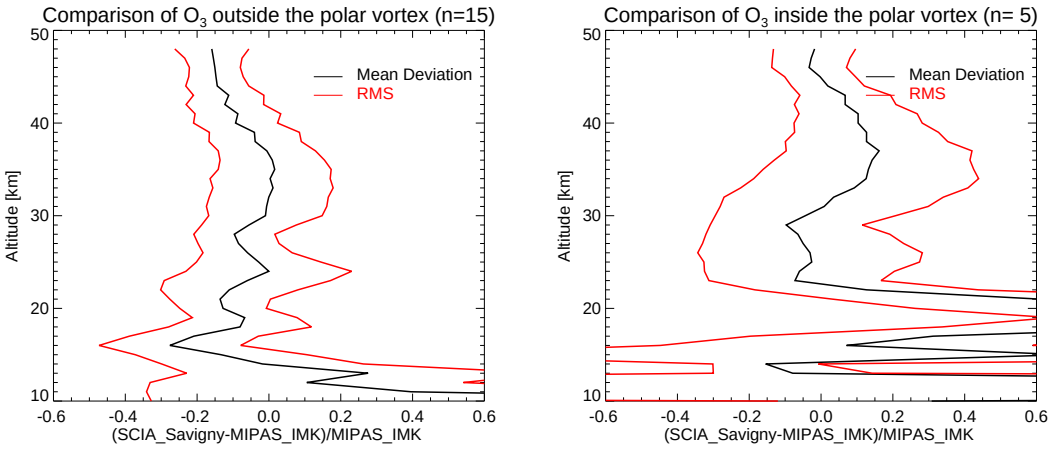

Figure 6.19: Statistics for ozone outside(left) and inside (right) the vortex.

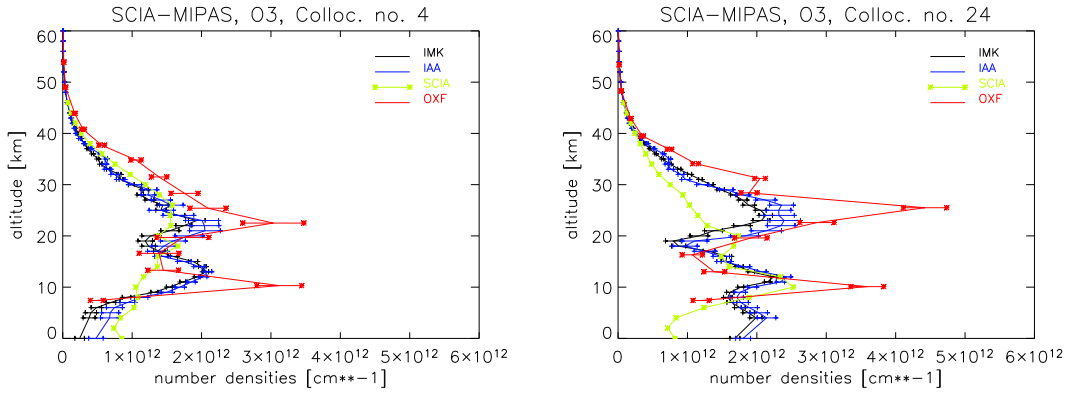

Figure 6.20: Ozone number density profiles. Collocations inside the vortex.

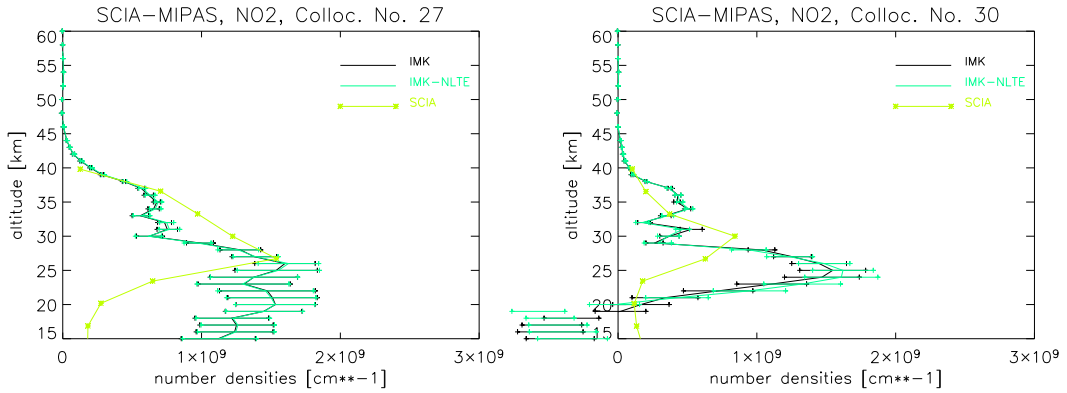

Figure 6.21: NO_2 number density profiles. MIPAS (IMK) results in black (incl. random error), IUP-SCIAMACHY result in yellow

Comparison to Further External Validation Data

The MIPAS-measured temperatures on 24 July and 20-27 September of 2002 are compared with those observed by a number of other satellites, including HALOE (Halogen Occultation Experiment) Version 19 L2 data, SABER (Sounding of the Atmosphere using Broadband Emission Radiometry) (Version 1.01 data), and UKMO (United Kingdom Meteorological Office) Stratospheric Assimilated Data (taken from BADC). The UKMO data are produced by analyzing a heterogeneous mixture of operational meteorological observations, including data from NOAA polar orbiters in addition to conventional meteorological observations such as radiosonde data.

Furthermore ozone profiles retrieved from GOME (Global Ozone Monitoring Experiment) measurements collocated with MIPAS measurements are compared. GOME is onboard ERS-2, which is on the same orbit as Envisat but with a delay of several minutes. Thus several collocations are available.

For the comparison individual paired-profile comparisons are conducted for those measurements with latitude and longitude differences smaller than 5 and 10 degrees, respectively. The time differences between the paired profiles are required to be less than 1 hour for the MIPAS/SABER and MIPAS/UKMO, but are allowed to be as large as 12 hours for MIPAS/HALOE due to the sampling characteristics of HALOE.

The paired profiles from SABER, HALOE, UKMO between 5 and 70 km are then interpolated to a common altitude grid as that used by the MIPAS-IMK data.

Total 208 MIPAS temperature profiles measured at different locations and seasons are compared with other satellite observations. The MIPAS data show general consistencies with those of the correlative HALOE, SABER and UKMO measurements on profile-by-profile basis.

The mean differences averaged over all available paired profiles are displayed here in Figure 6.22, left panel for 24 July, 2002 and, right panel, for five days of September 2002.

The MIPAS temperatures exhibit reasonable agreements with those of the three other satellite measurements. For solstitial measurements on 24 July (Figure 6.22), the MIPAS temperatures below 30 km are generally hotter than those of UKMO, but colder than those of SABER, with the differences less than 1 K and 2 K with respect to UKMO and SABER, respectively. At upper heights between 30 and 55 km, both HALOE and SABER are colder than MIPAS by 2-3 K, while UKMO hotter by 3-5 K. Larger deviations of 10-20 K are found above 60 km, where the upper boundary of the MIPAS observations is reached. The mean differences on 24 July of 2002 indicate that the MIPAS temperatures are colder than SABER by 2 K below 30 km (no HALOE data are available in the low altitudes), but hotter than both HALOE and SABER by 2-3 K at upper heights between 30 and 55 km. The discrepancies at the upper heights could be understood by the known

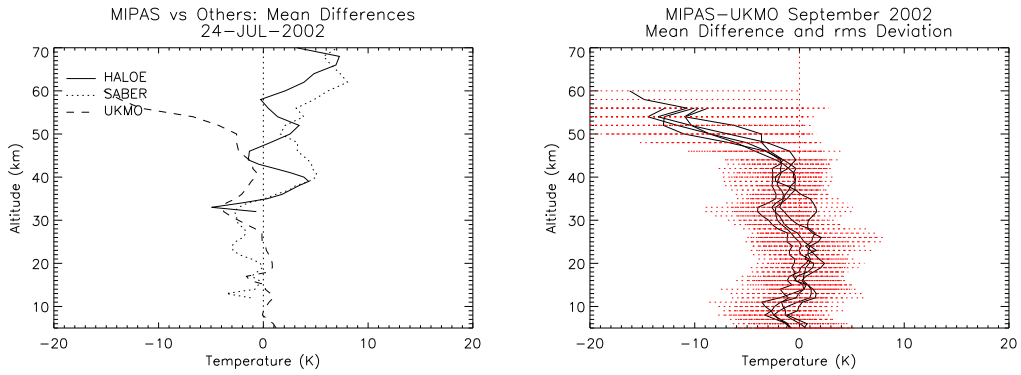

Figure 6.22: Left panel: Mean differences of MIPAS temeperatures with respect to the measurements of HALOE (solid), SABER(dotted), and UKMO (Dashed) (in Kelvin). The data are averaged over all available correlative profiles on 24 July, 2002. Right panel: Mean differences (solid) and root-mean-squared deviations (dotted) of MIPAS and UKMO temperatures (in Kelvin). The data are averaged over all available paired profiles during a day for the five days in September of 2002.

cold bias of SABER data.

Due to missing collocations of MIPAS and HALOE and reprocessing of the SABER data only comparisons of MIPAS and UKMO are presented for the days in September. As a consequence of the coincidence requirement MIPAS/UKMO collocations is available on 20,21,23,26, and 27 September. The mean differences and root-mean-squared deviations averaged over all available paired profiles for each day are displayed in Figure 6.22, right panel. Between 10 and 30 km, the daily mean differences are of about $\pm$(1-3) K, with larger magnitudes at the lowest and highest levels, and with apparent day-to-day variations. The resultant differences of the five days tend to be zero in this height region, suggesting no apparent systematical deviations between MIPAS and UKMO measurements. At upper heights above 30 km, the discrepancies generally increase with increasing height, with UKMO hotter than MIPAS by 10 -20 K at the upper boundary of UKMO and MIPAS measurements around 60 km. It is known that the UKMO temperatures are constrained and have a significant warm bias in the lower mesosphere. To further examine the statistical consistency between MIPAS and UKMO data, we compare the zonal mean differences between the correlative MIPAS and UKMO measurements. Figure 6.23 shows the daily zonal means of the differences during the four days of September. The zonal means of the differences between available correlative MIPAS and UKMO measurements revealed large discrepancies of maximum 6-8 K to occur around 25 km at higher latitudes of 60°S south, with MIPAS generally hotter than UKMO. This could be due to the deviations between the MIPAS observations and the current UKMO assimilation model, which may not fully reflect the unprecedented event.

Ozone retrievals from GOME and MIPAS have been compared for three collocations. The results are shown in Fig. (6.24). Both instruments reproduce the maximum and the

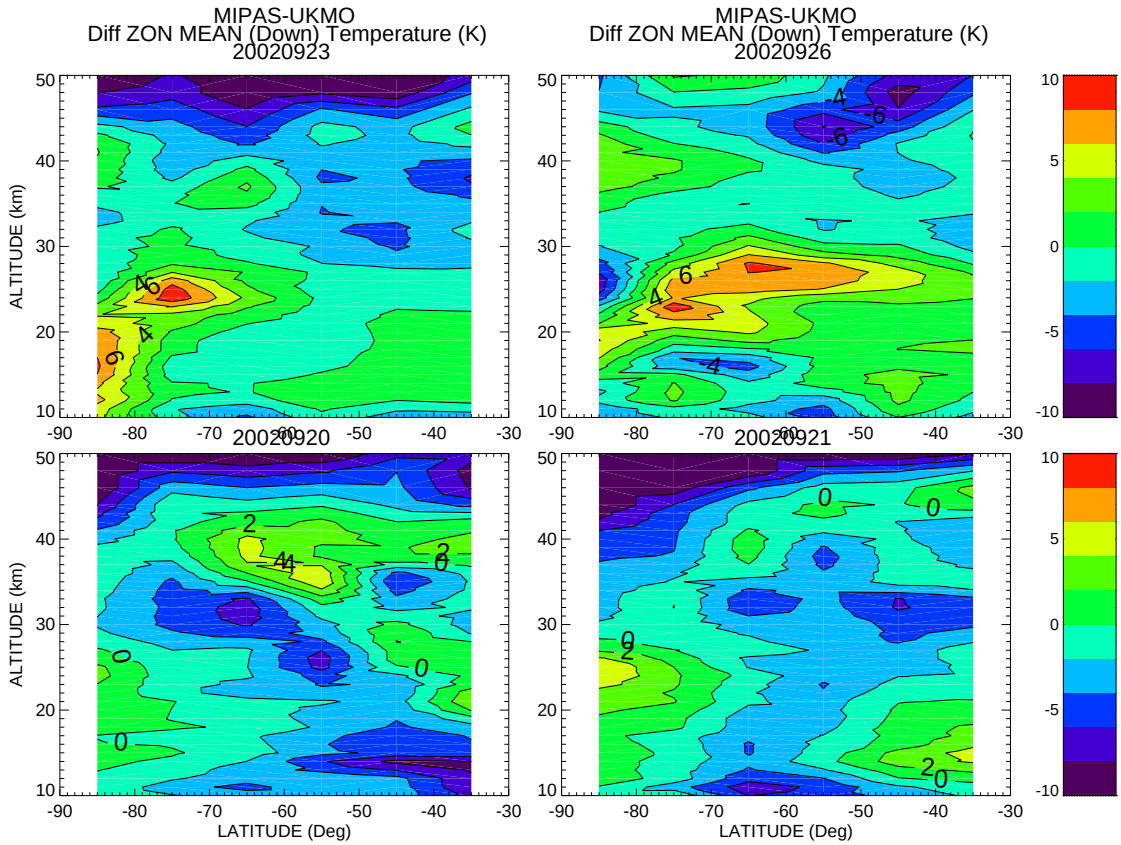

Figure 6.23: Daily zonally averaged temperature differences (in Kelvin) of correaltive MIPAS and UKMO measurements The temperatures are contoured by 2 K interval.

results look good. The altitude of the maximum is consistent for all MIPAS retrievals and the GOME profile. As the MIPAS results were obtained using different retrieval approaches and constraints the distribution varies, particularly in the maximum region. The IMK results seem to have lower maximum values than the others. For the observed cases the maximum of the GOME ozone profile shows slightly larger values than the MIPAS retrievals. Takeing into account the assumed random errors for MIPAS, MIPAS and GOMOS agree quite good.

Reference Algorithm Qualification

The functionalities inplemented in the IROE-I processor were exploited in this WP to re-process some MIPAS data sets with the aim of characterizing the accuracy of the retreived profiles with respect to some instrumental parameters that are assumed to be known in the ESA Level 2 processing chain. In particular, the following instrumental aspects were considered: Adequacy of the ILS shape as modelled in Level 1b processing, frequency and intensity calibrations, altitude dependence of the residual (uncorrected) instrumental offset.

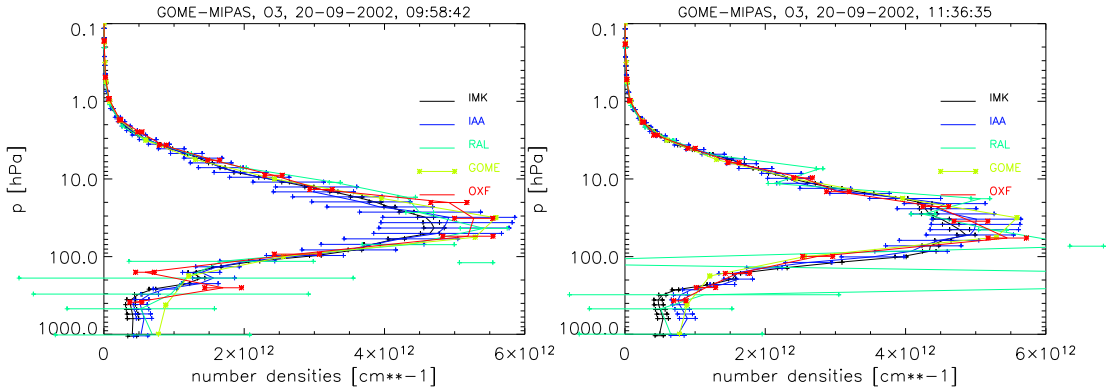

Figure 6.24: Ozone number density profiles for collocations of MIPAS and GOME. Results from GOME (yellow), IMK (black), IAA (blue), OXF (red) and RAL (green).

The analyses carried out under this WP have highlighted a frequency shift error in MIPAS measured spectra. A correction scheme was activated in Level 2 processor to correct the frequency scale of Level 1b spectra allowing to improve the retrieval accuracy. A recommendation was issued to improve the frequency calibration scheme implemented in MIPAS Level 1b processor (which did not properly allow for detectors non-linearity).

The retrieved instrument offset was found to be generally smaller than the measurement noise therefore, fitting of the residual instrument offset is an operation that could be avoided in routine retrievals.

6.4 Conclusions Including Socio-Economic Relevance, Strategic Aspects and Policy Implications

Four out of the six participating codes were developed to a maturity that they are now successfully used for scientific MIPAS data analysis. One further code can be used as multi-purpose work-bench reference code. Development of a sixth code had been slowed down for political (funding) reasons.

The availability of validated data analysis processors strengthens the participating groups in international scientific competition. The project contributed to the success of MIPAS which will have a positive impact to future Earth observation satellite missions. This strengthens the European space industry. Furthermore, AMIL2DA offered the chance to the participants to implement state-of-the-art software tools which are useful also beyond the MIPAS application. This is an advantage because these institutions are now able to contribute to future satellite missions without any additional delay and expenses which would be required if the software had to be created from the scratch as it would in some sense be the case without AMIL2DA.

The availability of improved spectroscopic data, and in particular the direct link between the retrieval community and the spectroscopy community strengthens their positions in international scientific competition.

The AMIL2DA project itself has provided a useful forum for our PhD students to gain wider experience of European research in their field, establish their own contacts with colleagues at the partner institutes, and acquire some understanding of the working of large international cooperative efforts. As such it has been a valuable part of their overall training.

Due to the upgrades developed under AMIL2DA, the spectroscopic database available for MIPAS level-2 data analysis is considered superior than commonly used databases available prior to AMIL2DA.

Cross-validation of radiative transfer models has put the consortium in a world-leading position in the area of forward modelling, since confidence in each of the codes under assessment has been considerably increased.

The climatology of vibrational temperatures delivered is the first of its kind and exceeds the needs of this particular AMIL2DA work-package by far. It can be considered the best ever obtained non-LTE populations dataset.

Retrieval of non-key species has been proven to be feasible. Some problems occur in the lowermost stratosphere, which could be assigned to the large aerosol loading of the reference atmosphere.

After this final step of processor validation, the European scientific community is ready to use their processors for science application, since the characteristics of the processors are well understood, and the characteristics of MIPAS radiance spectra and ancillary data are reasonably well understood. This allows the European MIPAS community to make valuable and timely contributions to atmospheric sciences. This strengthens the position of European research in worldwide competition. This also is advantageous for European space and remote sensing industry, because it proves the appropriateness of the technical concept behind the experiment and the quality of related engineering.

The ability of the European Earth observation community to scientifically analyse MIPAS radiance spectra allows to make major contributions to the research fields of ozone destruction, global change, and atmospheric pollution.

The construction of a parallel preprocessor and L2 retrieval has allowed feedback to be provided to ESA as part of the MIPAS Cal/Val activities.

6.5 Dissemination and Exploitation of Results

The data processors developed at the participating institutions will be used for analysis of MIPAS spectra. Resulting atmospheric data then will be distributed among the scientific community within the framework of dedicated co-operations. A major part of the scientific work done under AMIL2DA has been published in scientific journals. Developed understanding of MIPAS related instrument and retrieval problems was communicated to ESA and helped to improve the operational data processing. Spectroscopic data as well as some software developed under AMIL2DA are accessible by the scientific community. Beyond analysis of MIPAS data, the processors and tools developed under AMIL2DA will be used for definition studies of future satellite missions.

6.6 Main Literature Produced

T. von Clarmann, T. Chidiezie Chineke, H. Fischer, B. Funke, M. García-Comas, S. Gil-López, N. Glatthor, U. Grabowski, M. Höpfner, S. Kellmann, M. Kiefer, A. Linden, M. López-Puertas M. Á. López-Valverde, G. Mengistu Tsidu, M. Milz, T. Steck and G. P. Stiller, 2003, "Remote Sensing of the Middle Atmosphere with MIPAS", in *Remote Sensing of Clouds and the Atmosphere VII*, K. Schäfer, O. Lado-Bordowsky, A. Comerón and R. H. Picard, eds., Proc. SPIE, **4882**, 172–183, SPIE, Bellingham, WA, USA.

T. von Clarmann, M. Höpfner, B. Funke, M. López-Puertas, A. Dudhia, V. Jay, F. Schreier, M. Ridolfi, S. Ceccherini, B. J. Kerridge, J. Reburn and R. Siddans, 2003, "Modelling of atmospheric mid–infrared radiative transfer: the AMIL2DA algorithm intercomparison experiment", *J. Quant. Spectrosc. Radiat. Transfer*, **78**, 3-4, 381-407, doi:10.1016/S0022-4073(02)00262-5.

T. von Clarmann, N. Glatthor, U. Grabowski, M. Höpfner, S. Kellmann, M. Kiefer, A. Linden, G. Mengistu Tsidu, M. Milz, T. Steck, G. P. Stiller, D. Y. Wang, H. Fischer, B. Funke, S. Gil-López, and M. López-Puertas, 2003, "Retrieval of temperature and tangent altitude pointing from limb emission spectra recorded from space by the Michelson Interferometer for Passive Atmospheric Sounding (MIPAS)," J. Geophys. Res., accepted.

T. von Clarmann, S. Ceccherini, A. Doicu, A. Dudhia, B. Funke, U. Grabowski, S. Hilgers, V. Jay, A. Linden, M. López-Puertas, F.-J. Martín–Torres, V. Payne, J. Reburn, M. Ridolfi, F. Schreier, G. Schwarz, R. Siddans, and T. Steck, 2003, "A blind test retrieval experiment for infrared limb emission spectrometry", J. Geophys. Res., accepted.

A. Doicu, F. Schreier and M. Hess, 2003, "Iteratively Regularized Gauss–Newton Method for Bound–Constraint Problems in Atmospheric Remote Sensing", *Comp. Phys. Comm.*, **153** (1), pp. 59–65.

J.-M. Flaud, W. J. Lafferty, J. Orphal, M. Birk, and G. Wagner, 2003, "First high-resolution

analyses of the ν_8 and ν_8 + ν_9 spectral regions of $^{35}ClONO_2$: determination of the ν_9 band center," *Mol. Phys.*, **101**, 1527-1533.

J.-M. Flaud, J. Orphal, W.J. Lafferty, M. Birk and G. Wagner, 2002, "High resolution vib-rotational analysis of the ν_3 and ν_4 spectral regions of chlorine nitrate," *J. Geophys. Res.*, **107**, D24, ACH16-1-16-9.

J.-M. Flaud, A. Perrin, J. Orphal, Q. Kou, P.-M. Flaud, Z. Dutkiewicz and C. Piccolo, 2003, "New analysis of the $\nu_5 + \nu_9 - \nu_9$ hot band of HNO_3," *J. Q. S. R. T.*, **77**, 355-364.

J.-M. Flaud, C. Piccolo, B. Carli, A. Perrin, L. H. Coudert, J.-L. Teffo, and L. R. Brown, 2003, "Molecular line parameters for the MIPAS (Michelson Interferometer for Passive Atmospheric Sounding) experiment", *J. Atmospheric and Ocean Optics*, **16**, 172-182.

J.-M. Flaud, G. Wagner, M. Birk, C. Camy-Peyret, C. Claveau, M.R. De Backer-Barilly, A. Barbe, and C. Piccolo, 2003, "Ozone absorption around 10 μm", *J. Geophys. Res.*, **108**, doi:10.1029/2002JD002755.

G. Mengistu Tsidu, T. von Clarmann, H. Fischer, N. Glatthor, U. Grabowski, M. Höpfner, M. Kiefer, S. Kellmann, A. Linden, M. Milz, T. Steck, G. P. Stiller, B. Funke, and M. López-Puertas, 2002, "Validation of non-operational MIPAS-ENVISAT data products", in *Optical Remote Sensing of the Atmosphere and Clouds III*, *Proc. SPIE* **4891**.

M. Milz, M. Höpfner, T. von Clarmann, U. Grabowski, T. Steck, G. P. Stiller, and H. Fischer, 2002, "Measurements of water vapor and ice clouds in the tropical UT/LS region with MIPAS/ENVISAT", submitted to Adv. Space Res.

F. Schreier and U. Böttger, 2003, "MIRART, A Line-By-Line Code for Infrared Atmospheric Radiation Computations incl. Derivatives", Atmos. Oceanic Optics **16**, pp. 262–268.

G. P. Stiller, T. Steck, M. Milz, T. von Clarmann, U. Grabowski, and H. Fischer, 2003, "Approach to the cross-validation of MIPAS and CHAMP temperature and water vapour profiles", in *First CHAMP Mission Results for Gravity, Magnetic and Atmospheric Studies*, C. Reigber, H. Lühr, and P. Schwintzer, eds., pp. 551–556, Springer–Verlag Heidelberg.

G. P. Stiller, T. v. Clarmann, T. Chidiezie Chineke, H. Fischer, B. Funke, S. Gil-López, N. Glatthor, U. Grabowski, M. Höpfner, S. Kellmann, M. Kiefer, A. Linden, M. López-Puertas, G. Mengistu Tsidu, M. Milz and T. Steck, 2003, "Early IMK/IAA MIPAS/ENVISAT results", in *Remote Sensing of Clouds and the Atmosphere VII*, K. Schäfer, O. Lado-Bordowsky, A. Comerón and R. H. Picard, Proc. SPIE, **4882**, 184-193, SPIE, Bellingham, WA, USA

G. Wagner, M. Birk, F. Schreier and J.-M. Flaud, 2002, "Spectroscopic database for ozone in the fundamental spectral regions," *J. Geophys. Res.*, **107** (D22) 4626, doi: 10.1029/2001JD000818, ACH 10-1 – 10-18.

Appendix 1: Participants Information

Universität Karlsruhe, IMK
Kaiserstrasse 12
76128
Karlsruhe
Germany
Dr
von Clarmann
Thomas
Phone +49 7247 825946
Fax +49 7247 824742
e-mail thomas.clarmann@imk.fzk.de

Oxford University, Atmospheric, Oceanic and Planetary Physics
Parks Road
OX1 3PU
Oxford
United Kingdom
Dr
Dudhia
Anu
Phone +44-1865-272922
Fax +44-1865-272923
e-mail dudhia@atm.ox.ac.uk

DLR Oberpfaffenhofen
82230
Wessling
Germany
Dr
Schreier
Franz
Phone +49 8153 281234
Fax +49 8153 281446
e-mail franz.schreier@.dlr.de

IFAC - CNR
Via Panciatichi, 64
50127
Firenze
Italy
Dr
Ridolfi
Marco
Phone + 39 051 2093693
Fax + 39 051 2093693
e-mail ridolfi@fci.unibo.it

Rutherford Appleton Laboratory
Chilton, Didcot
OX11 0QX
Oxfordshire
United Kingdom
Dr
Kerridge
Brian J.
Phone +44-1235-445848
Fax +44-1235-446524
e-mail bjk@test76.ag.rl.ac.uk

Laboratoire de Photophysique Moleculaire
Batiment 213, Universite Paris 11, Campus d'Orsay
91405
Orsay Cedex
France
Prof Dr
Flaud
Jean-Marie
Phone +33 1 69416776
Fax +33 1 69416777
e-mail flaud@ccr.jussieu.fr

Instituto de Astrofisica de Andalucia CSIC
Apartado Postal 3004
18080
Granada
Spain
Dr
Lopez-Puertas
Manuel
Phone +34 958-121311
Fax +34 958-814530
e-mail puertas@iaa.es

Universität Bremen, IUP
P.O. Box 330440
28334
Bremen
Germany
Dr
Bovensmann
Heinrich
Phone +49-421-218-4081
Fax +49-421-218-4555
e-mail heinrich.bovensmann@gome5.physik.uni-bremen.de

Finnish Meteorological Institute, FMI, Geophysical Research Division
P.O. Box 503
00101
Helsinki
Finland
Dr
Kyrölä
Erkki
Phone +358-9-19294 640
Fax +358-9-19294 603
e-mail erkki.kyrola@fmi.fi